

EFFECT OF APPLIED PRESSURES ON THE RADON CHARACTERISTICS  
OF AN UNDERGROUND MINE ENVIRONMENT

by

Gerald Lawrence Schroeder

S.B., Massachusetts Institute of Technology  
(1959)

M.S., Massachusetts Institute of Technology  
(1961)

SUBMITTED IN PARTIAL FULFILLMENT OF THE

REQUIREMENTS FOR THE DEGREE OF

DOCTOR OF PHILOSOPHY

at the

MASSACHUSETTS INSTITUTE OF TECHNOLOGY

January, 1965

Signature of Author \_\_\_\_\_  
Department of Geology and Geophysics,  
11 January 1965

Certified by \_\_\_\_\_  
Thesis Supervisor

Certified by \_\_\_\_\_  
Thesis Co-Supervisor

Accepted by \_\_\_\_\_  
Chairman, Departmental Committee  
on Graduate Students



LINDGREN

EFFECT OF APPLIED PRESSURES ON THE RADON CHARACTERISTICS  
OF AN UNDERGROUND MINE ENVIRONMENT

by

Gerald Lawrence Schroeder

Submitted to the Department of Geology and Geophysics on  
11 January 1965 in partial fulfillment of the requirement for  
the degree of Doctor of Philosophy.

ABSTRACT

Investigations were conducted at two underground locations, foreman's room and 5702 area, of the Kermac Nuclear Fuels Corp. uranium mining installation, Ambrosia Lake, New Mexico. The rock environment is stratified sandstone. Pressures were varied from -0.4 cm Hg to +3.8 cm Hg with respect to barometric pressure, and were maintained for periods ranging from several hours to 21 days. Variables measured were: room air radon-222 (Rn) and Rn daughter-product concentrations, humidity, temperature, interstitial Rn concentrations at depths to 15 ft. within rock, and air consumption required to maintain the chosen overpressure.

Reduction of the flux of Rn from adjacent rock into the mine during overpressure is sizable. One cm Hg overpressure (~1.5% of normal barometric pressure) produced a 20-fold decrease in Rn flux into the foreman's room as compared to the Rn flux observed during dilution ventilation. The 5702 area experienced a 5-fold decrease in Rn flux for a similar overpressure. During 21 days of continuous 1 cm Hg overpressure in the 5702 area this reduced Rn flux was maintained. The smaller reduction in flux for the 5702 area results in part from the proximity of the foreman's room to a non-pressured area and the presence of a shale lens overlying the ceiling of the 5702 area. A 0.4 cm Hg underpressure of the 5702 area increased the Rn flux into the area by 3-fold over the non-pressured value.

A barometric pressure influence on Rn flux into the mine and on air Rn concentrations in non-pressured areas of the mine was measured. A falling barometric pressure causes an increase in the flux of interstitial gas into the mine; a rising barometric pressure decreases this flux. These effects are not seen in overpressured mine areas.

In the 5702 area, during dilution ventilation, the ratio of activities of air-suspended Rn daughter products to Rn is 50% of the equilibrium value. During overpressure this ratio is reduced to 25%.

Radon concentrations in rock interstices show, during overpressure, decreases at all locations monitored except in the immediate vicinity of the shale lens above the 5702 area ceiling. These reductions are the result of air flowing from the mine into the rock interstices under the influence of the pressure gradient induced by the overpressure.

The relative humidity of the 5702 area was reduced after 2 days of 1 cm Hg overpressure from a pre-overpressure value of 96% to 81%.

A theoretical treatment of convection and counter diffusion of miscible compressible fluids moving through an anisotropic porous medium is presented. This leads to an analytic expression for the distribution of Rn within the interstices of a stratified sandstone surrounding an overpressured area. When measured permeabilities and observed interstitial pressure gradients are introduced into this expression the results are in good agreement with the Rn concentrations observed during overpressure.

Thesis Supervisor: Robley D. Evans  
Title: Professor of Physics

Thesis Co-Supervisor: John W. Winchester  
Title: Associate Professor of Geochemistry

## TABLE OF CONTENTS

	<u>Page</u>
Abstract	2
List of Figures	6
List of Tables	10
1. Introduction	14
2. Experimental Installations	17
3. Experimental Procedure	25
4. Experiments	29
5. Empirical Results and Interpretation	30
a. Radon Concentrations in Interstitial Gas	32
b. Radon Flux	50
c. Room Air Radon Concentrations	55
d. Radon Daughter-Product Working Levels and Radon-Radon Daughter-Product Disequilibria	60
e. Temperature, Relative Humidity, and Moisture	62
6. Analytic Description of Interstitial Radon Concentrations During Mine Overpressure	64
7. Bibliography	79
APPENDIX	
8. Experimental Installations	82
9. Experiments	88
10. Radon Concentrations in Interstitial Gas	93
11. Radon Flux Measurements	105
12. Room Air Radon Concentrations	108

	<u>Page</u>
13. Diffusion Coefficient of Radon in Sandstone	121
14. Permeability of Test Site Environment	124
15. Permeability of the Mathematically Transformed Mine Environment	128
16. Comparison of Observed and Predicted Rates of Air Consumption in the Foreman's Room	130
17. Theoretical Description of Interstitial Radon Concentrations in Rock Adjacent to a Mine Tunnel During Non-pressure Conditions	135
18. Derivation of Equation (24), an Analytic Description of Interstitial Radon Concentrations in Rock Surrounding an Overpressured Area	140
19. Determination of Interstitial Radon Production Rate in Rocks for Low and High Interstitial Radon Concentrations	146
20. Radon and Radium in Mine Recycle Waters	149
21. Bibliography to the Appendix	157
ACKNOWLEDGEMENTS	158
BIOGRAPHICAL NOTE	159

## LIST OF FIGURES

<u>FIGURE</u>		<u>PAGE</u>
1	Plan View of Sampling Installation Foreman's Room	18
2	Plan View of 5702 Test Area	19
3	Profile of Sampling Sites in Drift of 5702 Test Area	21
4	Interstitial Radon Concentration for Pre-overpressure Periods and for 0.9 cm Hg Overpressure vs. Depth, Foreman's Room	34
5	Interstitial Radon Concentration vs. Time, Varied Overpressure Test, Foreman's Room	35
6	Interstitial Radon Concentration vs. Time, 3.8 cm Hg Overpressure Test, Foreman's Room	37
7	Interstitial Radon Concentration vs. Depth Parallel to Bedding, 21 day overpressure test, 5702 area	40
8	Interstitial Radon Concentration vs. Depth Perpendicular to Bedding, 21 day overpressure test, 5702 area	41
9	Interstitial Radon Concentration vs. Depth, 21 day overpressure test, 5702 area	42
10	Pressure Difference Between Sampling Probe and Test Area vs. Depth, 21 day overpressure test, 5702 area	44
11	Pressure Difference Between Sampling Probe and Test Area vs. Depth, underpressure test, 5702 area	47
12	Total Radon Flux into Foreman's Room vs. Applied Overpressure	51
13	Total Radon Flux into 5702 Area vs. 5702 Area Pressure Relative to Local Barometric Pressure	52

<u>FIGURE</u>		<u>PAGE</u>
14	Comparison of Observed and Predicted Interstitial Radon Concentrations vs. Depth, 0.9 cm Hg Overpressure, Foreman's Room	75
15	Comparison of Observed and Predicted Interstitial Radon Concentrations vs. Depth, 1.4 cm Hg Overpressure Foreman's Room	76
16	Plan View of Sampling Installation at Foreman's Room	83
17	Profile of Sampling Installation, Foreman's Room	84
18	Plan View of Sampling Sites in Drift of 5702 Test Area	85
19	Profile of Sampling Sites in Stope of 5702 Test Area	86
20	Interstitial Radon Concentration vs. Time, 21 day overpressure test, 5702 area	94
21	Interstitial Radon Concentration vs. Time, 21 day overpressure test, 5702 area	95
22	Interstitial Radon Concentration vs. Time, 21 day overpressure test, 5702 area	96
23	Interstitial Radon Concentration vs. Time, 21 day overpressure test, 5702 area	97
24	Interstitial Radon Concentration vs. Time, 21 day overpressure test, 5702 area	98
25	Interstitial Radon Concentration vs. Time, underpressure experiment, 5702 area	100
26	Interstitial Radon Concentration vs. Time, underpressure experiment, 5702 area	101
27	Interstitial Radon Concentration vs. Time, underpressure experiment, 5702 area	102

<u>FIGURE</u>		<u>PAGE</u>
28	Room Air Radon Concentration vs. Time, varied overpressure test, foreman's room	109
29	Room Air Radon Concentration vs. Time, 21 day overpressure test, 5702 area	110
30	Room Air Radon and Radon Daughter-product Concentrations During Stated Air Dilution Conditions vs. Time, 5702 Area	111
31	Room Air Radon and Radon Daughter-product Concentrations During Stated Overpressure Conditions vs. Time, 5702 Area	113
32	Room Air Radon and Radon Daughter-product Concentration vs. Time, underpressure experiment, 5702 area	114
33	Barometric Pressure at Grants, New Mexico, vs. Time	116
34	Air Radon Concentration for Stated Dilution and Overpressure Conditions vs. Time, 5702 area	117
35	Radon Diffusion Coefficient (D) as Predicted from Interstitial Radon Concentration Gradient ( $dc/dx$ ) in Bulk Rock and Observed Radon Flux (J) Across Total Rock Surface vs. Overpressure, Foreman's Room	122
36	Apparatus for Determination of Permeability of Rock Samples	125
37	Pressure Difference Between Sampling Probe and Test Area for Stated Overpressure vs. Depth, Foreman's Room	131
38	Approximation of the Profile of Foreman's Room	132
39	Observed and Predicted Air Input Rate to Foreman's Room During Overpressure vs. Applied Overpressure	133



<u>FIGURE</u>		<u>PAGE</u>
40	Theoretically Predicted Interstitial Concentrations in Rock Surrounding a 10 Foot Diameter Tunnel and Interstitial Radon Concentrations Observed in Rock Adjacent to Foreman's Room vs. Depth; Normal Pressure	138
41	Solutions of $D \nabla^2 C - \frac{1}{S} \text{div}(VC) + \phi - \lambda C = 0$ using Stated Parameters	143
42	Solutions of $D \nabla^2 C - \frac{1}{S} \text{div}(VC) + \phi - \lambda C = 0$ and $-\frac{1}{S} \text{div}(VC) + \phi - \lambda C = 0$	145
43	Apparent Interstitial Radon Production Rate as Determined by Purging vs. Pressure Differential Across Rock Sample	148
44	Plan View of Water and Air Sampling Area, 20 September 1963	150
45	Radon Content of Water vs. Distance of Flow in Drift	151
46	Dissolved Radium Content of Water vs. Distance of Flow in Drift	151
47	Radon Concentration in Air vs. Distance from End of 09 Drift	152
48	Plan View of Water and Air Sampling Area, 57 Drift, 27 February 1964	155

## LIST OF TABLES

<u>TABLE</u>		<u>PAGE</u>
1	Effect of Applied Pressures on Radon Characteristics of 5702 Area	58
2	Sampling Probes in Foreman's Room, June 1963	87
3	Permeability of Sandstones from Foreman's Room and 5702 Area	127
4	Values of E: Ratio of Interstitial Radon Production Rate in Low Radon Atmosphere to Interstitial Production Rate in High Radon Atmosphere	147

The following text through section 7 is to be submitted for publication.

EFFECT OF APPLIED PRESSURES ON THE RADON CHARACTERISTICS  
OF AN UNDERGROUND MINE ENVIRONMENT

by

Gerald L. Schroeder and Robley D. Evans

ABSTRACT

Investigations were conducted at two underground locations, foreman's room and 5702 area, of the Kermac Nuclear Fuels Corp. uranium mining installation, Ambrosia Lake, New Mexico. The rock environment is stratified sandstone. Pressures were varied from -0.4 cm Hg to +3.8 cm Hg with respect to barometric pressure, and were maintained for periods ranging from several hours to 21 days. Variables measured were: room air radon-222 (Rn) and Rn daughter-product concentrations, humidity, temperature, interstitial Rn concentrations at depths to 15 ft. within rock, and air consumption required to maintain the chosen overpressure.

Reduction of the flux of Rn from adjacent rock into the mine during overpressure is sizable. One cm Hg overpressure (~1.5% of normal barometric pressure) produced a 20-fold decrease in Rn flux into the foreman's room as compared to the Rn flux observed during dilution ventilation. The 5702 area experienced a 5-fold decrease in Rn flux for a similar overpressure. During 21 days of continuous 1 cm Hg overpressure in the 5702 area this reduced Rn flux was maintained. The smaller reduction in flux for the 5702 area results in part from the proximity of the foreman's room to a non-pressured area and the presence of a shale lens overlying the ceiling of the 5702 area. A 0.4 cm Hg underpressure of the 5702 area increased the Rn flux into the area by 3-fold over the non-pressured value.

A barometric pressure influence on Rn flux into the mine and on air Rn concentrations in non-pressured areas of the mine was measured. A falling barometric pressure causes an increase in the flux of interstitial gas into the mine; a rising barometric pressure decreases this flux. These effects are not seen in overpressured mine areas.

In the 5702 area, during dilution ventilation, the ratio of activities of air-suspended Rn daughter products to Rn is 50% of the equilibrium value. During overpressure this ratio is reduced to 25%.

Radon concentrations in rock interstices show, during overpressure, decreases at all locations monitored except in the immediate vicinity of the shale lens above the 5702 area ceiling. These reductions are the result of air flowing from the mine into the rock interstices under the influence of the pressure gradient induced by the overpressure.

The relative humidity of the 5702 area was reduced after 2 days of 1 cm Hg overpressure from a pre-overpressure value of 96% to 81%.

A theoretical treatment of convection and counter diffusion of miscible compressible fluids moving through an anisotropic porous medium is presented. This leads to an analytic expression for the distribution of Rn within the interstices of a stratified sandstone surrounding an overpressured area. When measured permeabilities and observed interstitial pressure gradients are introduced into this expression the results are in good agreement with the Rn concentrations observed during overpressure.

## 1. Introduction

The control of harmful or noisesome gases which emanate into underground mining areas from surrounding rocks is often a costly necessity. In uranium (U) mines this problem is presented by the high interstitial concentrations of radon-222 (Rn), a radioactive noble gas of 3.82-day half-period, formed in the decay scheme of  $U^{238}$ , and the relative ease with which this noble gas diffuses from its parent rock into the interstices of the rock and then to a working area. Long-term exposure to moderate concentrations of Rn (3000  $\mu\mu\text{c}/\text{l}$ ) and its short-lived alpha-ray emitting daughter products, RaA ( $\text{Po}^{218}$ ) and RaC' ( $\text{Po}^{214}$ ), has been found to result in an increased incidence of bronchial carcinoma (C-1). The acceptable limit of Rn daughter products in a mine atmosphere is presently set at a concentration of short-lived radon daughters which would be in equilibrium with 100  $\mu\mu\text{c}$  of Rn/l. of air.

Ventilation of mines is conventionally accomplished by continuously diluting the mine air with fresh air brought in by fan or natural convection from above ground surface. The diluted air is allowed to vent freely to the atmosphere. This process does nothing to retard the rate at which gases (including Rn) diffuse into the mine from surrounding rock. It merely reduces the concentrations of these gases within the mine.

It is suggested that in a sufficiently permeable rock environment a slight pressurization of the mine air may induce air flow from the mine into the interstices of rock surrounding the mine. This convective flow of comparatively fresh air will reduce the concentration and the concentration gradient of undesirable gases in the rock interstices adjacent to the mine and hence reduce the flux of these gases into the mine.

An investigation into the effect which applied pressures have upon the Rn characteristics of a mine atmosphere has been in progress at the Kermac Nuclear Fuels Corp. uranium mines, Ambrosia Lake (near Grants), New Mexico, since June 1963. In rock interstices adjacent to the mine and in the mine atmosphere the rate, magnitude, and duration of induced changes in Rn concentration were measured for pressures ranging from -0.4 cm Hg (-2.1 in. water gauge) to 3.8 cm Hg (20.0 in. water gauge) with periods of continuous pressurization varying from 1 day to 21 days. During the tests, humidity in the mine atmosphere, transmitted pressures in the interstices of the adjacent rock, and air consumption required to maintain the desired pressure were also recorded.

Results were intended, in part, to indicate whether an overpressure of several cm Hg in an underground area would reduce the Rn flux into a mine sufficiently to warrant further

investigation into the practicality of this technique as a method of general mine ventilation. Monitoring of Rn concentrations and transmitted overpressures in the interstices of adjacent rock allows a comparison of these values with theoretical predictions, and aids in the understanding of the changes observed in the mine atmosphere.

Analytically, the overpressure problem is one of miscible displacement by compressible fluids flowing through an anisotropic porous medium: moderately pressurized air from the mine flows into a layered sedimentary rock and convectively displaces part of the Rn-rich interstitial gas. Radon diffuses counter-current to this convective flow at a rate proportional to its concentration gradient. In time, a steady state of convection and counter diffusion is established. The Rn flux into the mine is never reduced to zero, and only asymptotically approaches zero as the overpressure (and hence the convective velocity of purging air) approaches infinity.

Radon concentrations during overpressure are described mathematically by a steady-state form of Fick's second law of diffusion taking into account Rn production from radium ( $\text{Ra}^{226}$ ) in the rock and Rn decay, with an additional term to account for the convective displacement of the gases.



## 2. Experimental Installations

Two locations in the Kermac mines were used: an abandoned foreman's lunch room (referred to as the foreman's room), mine section 24, 1-4 level, and an area consisting of a stope and adjoining drifts off 57 drift 02 raise (referred to as the 5702 area), mine section 26. The areas are approximately 800 feet and 600 feet below ground level, respectively, and are remote from present mining operations.

Figure 1 shows the foreman's room in plan. Probes for sampling interstitial gas are indicated in the figure. They are from an experiment performed here. The probes are located in the ribs and floor of the room. The room is nominally 25 ft. long, 9-12 ft. wide and 8 ft. high, with a surface area of about 1100 sq. ft. and volume of about 2100 cu.ft. It is cut into the wall of a main haulageway. The rock surfaces are free of major obstructions to the passage of Rn. The environment is a moist, soft, stratified, uranium-bearing sandstone of low grade and of moderate permeability ( $14 \times 10^{-9} \text{ cm}^2$  perpendicular to, and  $22 \times 10^{-9} \text{ cm}^2$  parallel to stratifications). Stratifications are approximately horizontal. The floor is covered with 1-2 ft. of crushed, packed sandstone.

Figure 2 shows the 5702 area in plan. This area offers the opportunity of working with typical mining geometries

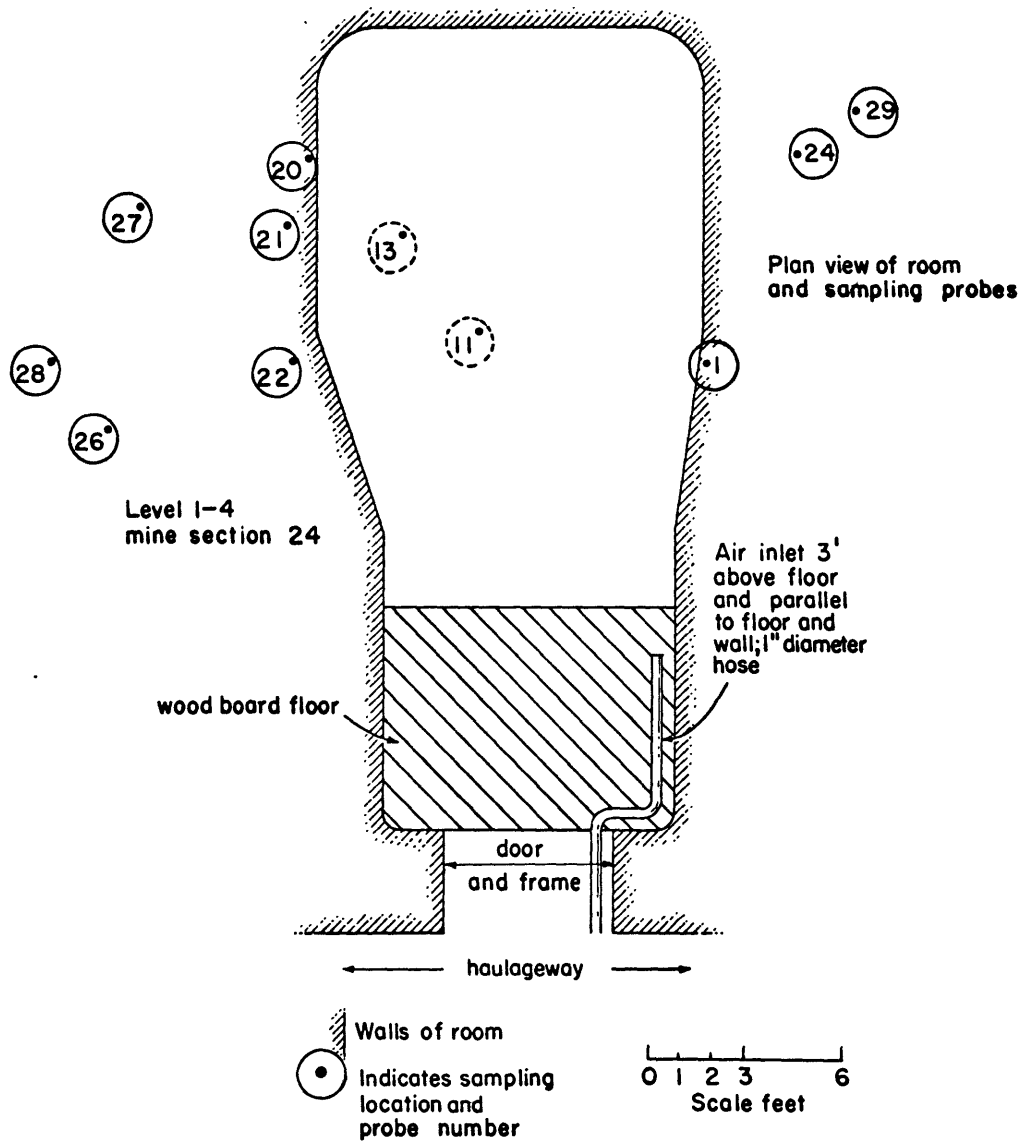


FIGURE 1. PLAN VIEW OF SAMPLING INSTALLATION FOREMAN'S ROOM

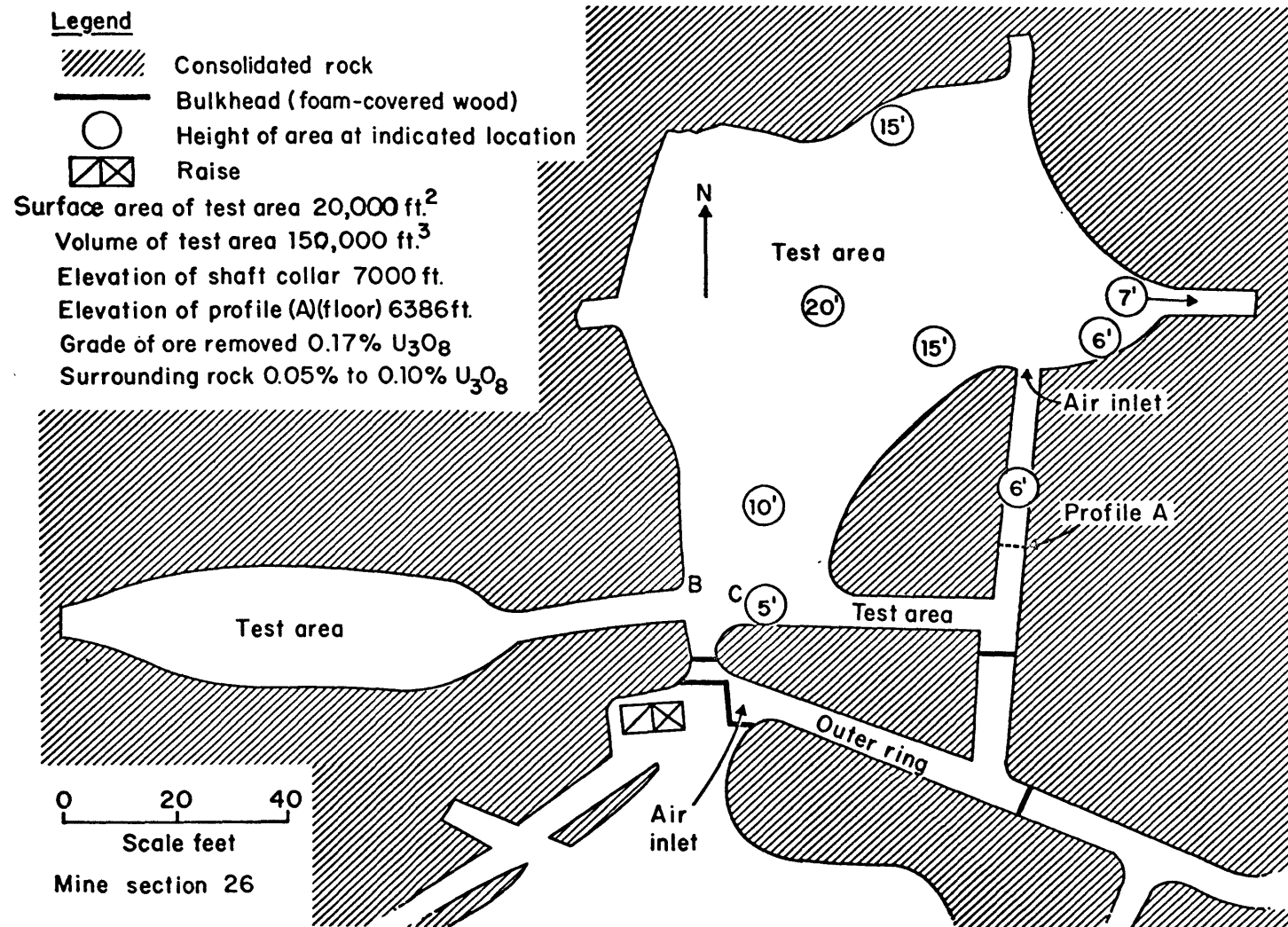


FIGURE 2. PLAN VIEW OF 5702 TEST AREA

including stopes, drifts, and enclosed pillars. Nominally the surface area of 5702 area is 20,000 sq. ft. and the volume is 150,000 cu. ft. Interstitial gas sampling probes are located in the vicinity of areas A, B, C, Fig. 2. The environment is stratified sandstone of fair-to-high grade ore and is not completely mined out. Permeability of the rock is not uniform; a representative permeability is about  $55 \times 10^{-9} \text{ cm}^2$  parallel to and  $33 \times 10^{-9} \text{ cm}^2$  perpendicular to stratifications. Stratifications are approximately horizontal. In a section of the stope ceiling a portion of a shale lens was visible. Mine geologists stated that this lens was no more than several feet in thickness. Water dripped from much of the stope ceiling in the vicinity of the exposed shale prior to the application of overpressure. Several test holes drilled into the drift ceiling near profile A (Fig. 2) produced water at the rate of a very slow drip. Relative humidity was 96% prior to overpressure. Figure 3 shows, in profile, a portion of the drift near profile A, Fig. 2. Location of sampling probes are indicated in Fig. 3.

During overpressure experiments, the outer ring of the 5702 area (Fig. 2) was maintained, by separate air supply, at a pressure close to that of the test area. This ensured that all air utilized in the test area passed into the rock of the area and did not leak out around the inner bulkhead air seals.

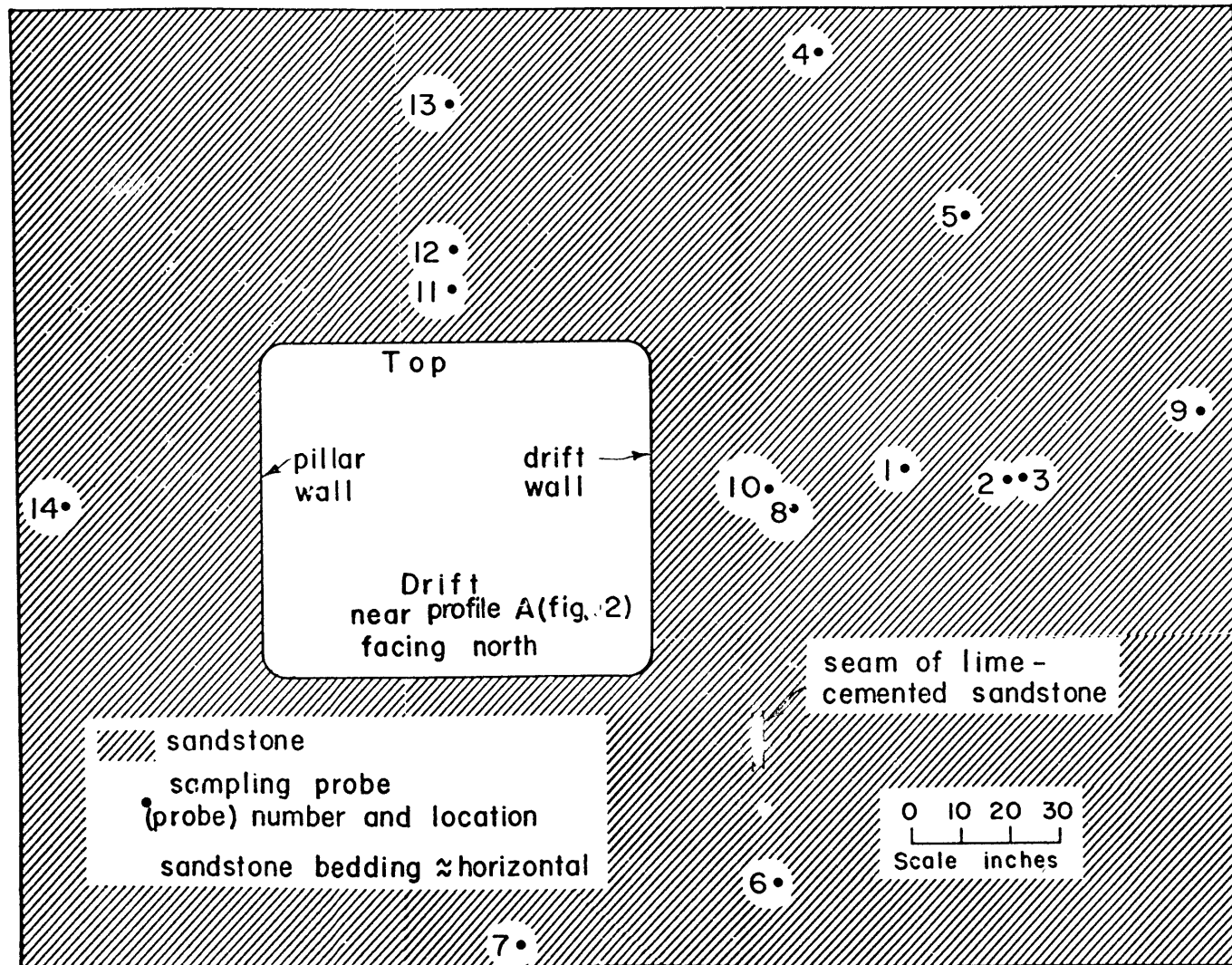


FIGURE 3. PROFILE OF SAMPLING SITES IN DRIFT OF 5702 TEST AREA

This precaution was taken since a significant portion of the air consumed in the foreman's room during overpressure experiments was believed to have left the room through the rock immediately surrounding the sealed door to the room. All bulkheads were constructed of a rigid plastic foam sprayed over wood.

Probes for sampling room air were mounted at two locations in each test area. Pitot tubes, used to estimate the volume rate of air input to the test area, were mounted within the air input hoses, 8 in. to 12 in. from the exhaust end of these hoses.

In both test areas, probes for sampling interstitial gas were placed in several directions with respect to the bedding planes in order to investigate effects which rock stratifications have on final Rn concentrations. These same probes were also used to measure overpressures transmitted from the test area into the interstices of the sandstone.

Although spatial location of the sampling probes is varied with respect to the mine test areas, their installation was similar in all cases and was as follows: using an air-driven  $3/4$  to  $1\frac{1}{2}$  in. dia. star drill, holes were drilled into the rock at selected sites. Holes in the foreman's room were drilled with the aid of water; holes in the 5702 area were drilled

dry. At each location a length of standard 3/16 in. OD (1/8 in. OD for holes less than 6 in. deep), 0.030 in. wall, copper tubing, 5 in. longer than the hole depth, served as the primary sampling probe. A tuft of glass wool which acted as a filter was fixed over the opening of one end of the copper tube; this end was inserted into the drilled hole. A 2 in. ball of crumpled paper, glass wool, or powdered sandstone was then packed into the hole to insulate the sampling end of the tubing from the subsequent sealant. A 1 in. plug of hardening sealant (e.g., expanding cement) was tamped into the hole and allowed to set. The hole was filled with a nonporous sealant [e.g., epoxy, common nonhardening roofing tar, water-emulsified asbestos]. In the case of holes where the sealant could not flow into the hole under force of gravity the sealant was forced in using a plunger arrangement similar to a grease gun with an extended greasing hose.

Lengths of 3/16 in. OD copper tubing were attached by short pieces of rubber pressure tubing to the test probes and pitot tubes and were strung from the holes through the wooden frames of the bulkheads which isolate the test area. This allowed sampling of interstitial gas, room air, and pressures without disturbing the areas. Differential manometers, oil (sp. gr. 0.826) or Hg, were used to measure the pressure

difference between the test area and the immediately adjacent unpressurized area.

Interstitial gas and room air samples were taken in 1-liter glass flasks. For sampling, a previously evacuated flask was attached by a short rubber tube to the selected sampling probe. The connecting valves were opened and the liter of gas was drawn into the flask.



### 3. Experimental Procedure

The exact program of each experiment is unique; however, the general pattern of sampling and data recording was similar in all cases.

Prior to the start of each experiment the test area was left unventilated for several days. The bulkheads were usually sealed. Two complete pre-experiment sets of interstitial gas and air samples were taken with a several-hour interval between the sets, the second set being taken shortly before commencing air input. With the start of an experiment, the desired pressure or air volume input rate was established as rapidly as possible, usually in a matter of minutes. This condition was then maintained, within conventional mine operational limits, for the duration of the experiment. During the course of an experiment, the applied parameter (e.g., volume rate of air input) rarely varied from the desired value by more than 10 percent.

Air was supplied from the mine compressed-air system except as noted. Interstitial gas and room air samples, and pressure readings in the adjacent rock, were taken at intervals dependent upon the specific nature of the experiment. Occasionally the 5702 test area was entered during experiments in order to measure relative humidity and Rn daughter-product

concentrations. Since the outer ring formed an air-lock these entries caused only slight perturbations in the pressure conditions of the area.

All gas samples were shipped in the 1-liter sampling flasks via Continental Trailways bus or Railway Express from Grants to Albuquerque. A transfer agent delivered the samples to the airport from which they were sent air express to the M.I.T. Radioactivity Center. Radon analyses of these samples were performed using  $\gamma$ -ray spectroscopy with a 4 in. x 4 in. NaI(Tl) crystal in a low background facility, or by  $\alpha$ -ray counting with a ZnS(Ag)-coated scintillation chamber. Normally each sample was analyzed twice.

When using the NaI(Tl) crystal for analysis, activity of the 0.61 Mev  $\gamma$  ray of RaC ( $\text{Bi}^{214}$ ) was measured. One-liter gas samples containing greater than  $10^5 \mu\mu\text{c}$  of Rn could readily be analyzed in this manner by presenting the sample, in its flask, to the crystal. The Rn content of a sample was determined by comparing the measured activity of the sample with the measured activity of a known amount of Rn in equilibrium with its daughter products. The Rn standard, contained in a routine glass sampling flask, was placed before the crystal in the same position as a gas sample. The Rn standard was obtained by deemanating a  $0.2 \times 10^{-6} \text{ c}$   $\text{Ra}^{226}$  standard into

the sampling flask when the Rn in the standard was in near-equilibrium with the Ra. Aged nitrogen was used for the deemanation.

For samples containing less than  $10^5 \mu\mu\text{c Rn/l ZnS(Ag)}$ -coated chambers (K-2) were used. This apparatus consists of a 0.5-liter lucite cylinder, coated on all internal surfaces with ZnS(Ag). A 5 in. photomultiplier tube views each of the two end plates. The PM tube signals are summed and fed into a cathode follower, then to an amplifier and discriminator, and finally to a scaler. To analyze a gas sample, the ZnS(Ag) chamber was evacuated and the one-liter gas sample was shared with this 0.5 liter chamber volume. Hence, about 1/3 of the sample entered the chamber. The portion of sample remaining in the flask was saved for a second analysis. For calibration, a  $10^{-9} \text{ c NBS Ra}^{226}$  standard was deemanated into a sampling flask. This known amount of Rn was then shared with the ZnS(Ag) chamber following the same procedure as in the routine analysis of a gas sample and the activity was monitored. Samples having Rn concentrations of about  $10^5 \mu\mu\text{c/l}$  were occasionally analyzed on both units to provide a cross-check on the calibrations.

Analysis of concentration of air-suspended Rn daughter products was performed at the mine by Mr. William Lane of

Kermac. A known quantity of air, between 10 and 30 cu. ft., was drawn through a membrane filter (e.g., Gelman AM-4). The alpha activity retained on the surface of this filter was measured and, knowing the time that had passed since the sample was taken, this activity was extrapolated to a concentration at the time of sampling. In this case one must assume a relative ratio of the short-lived Rn daughters, RaA ( $\text{Po}^{218}$ ), RaB ( $\text{Pb}^{214}$ ), RaC ( $\text{Bi}^{214}$ ), RaC' ( $\text{Po}^{214}$ ), present at time of sampling. The procedure has been described by D.A. Holaday et al. (H-1).

#### 4. Experiments

It was necessary first to learn whether overpressure could reduce the Rn flux into a chosen mine for periods of at least several days and then to determine empirically the quantitative relationship between Rn flux and amount of mine overpressure.

Initial experiments were performed in the foreman's room. These included 68 hours of continual 3.3 to 3.8 cm Hg overpressure, direct measurements of Rn flux through the foreman's room floor into the test area prior to and after overpressure (for this a previously developed flux can, was used; it is described in E-2), and an incremental variation of overpressure from 0.5 cm Hg to 3 cm Hg with each chosen pressure maintained for a 24 hour period.

Subsequent experiments were carried out in the 5702 area. These included 21 days of continual overpressure at 1 cm Hg, overpressure at 0.6 cm Hg for several days, ventilation of the test area by dilution only (i.e., no overpressure) and by overpressure combined with dilution, and finally, an underpressuring of the area. The underpressure test was to demonstrate the effect which a slight vacuum in a mine has upon the Rn characteristics of the mine. The results are of interest since mines are often ventilated by having an exhaust fan vent air from the mine and allowing fresh air, under the influence of the vacuum created by the exhaust fan, to enter the mine at another shaft.

## 5. Empirical Results and Interpretation

The results of all experiments related to this investigation of overpressure as a means of mine ventilation confirm the initial suppositions on which the project was based: moderate pressurization of the mine areas studied does induce a flow of air from the mine into the interstices of the surrounding rock; this flow of relatively fresh air purges and hence reduces the Rn concentration and concentration gradient in the interstices of rock adjacent to the pressurized area; such a reduction lowers the Rn flux into the mine. Since less Rn enters the mine area during overpressure, the amount of dilution air needed to attain a given Rn concentration in the mine atmosphere is less than that required with simple dilution techniques of ventilation. Underpressure does induce a convective flow of interstitial gas into the underpressured area. This flow results in a significant increase of the Rn flux into the mine.

Figures 12 and 13, (section 5b), and Table 1, (section 5c), present the essence of the effects which applied pressures have on the Rn and Rn daughter-product concentrations of the mine environments studied. Figures 12 and 13 describe as a function of applied pressure the Rn flux into the foreman's room and the 5702 area respectively. Figure 13 includes data for under- and overpressures. In both test areas, the sharp decrease in flux during overpressure as compared with zero

applied pressure is evident. The difference in the absolute magnitude of decrease in the flux between the foreman's room and the 5702 area, for a given overpressure, is attributable in part to the proximity of the foreman's room to a non-pressured haulageway and the presence of a shale lens overlying much of the 5702 area. For small applied pressures, underpressuring an area seems to increase the Rn flux as readily as overpressure decreases it (Fig. 13). Table 1 demonstrates the air economy of overpressure in the 5702 area. Using  $130 \text{ ft}^3/\text{min.}$  total rate of air change, the air Rn concentration at zero applied pressure is 6 times the air Rn concentration observed when  $130 \text{ ft}^3/\text{min.}$  air is supplied at 1 cm Hg overpressure. The air-suspended Rn daughter-product concentration during these 1 cm Hg overpressure conditions is 10 times lower than during zero applied pressure,  $130 \text{ ft}^3/\text{min.}$  air change rate. The larger decrease in Rn daughter-product concentration than Rn during overpressure is possibly the result of the daughters being carried convectively to the mine walls by the purging air as it enters the mine walls.

Error limits have not been assigned to the data because of uncertainties of precision and accuracy inherent in field investigations in which sample analysis is performed a great distance from the sampling site. The analysis of gas samples for Rn is estimated to be accurate to  $\pm 10$  percent. This value

is derived from observed variations of the order of  $\pm 5$  percent experienced between routine calibrations of the ZnS(Ag) chambers, and  $\pm 10$  percent experienced in calibrations of the NaI(Tl) crystal. These variations are consistent with source geometry reproducibility and electronic stability of the system. Moreover, inhomogeneities of the mine environment (e.g., variations in Ra content and permeability of the rock) make any one point of sampling only an indication of the general trend occurring at all similar locations (given depths, given angles within the mine wall). It is not surprising occasionally to find sampling sites that yield absolute Rn concentrations which are different from concentrations observed in similar sampling sites. No error is assigned to the data in an attempt to include the naturally anomalous sites in the general trend.

a. Radon Concentrations in Interstitial Gas.

The concentration of Rn in the interstices of rock surrounding a non-pressured mine increases within the first few feet of rock from the low value at the wall surface, equal to the mine air Rn concentration, to nearly the maximum concentration able to be supported by the emanating Ra in the parent rock. It is because of this very rapid rise in Rn concentration within the surface layers of a mine wall that the diffusion-



driven flux of Rn into a mine is high. The flux of a diffusing substance, it is recalled, is directly proportional to the concentration gradient of that substance. With the high specific flux of Rn across the wall-air interface, it is not surprising that a mine area unventilated even for a few hours accumulates high Rn and Rn daughter-product concentrations. The ability of overpressure to decrease significantly the interstitial Rn concentration in rock surrounding a mine is fundamental to its applicability as a possible ventilation mechanism.

Radon concentrations are listed as interstitial concentrations, i.e.,  $\mu\mu\text{c/l}$  of interstitial volume and not per liter of bulk rock.

The data in Fig. 4 pertaining to preoverpressure interstitial Rn concentrations demonstrate the high concentrations of Rn found in the interstitial gas of sandstone immediately surrounding the foreman's room. Within the surface 40 in. of rock, the Rn concentration closely approaches the maximum steady-state value of about  $6 \times 10^5 \mu\mu\text{c/l}$  for this rock.

In Figs. 4 and 5 it is seen that interstitial Rn concentrations at the depths studied within the surrounding medium decrease regularly with increasing overpressure. This is the result of convective transport (with air forced by overpressure

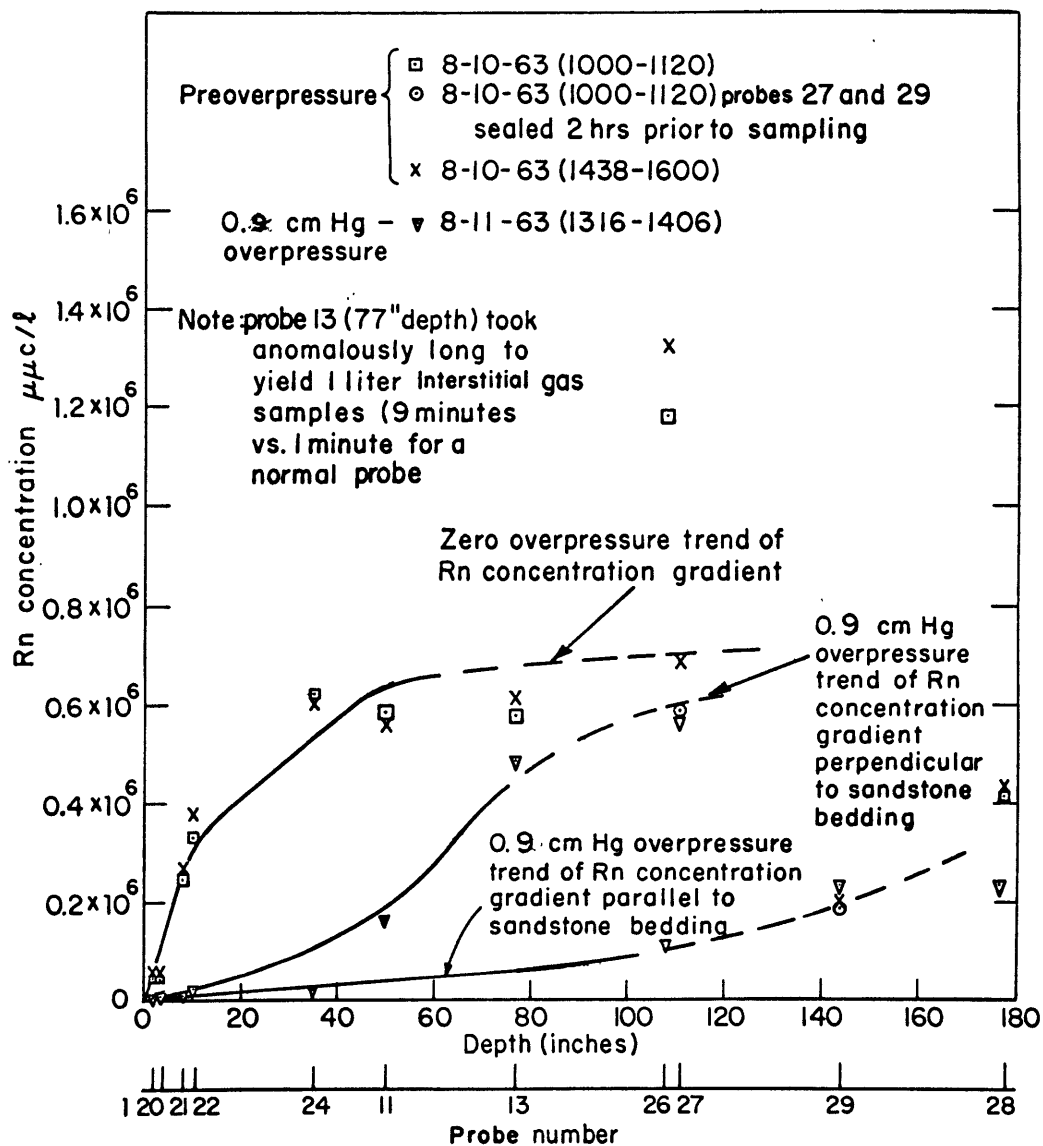


FIGURE 4. INTERSTITIAL RADON CONCENTRATION FOR PREOVERPRESSURE PERIODS AND FOR 0.9cm Hg OVERPRESSURE VS. DEPTH, FOREMAN'S ROOM

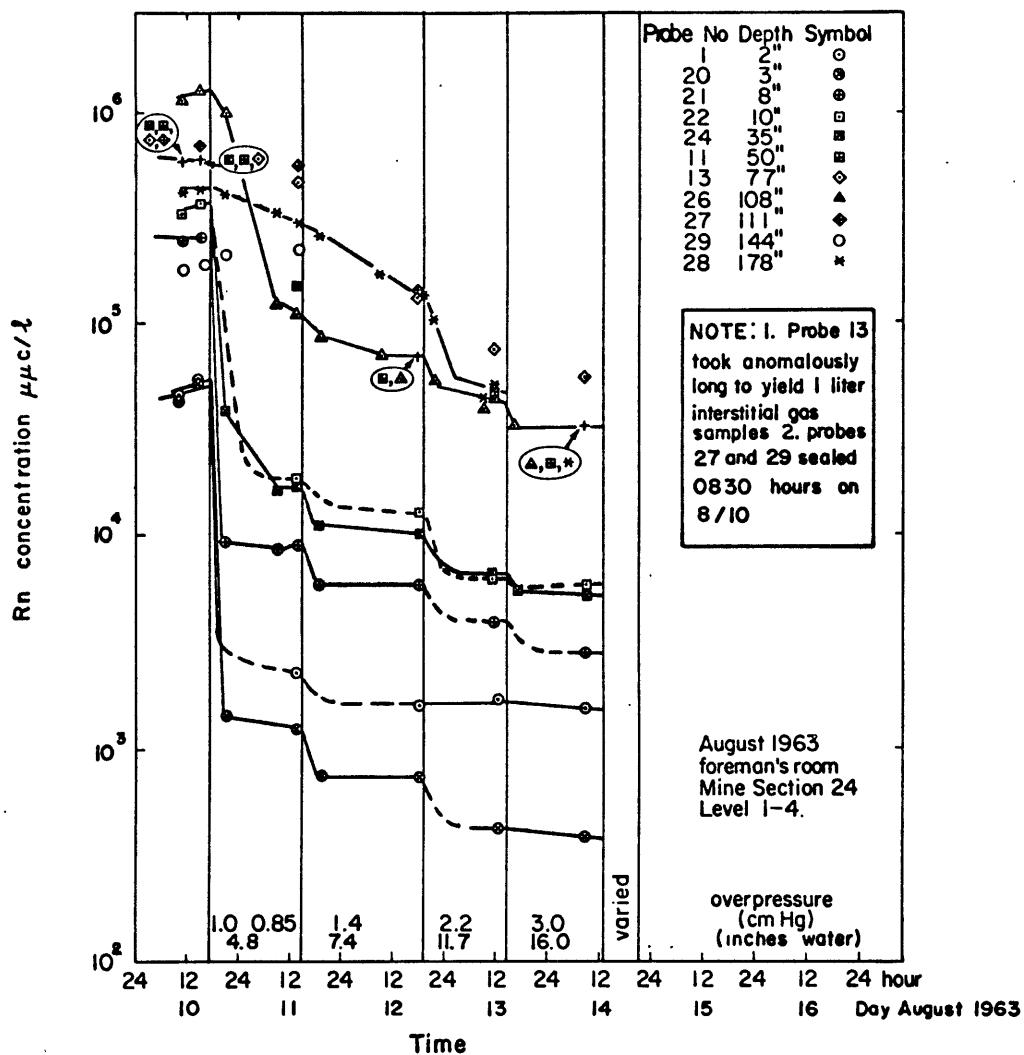
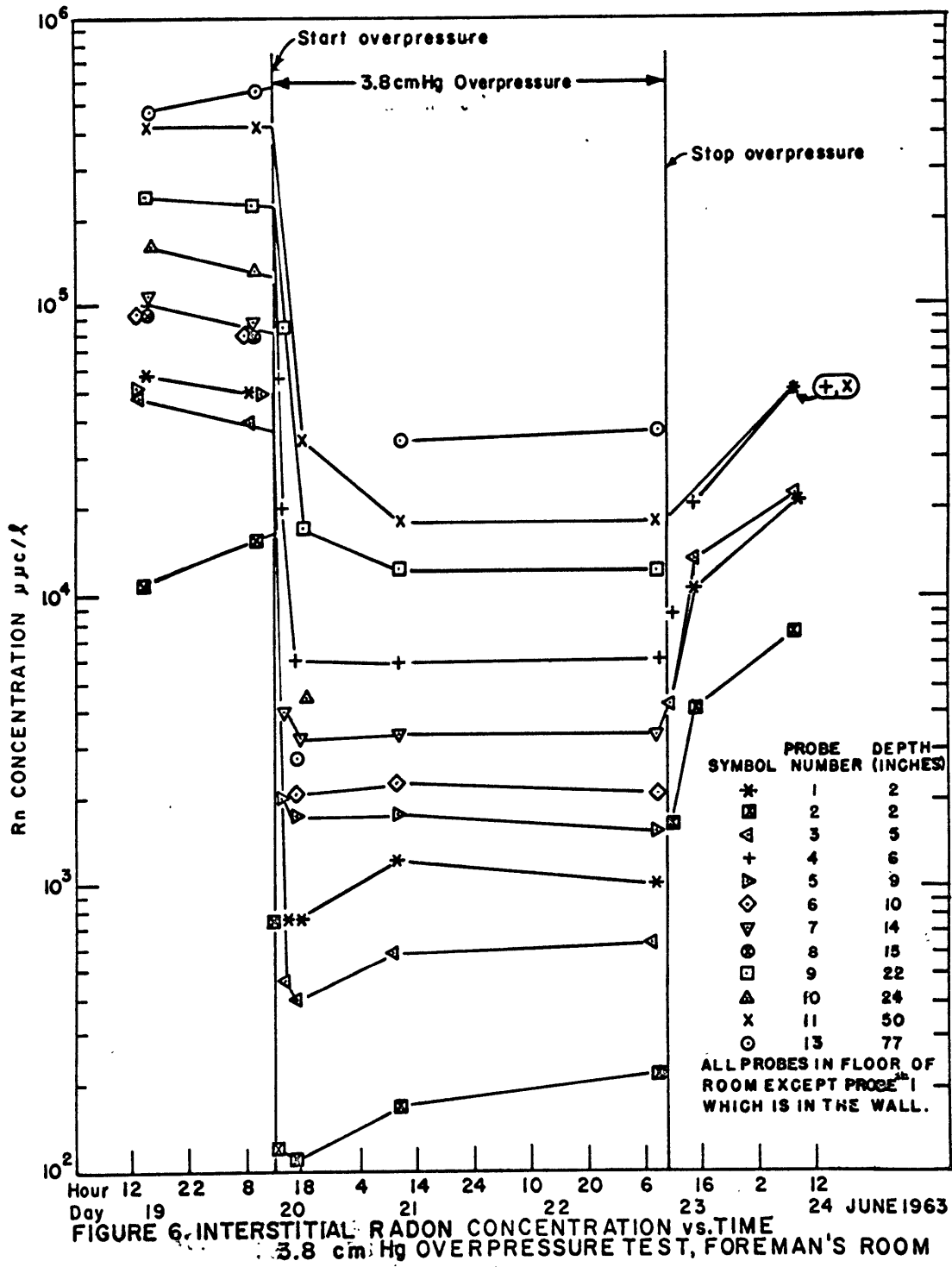


FIGURE 5. INTERSTITIAL RADON CONCENTRATION VS. TIME,  
VARIED OVERPRESSURE TEST, FOREMAN'S  
ROOM

into the rock) of Rn from the shallow interstices of the rock to greater depths. Observe that in the surface 3 feet of rock during 0.9 cm Hg overpressure the Rn concentration is 5 percent of the pre-overpressure concentration, a twentyfold decrease! The large depression of the concentration gradient during overpressure is indicative of a corresponding decrease in the Rn flux.

The rate at which an interstitial Rn concentration is reduced by overpressure is dependent upon the magnitude of overpressure, the depth under study, and the permeability of the rock. Generally, for overpressures of about 1 cm Hg and rock permeabilities similar to those of the test areas, the adaptation of Rn concentrations in the surface 30 in. of rock to the overpressure is completed within the first 24 hours of overpressure; for depths between 30 in. and 110 in. concentration changes are completed in less than 4 days. In both test areas, the major portion of the pressure-induced Rn changes in the surface 100 in. of rock occur within the initial 20 hours of overpressure.

That the interstitial Rn concentrations only gradually return to their pre-overpressure values following a period of overpressure was confirmed at the termination of the 68 hour, 3.8 cm Hg, overpressure test, foreman's room (Fig. 6). Twelve



hours after the removal of overpressure the Rn concentrations in the initial 20 in. of rock had returned to only 1/3 of their original values; at deeper levels the fraction of re-establishment was considerably less (e.g., at 50 in. the Rn concentration had reached 1/12 of its pre-overpressure level 12 hours after the end of overpressure). These results are consistent with observations in 5702 area.

The conception that during overpressure Rn will be held in rock interstices only to flow rapidly out at the termination of overpressure is, of course, unfounded. Radon that is held within the interstices will decay there and never enter the mine area. At the termination of overpressure the Rn returns at a rate solely determined by its rate of diffusion through rock.

The interstitial Rn concentration data for the 0.9 cm Hg overpressure test shown in Fig. 4 give an indication of the directional variation of rock permeability to convective flow of air. The sampling probes located most vertically below the foreman's room tend to suffer a smaller percentage decrease in Rn concentration than probes located to the side of the room. In the vicinity of the foreman's room, sandstone bedding is horizontal. Measurements of the permeability of rocks taken from the mine show that there is less resistance to air motion parallel to stratifications than perpendicular to the

stratifications. In the foreman's room, permeability of the rock parallel to the stratifications is about  $22 \times 10^{-9} \text{ cm}^2$  and perpendicular to the stratifications it is  $14 \times 10^{-9} \text{ cm}^2$ .

The 21-day overpressure test, 5702 area, demonstrated that at least for an environment similar to this test area, overpressure is an effective method of reducing interstitial Rn concentrations, and hence Rn flux, for periods equal to or greater than 21 days (Figs. 7-9). Once equilibrium overpressure conditions were established (taking 1 day for depths up to 30" and less than 4 days for depths up to 113") no varying trends in Rn flux or air consumption were observed for the duration of the experiment.

From data in Figs. 7, 8, and 9 (21 day overpressure test, 5702 area) it is at once apparent that there is an anomalous factor affecting sampling sites located above the 5702 area ceiling (5702 area, probes 4, 11, 12, 13). At all of these sites, with the possible exception of probe 11, the pre-overpressure Rn concentration is considerably lower than that experienced at sites of comparable depths but located at lower absolute elevations. More dramatic in these ceiling sites is the absence of change in interstitial Rn concentrations from the pre-overpressure values throughout the entire 21-day period of overpressure. A comparison of the pressures at the various

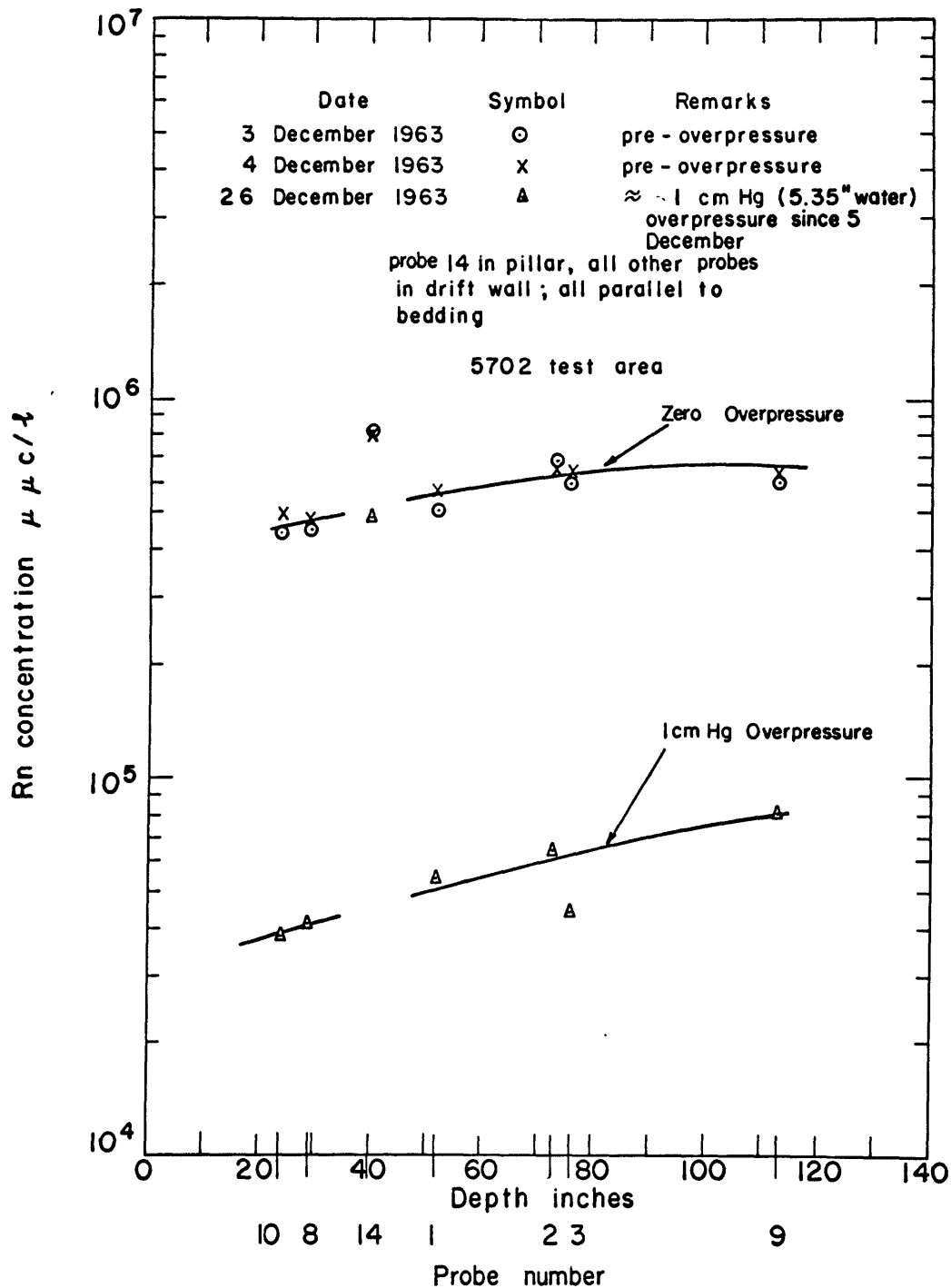


FIGURE 7. INTERSTITIAL RADON CONCENTRATION VS. DEPTH  
PARALLEL TO BEDDING  
21 Day overpressure test, 5702 area



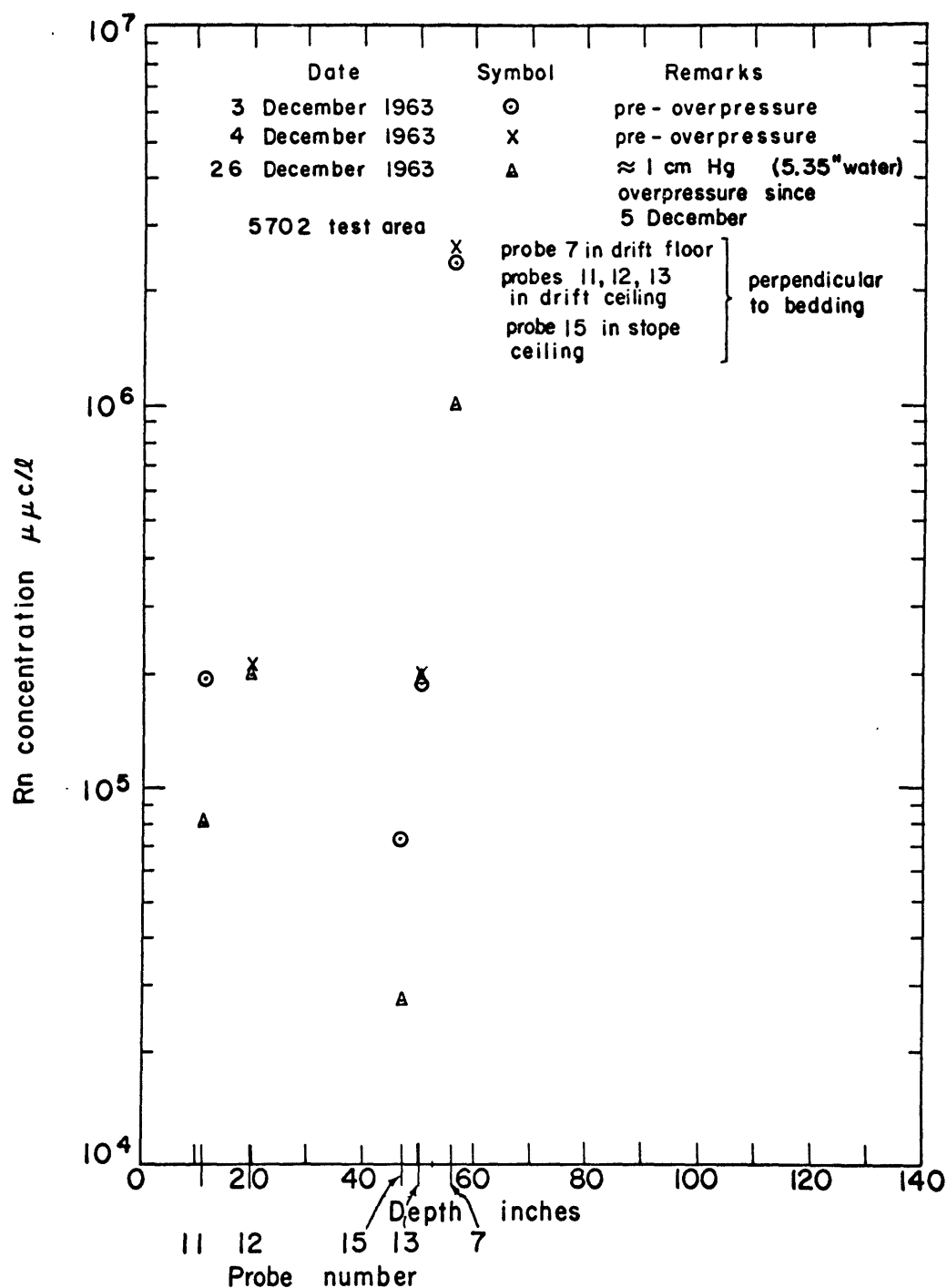


FIGURE 8. INTERSTITIAL RADON CONCENTRATION VS. DEPTH  
 PERPENDICULAR TO BEDDING  
 21 Day overpressure test, 5702 area

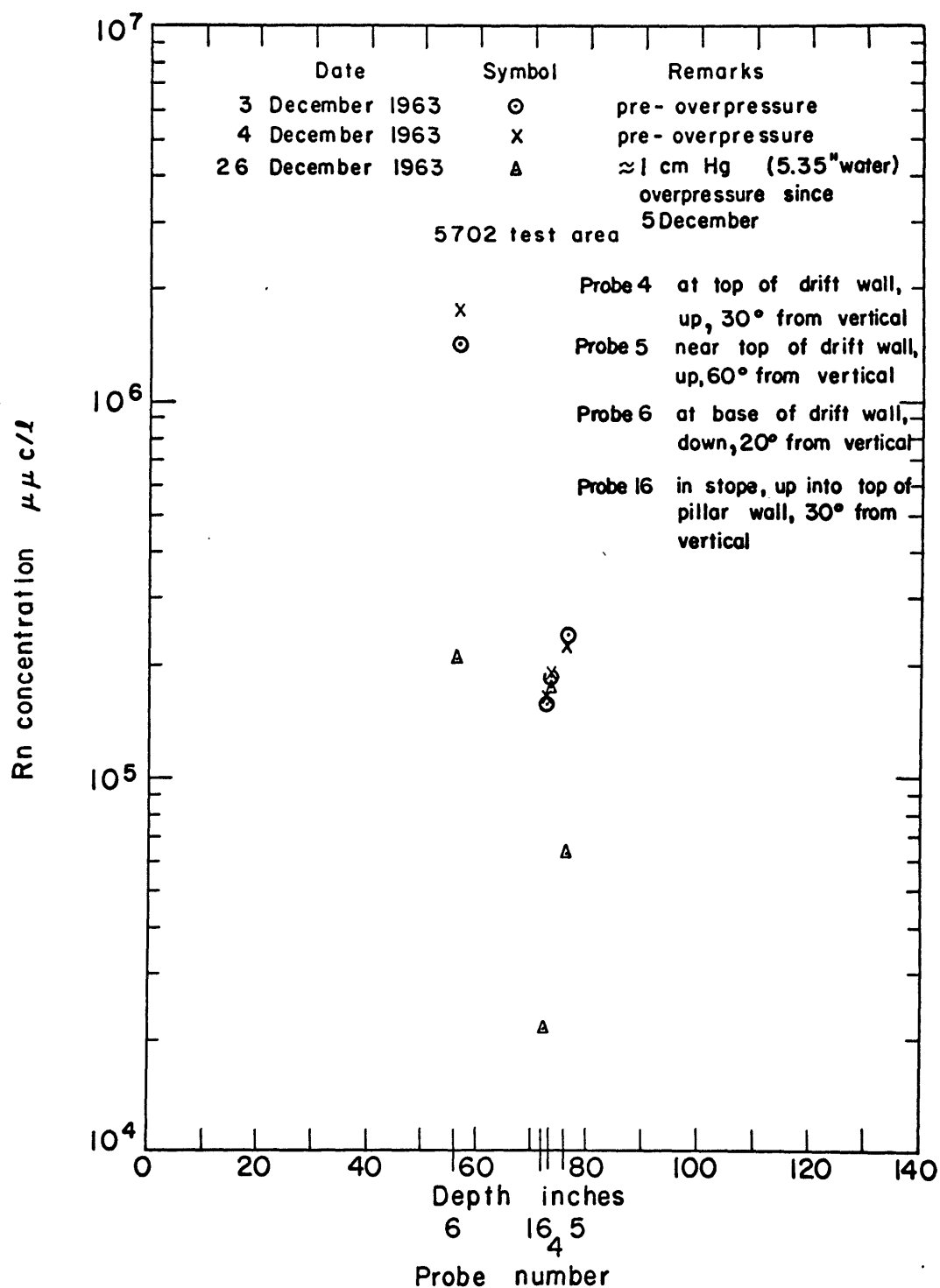


FIGURE 9 INTERSTITIAL RADON CONCENTRATION VS. DEPTH  
21 Day overpressure test, 5702 area

sampling probes with room pressure shows that probes located above the drift ceiling, regardless of depth, had pressures very similar to the room pressure (Fig. 10). For example, probe 4, 73 in. deep in ceiling, has a pressure only 0.08 cm oil below room pressure. At the same time, probe 2, 73 in. deep in wall, has a pressure of 1.40 cm oil below room pressure. The flow-inducing pressure gradient is much greater in the direction of probe 2. The interstices of the rock in this ceiling area had become pressurized. Because of the similarity of pressure between the rock interstices and the room there was little or no driving force (pressure gradient) to cause purging air to flow into the rock. A pressure gradient is essential to cause air flow. The volume of flow, for a given rock permeability, is proportional to the pressure gradient. A likely supposition was that the shale lens, visible some 60 ft. away in the stope where portions of the ceiling had fallen, extended over these test holes in the drift. Subsequent investigation indicated that this lens did extend above much of the 5702 area ceiling and for several hundred feet beyond the test area. Because the shale lens has an extremely low permeability, the air cannot easily pass through it. It also appears that the shale and a perched water table above it offer considerable resistance to the diffusion of Rn.

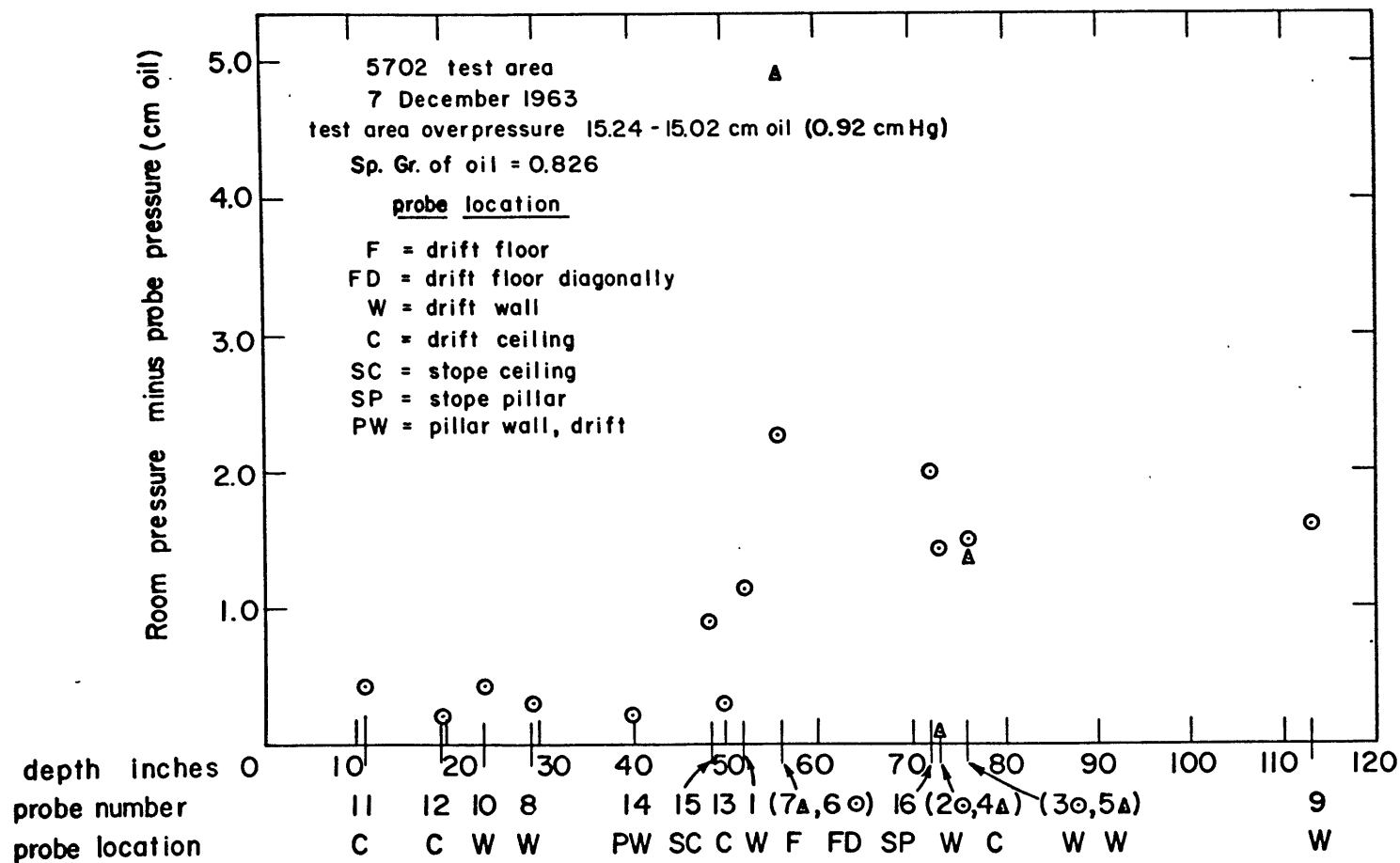


FIGURE 10. PRESSURE DIFFERENCE BETWEEN SAMPLING PROBE AND TEST AREA VS. DEPTH, 21 DAY OVERPRESSURE TEST, 5702 AREA

The low interstitial Rn concentrations experienced at sites above the drift ceiling indicate that a barrier is present which stops the diffusional flow of Rn from depth into the rock below the low-permeability lens. With the supply of Rn from depth blocked, the concentration becomes depleted. Since the Rn flux is proportional to the Rn concentration gradient, these areas will have a low Rn flux. Interestingly, effects cancel: the Rn-purging and hence flux-reducing air cannot enter the interstices of this area of rock because of the impermeable backing; however, this same impermeable backing reduces the flux by its very presence.

Figure 7 shows the tenfold decrease in the Rn concentrations measured parallel to rock bedding at depths between 24 in. and 113 in. when 1 cm Hg overpressure was applied. This indicates at least a tenfold decrease in the Rn flux into the mine atmosphere from the walls of the mine.

The one probe (probe 14, 40 in. deep) in a pillar surrounded entirely by pressurized air had slightly under a factor of two decrease in interstitial Rn concentration during overpressure. Because the pillar is surrounded by pressurized air, purging air entering the pillar can leave only through the top and bottom. This decreases the efficacy of purging.

Purging of interstitial gas in layers perpendicular to stratifications yielded a 2.5-fold decrease in Rn concentration

(Fig. 8, probes 7, 11, 15). If this is indicative of a 2.5 fold decrease in the interstitial Rn concentration gradient, the Rn flux into the mine from the floors and ceilings will be reduced during overpressure by a factor of 2.5.

Underpressuring a mine area that is located in a permeable rock environment establishes a system of pressures which increase from the low value in the mine to the normal atmospheric pressure at depth in the interstices of surrounding rock. Such a pressure gradient induces a flow of gas from the rock interstices into the mine.

Figure 11 describes differences in pressure between test probes in rock adjacent to the 5702 area and the 5702 area itself, during 0.43 and 0.27 cm Hg (2.3 and 1.4 inches water respectively) underpressure of the 5702 area. In all cases the pressure within the interstices of adjacent rock is greater than that of the 5702 area. The overpressure experiments have shown this rock to be permeable to the flow of air. Thus, existence of the pressure gradient establishes the fact that there is a convective transport of the interstitial gas within this region toward the underpressured area.

Although interstitial gas was not sampled extensively during the underpressure tests, the data obtained follow expected trends. Probes located at large depths ( where Rn

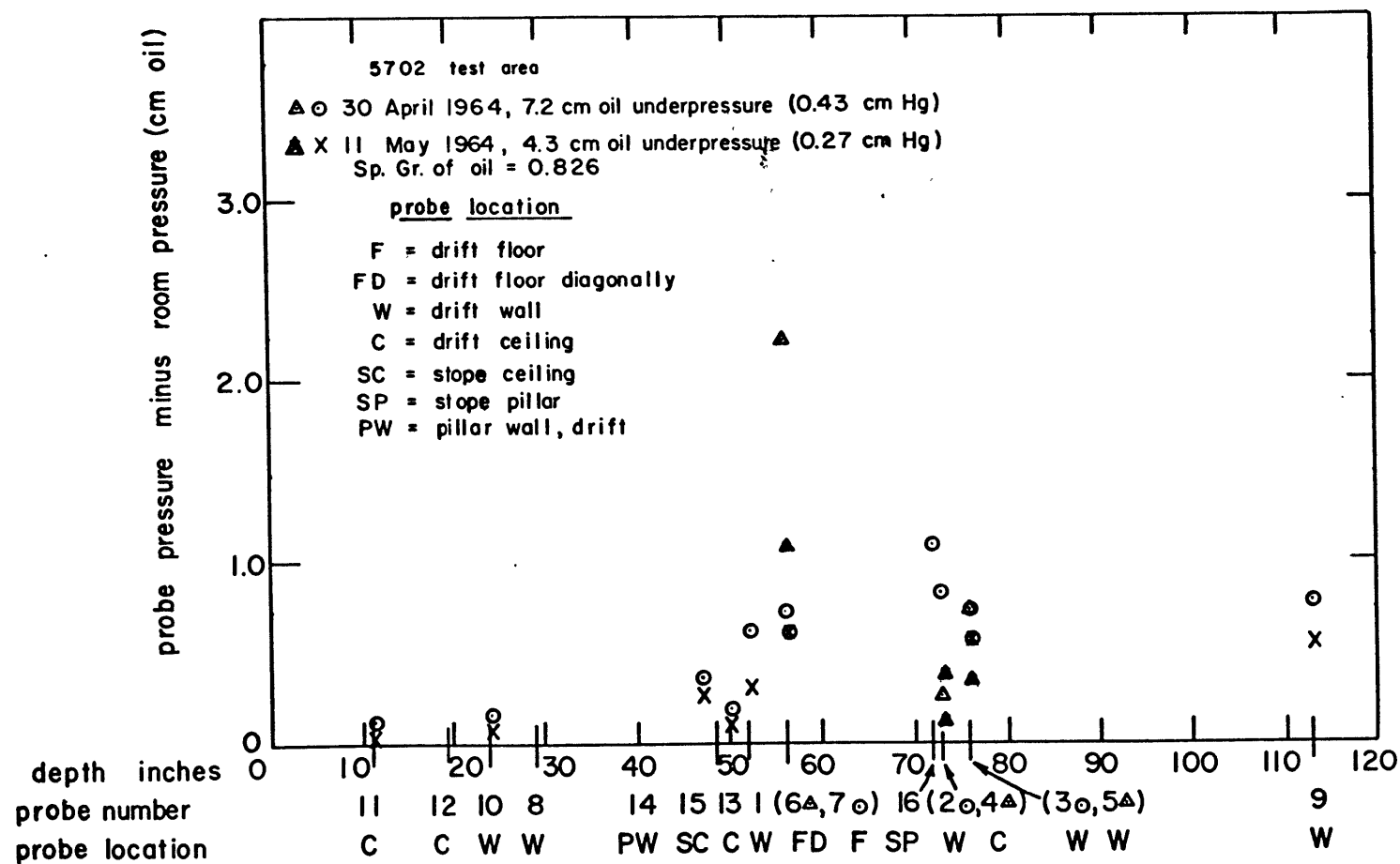


FIGURE II. PRESSURE DIFFERENCE BETWEEN SAMPLING PROBE AND TEST AREA VS. DEPTH, UNDERPRESSURE TEST, 5702 AREA

concentration during normal barometric conditions is constant regardless of increasing depth) show no change in concentration during underpressure even though there is a pressure difference between the probe and the 5702 area. The pressure decreases in the direction of the test area; flow is from depth into the area. Since in these deep regions the Rn concentration does not change with increasing depth, gas from depth flowing past these probes toward the test area has the same Rn concentration as the gas initially at these probes.

At intermediate and shallow depths significant increases in Rn concentration were observed during underpressure. During non-pressure condition, this region has its Rn concentration depleted by diffusion of Rn into the test area. During underpressure gas from greater depths, and hence higher Rn concentration regions, flows past these probes toward the test area increasing the local Rn concentration.

Sampling probes located in the ceiling of the 5702 area showed little or no equilibrium Rn concentration change during underpressure. This is attributed to the presence of the low-permeability shale lens overlying the area. Consistently probes located at elevations above the drift ceiling and hence near the shale lens, have pressures more similar to the 5702 area pressure than



probes located at comparable depths but lower absolute elevations (c.f., probe 4 vs. probe 2, probe 13 vs. probe 1, Fig. 11). The small pressure gradient indicates a reduced convective flow in this region.

A drop in the interstitial Rn concentration at several probes was observed on the first day of underpressure and at no other time during the underpressure experiment. The origin of this transient decrease is uncertain. It would be expected that with the establishment of underpressure, flow into the test area from the rock interstices would begin. This, as previously described, would increase shallow depth Rn concentrations. The initial decrease in Rn concentration may indicate an initial flow of Rn deficient air from a non-underpressured tunnel outside the test area. The closest non-underpressured area is 50 ft. from the sampling probes.

A study of the naturally occurring Rn concentrations as a function of depth shows that, for the locations sampled, concentration is not necessarily related to depth. Mine analyses have shown that large variations in the Ra content of rocks in the mine exist. When not in the immediate vicinity of a tunnel, Rn concentration in interstitial gas is dependent upon emanating Ra concentration in the rock.

b. Radon Flux.

Consistent with the previously described reduction of the interstitial Rn concentration gradient in rock adjacent to an overpressured area, the Rn flux into an overpressured area is depleted from its pre-overpressure level, the extent of the depletion being related to the magnitude of the actual overpressure. Figure 12 describes the total flux of Rn into the foreman's room as a function of overpressure. The empirical relationship shown indicates how very significantly the Rn flux is reduced for modest overpressures. The flux of Rn into the foreman's room with no overpressure is estimated from flux data gathered in June 1963, to be about  $4 \times 10^{-8}$  c/sec, nearly 20 times higher than flux during 1 cm Hg overpressure.

Figure 13 shows the total flux of Rn into the 5702 area as a function of overpressure and underpressure. Overpressure of 1 cm Hg produces a 5-fold decrease from the zero overpressure flux. This reduction, while not as extensive as the reduction experienced in the foreman's room, is still formidable. The 5702 area provided a more rigorous test of the overpressure principle as an application to general mine ventilation than did the foreman's room. This area is more distant from non-pressured areas than is the foreman's room, and a shale lens overlies much of the 5702 area ceiling. Proximity to a non-

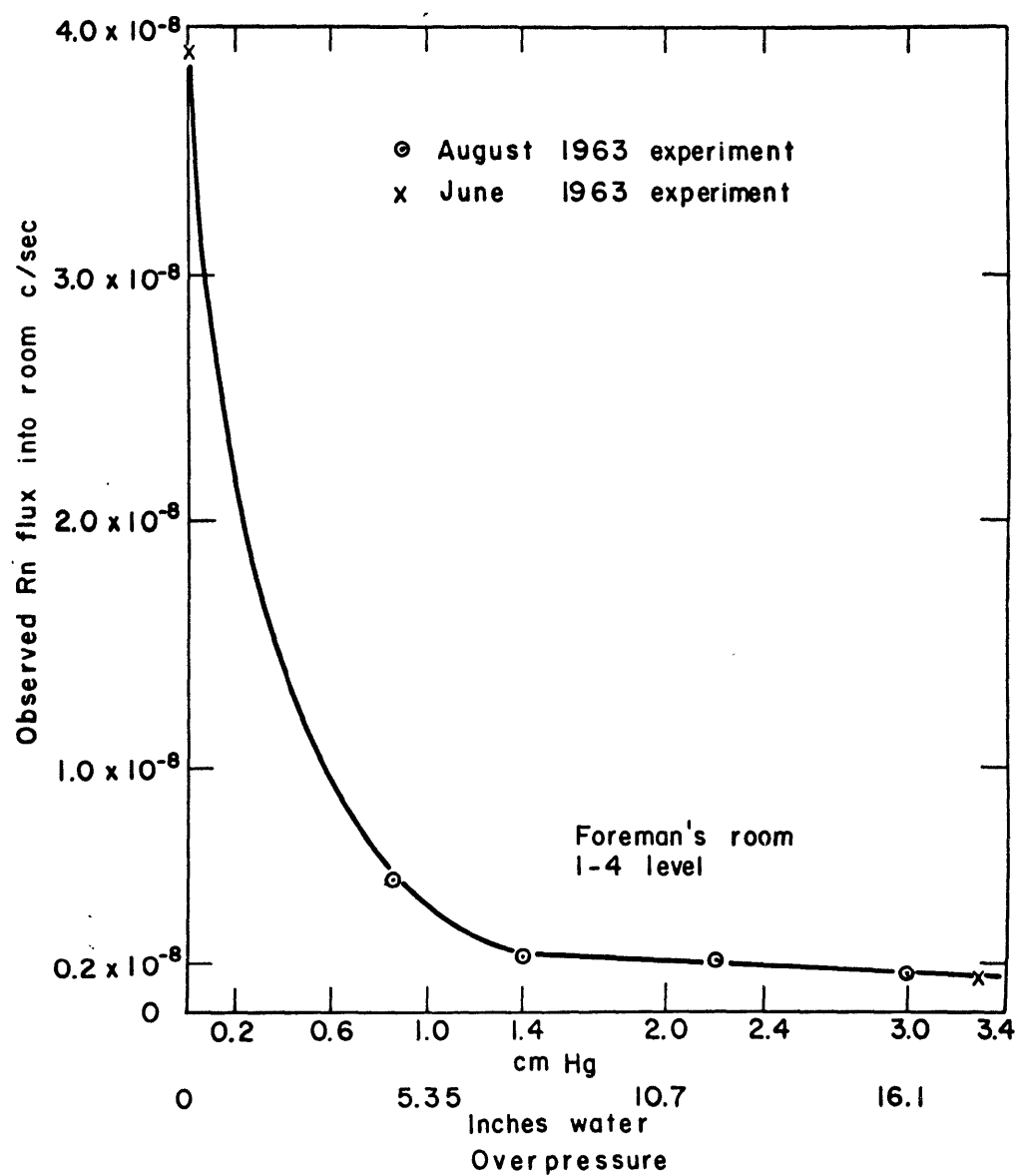


FIGURE 12. TOTAL RADON FLUX INTO FOREMAN'S ROOM VS. APPLIED OVERPRESSURE

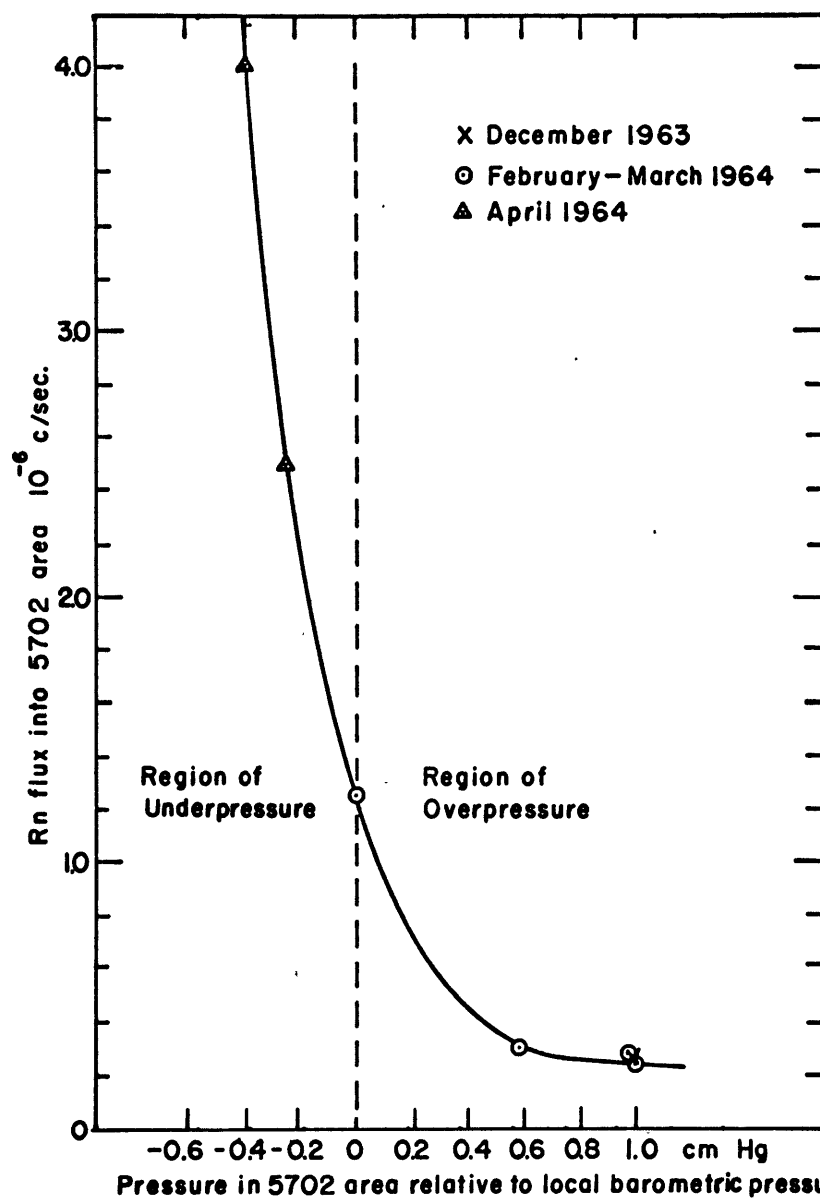


FIGURE 13. TOTAL RADON FLUX INTO 5702 AREA vs 5702 AREA PRESSURE RELATIVE TO LOCAL BAROMETRIC PRESSURE.

pressured area causes the pressure gradient in the rock adjacent to the test area to be steeper than if the area were surrounded by an infinite rock medium. The steeper pressure gradient increases the velocity of purging flow within the rock and hence allows a greater reduction in the interstitial Rn concentration. This is reflected in a greater decrease in Rn flux in areas of steep pressure gradients. Pressure gradients within rock adjacent to the foreman's room are 5 to 10 times steeper than in rock adjacent to the 5702 area. This reflects, in part, the difference in permeabilities and geometries of the two areas, and in part, the fact that one end of the foreman's room is separated from a non-pressured haulageway by only a few feet of rock.

The shale lens that extends over and beyond much or all of the 5702 ceiling prevented purging air from flowing efficiently into the ceiling rock. The Rn flux into the 5702 area from the ceiling surface was therefore not reduced as significantly as it might have been had no barrier been present. Fortunately, this low permeability lens itself reduces the Rn flux from this area permanently. The enclosed pillar in the 5702 area, which had a large surface area and pre-over-pressure Rn concentrations consistent with sites in the 5702 drift wall, could not be efficiently purged since it was sur-

rounded by pressured air.

For the pressure ranges studied, underpressure seems as efficient in increasing the Rn flux into a mine as overpressure is in reducing this flux. In the 5702 area, a 0.43 cm Hg underpressure results in a 3-fold increase in the Rn flux while a 0.43 cm Hg overpressure decreases the flux by about the same factor (Fig. 13). The mechanism of the increase in flux during underpressure is a convective introduction of interstitial gas, rich in Rn, to the test area. During 0.43 cm Hg underpressure in the 5702 area approximately 30 ft<sup>3</sup>/min. of interstitial gas are drawn into the area.

The total zero overpressure Rn flux into the 5702 area is approximately  $12.5 \times 10^{-7}$  c/sec. The corresponding flux into the foreman's room is  $4 \times 10^{-8}$  c/sec. This indicates an average Rn flux per unit area in the 5702 site of  $6.5 \times 10^{-14}$  c/cm<sup>2</sup> sec and in the foreman's room of  $4 \times 10^{-14}$  c/cm<sup>2</sup> sec. Since the Rn flux from the 5702 ceiling is lowered by the presence of a shale lens, the flux per unit area from the rest of the 5702 surfaces must be greater than the above value to compensate for this. The floor and walls of the 5702 stope contain moderately high grade uranium ore and hence are capable of producing a high Rn flux.

c. Room Air Radon Concentrations.

The reduction of Rn flux into a mine area during overpressure indicates that for a given rate of air consumption a lower ambient Rn concentration will be achieved if an area is overpressured than if the same area is ventilated by dilution techniques. During the 21 day, 1 cm Hg overpressure test, in the 5702 area the equilibrium room air Rn concentration was 4500  $\mu\mu\text{c/l}$ ; the rate of air consumption to maintain this overpressure was 100  $\text{ft}^3/\text{min}$ . Several weeks after the termination of overpressure the area was ventilated by dilution using 102  $\text{ft}^3/\text{min}$ . The equilibrium Rn concentration with dilution was 23,000  $\mu\mu\text{c/l}$ . This is 5 times the Rn level achieved with overpressure although the air consumption was essentially the same in both cases. To reduce the Rn concentration to 4500  $\mu\mu\text{c/l}$ , pure dilution would require at least 500  $\text{ft}^3/\text{min}$ .

Attempts to use dilution plus overpressure as a combined ventilation technique were hampered by the unavailability of large volumes of fresh air at the very remote location of the 5702 area. At 1 cm Hg, 30  $\text{ft}^3/\text{min}$ . of dilution air was added to the 100  $\text{ft}^3/\text{min}$ . pressurizing air. This was accomplished by having restricted vents at the bulkheads. The equilibrium air Rn concentration for these conditions was 3300  $\mu\mu\text{c/l}$ . Had no dilution occurred the Rn concentration would have been about  $3300 \times \frac{130}{100} = 4300 \mu\mu\text{c/l}$ . This is very similar to the results

of the previous 1 cm Hg overpressure test. The observation indicates that although there is more turbulence in the overpressured area as a result of the passage of additional dilution air, the Rn flux from the walls is not increased above the pure overpressure value. Additions of large volumes of Rn-contaminated diluting air (up to 1200 ft<sup>3</sup>/min.) during 1 cm Hg overpressure also did not increase the Rn flux. In fact one can expect a decrease in the flux when adding diluting air since the purging air which enters the rock interstices will have a lower Rn content.

For a given rate of air change an area will have higher room air Rn concentrations when it is underpressured than when the ventilation occurs at a pressure equal to or greater than local barometric pressure.

Pertaining to the following comments and Table 1, it is noted that for conditions of constant Rn flux (i.e., fixed pressure conditions) the air Rn concentration in the test area does not change in direct proportion to changes in the air dilution rate. With high dilution rates, the concentration of Rn is lowered and hence the amount of Rn in the test area that is "removed" by decay is decreased. Calculations must account for Rn removed by decay as well as by the convective displacement of the diluting air.



During 0.43 cm Hg underpressure in the 5702 area, a total of approximately  $30 \text{ ft}^3/\text{min.}$  of air was removed from the area. The air Rn concentration was  $170,000 \text{ } \mu\mu\text{c/l.}$  Had the 5702 area been ventilated at normal barometric pressure by  $30 \text{ ft}^3/\text{min.}$  of Rn-free dilution air, the equilibrium Rn concentration would have been about  $54,000 \text{ } \mu\mu\text{c/l.}$

Table 1 summarizes the effects which different pressure applications have on the Rn characteristics of the 5702 area. Data in lines 2, 4, and 5 of Table 1 are normalized for a total air change rate of  $130 \text{ ft}^3/\text{min.}$  moving through the test area.

An influence of barometric changes on air Rn concentrations and hence on Rn flux appears to be evident in areas ventilated by dilution. A change in barometric pressure is similar to an over- or under-pressuring of a mine. As pressure changes air enters or leaves the mine. The pressure in the free mine atmosphere changes more rapidly than the air pressure in the rock interstices. A pressure gradient is established and air flows through the surrounding rock until the pressure within the interstices is equal to the pressure in the mine. This interstitial passage of air performs the same function as it does during an applied pressure.

The following data were recorded while the 5702 area was ventilated by dilution. During the 12 hours prior to sampling on 24 January 1964, the barometer rose by 0.48 cm Hg (0.19 in.

TABLE 1.

Effect of Applied Pressures on Radon Characteristics of 5702 Area\*

Pressure of test area relative to local barometric pressure [cm Hg (in. water)]	Total rate of air change in test area (ft <sup>3</sup> /min)	Rn flux into test area (10 <sup>-7</sup> c/sec)	Air Rn con- centration (μμc/l)	Working*** level (WL, Rn daughter- product con- centration)
-0.43 (-2.3)	30	40	170,000	1300
-0.43 (-2.3)**	130	40	57,000	280
0	0	12.5	120,000	1200
0	130	12.5	18,000	90
1.0 (+5.4)	130	2.5	3,300	9

\* Volume of 5702 area = 150,000 ft<sup>3</sup>; location: mine section 26.

\*\* Data pertaining to 0.43 cm Hg underpressure and 130 ft<sup>3</sup>/min. air change are extrapolated from measurements taken at 0.43 cm Hg underpressure and 30 ft<sup>3</sup>/min. air change.

\*\*\* One working level (WL) is that concentration of Rn daughter products which would be in equilibrium with 100 μμc Rn/l.

Hg). The flux into 5702 area was measured to be  $8.2 \times 10^{-7}$  c/sec. During the 12 hrs. prior to sampling on 27 January barometric pressure rose 0.25 cm Hg (0.1 in. Hg). Measurements in the 5702 area indicate a Rn flux of  $9.5 \times 10^{-7}$  c/sec. The Rn flux into 5702 area on 13 February was  $7.7 \times 10^{-7}$  c/sec. Immediately prior to sampling barometric pressure was rising slowly; however, during the 20 hrs. prior to sampling the total rise in pressure was 0.38 cm Hg (0.15 in. Hg). Recall that the Rn flux into 5702 area during stable barometric conditions and no overpressure is  $12.5 \times 10^{-7}$  c/sec. All of the above-mentioned flux values are lower than this as a result of the rising barometric pressure prior to sampling.

When an area is overpressured the influence of barometric pressure changes on the Rn flux is not evident. Between 28 February and 1 March 1964, a period of 0.6 cm Hg overpressure, air Rn concentrations, and therefore Rn flux, remained constant to within a total spread of 10 percent. During this period barometric pressure had changes of twice the magnitude of those that produced the 40 percent changes in Rn flux observed during ventilation by dilution.

Pressure surges similar in amplitude to barometric pressure changes but of shorter periods are created within the mine by changes in the position of air-regulating doors. Such surges likely affect Rn flux into the mine in a manner quali-

tatively similar to barometric pressure changes.

Changes in barometric pressure may be the initial cause of more hazardous events in mines than changes in Rn flux. The major mine disasters of the world have taken place in the months between December and April (N-1). A compilation of all coal mine disasters in the United States having greater than 9 fatalities shows a frequency peak between November and April (B-1, H-2, M-1). These are the very months of the most dynamic barometric changes. Since many or most disasters involving more than a few men are the result of explosions, one may theorize that a falling barometer prior to an accident drew potentially explosive interstitial gases into the mine. Upon mixing with the oxygen in the mine, the gases became explosive and needed only to be ignited.

d. Radon Daughter-Product Working Levels and Radon-Radon Daughter-Product Disequilibria.

When concerned with mine ventilation, of particular interest is the concentration of the air born Rn daughter products: RaA ( $\text{Po}^{218}$ ;  $\alpha$ , 3.05 m), RaB ( $\text{Pb}^{214}$ ;  $\beta$ , 26.8 m), RaC' ( $\text{Bi}^{214}$ ;  $\beta$ , 19.7 m), RaC' ( $\text{Po}^{214}$ ;  $\alpha$ , 164 $\mu$ s). These nuclides, being solids, readily adhere to other solids and so tend to plate out in the bronchial tree when air containing them is drawn into the lungs. The resulting localized alpha-ray dose is experienced over sev-

eral years increases the probability of the development of a carcinoma (C-1, D-2). A reduction of the Rn concentration in air will lower the production rate of these suspended nuclides. A reduction of the ratio between the suspended Rn daughter products and Rn will further decrease the dose to the bronchial tree. Concentrations of the daughter products are listed in working levels (WL). One WL is the concentration of Rn daughter products that would be in secular equilibrium with  $100 \mu\mu\text{c Rn/l}$ .

In the 5702 area, the Rn daughter-product concentration during ventilation by  $102 \text{ ft}^3/\text{min}$ . dilution was measured to be about 120 WL; the Rn concentration was measured to be  $23,000 \mu\mu\text{c/l}$ . Thus with this rate of dilution, the Rn daughters are present at slightly greater than 50 percent of the equilibrium value with their Rn parent. On 10 March 1964, during 1 cm Hg overpressure,  $130 \text{ ft}^3/\text{min}$ . of air was consumed (including  $30 \text{ ft}^3/\text{min}$ . of dilution air). The room air Rn concentration was  $3300 \mu\mu\text{c/l}$ . The Rn daughter-product concentration was 9 WL. The daughter products are now approximately 25 percent of the concentrations which would be in equilibrium with their Rn parent. The air consumption was very nearly the same in both cases. This lower Rn daughter-Rn ratio during overpressure is perhaps indicative of a general convective sweeping of the daughters toward and onto the walls of the test area by air

entering the rock interstices.

e. Temperature, Relative Humidity, and Moisture.

Prior to the start of the 21 day, 1 cm Hg, overpressure experiment in the 5702 area the site was very damp. Portions of the stope ceiling had water dripping at a moderate rate; a test hole drilled 20 in. into the drift ceiling near profile A (Fig. 2) produced water at a very slow rate.

On 15 November, several weeks prior to overpressure, the area had a dry-bulb temperature of 63.5°F and a relative humidity of 96 percent. The pressurizing air dry-bulb temperature was 63°F and its relative humidity was 10 percent. This air is the normal source of compressed air for the entire mine.

On 7 December 1963, 2 days after the start of overpressure, and on 18 December, 13 days after the start of overpressure, the inner area was entered for inspection. On 7 December, relative humidity was 81 percent, dry-bulb temperature 61°F. The temperature outside the area was 65°F. On both days water was no longer dripping from the stope ceiling, and qualitatively, the area had dried up considerably as compared with the pre-overpressure condition.

The termination of water entering the stope from the ceiling is possibly related to the shale lens that overlies the stope and a layer of water (a perched water table) that

may be supported by this lens. Water will seep through the shale at a rate in part determined by the head of water above the shale. Since shale is such a low-porosity and low-permeability substance, the pressurized air may effectively retard this seepage of water. Water will accumulate above the shale. If the lens is of limited horizontal dimensions, the water will eventually spill over the edges of it; if the lens is large, the increase in water head may eventually allow the water to overcome the effect of the pressurized air below it, or the water head may be continuously relieved by seepage through a portion of the shale lens not overlying a pressurized area (i.e., a portion that is removed from mining operations). It is to be noted that in this case we are dealing with a perched water table supported by a low permeability lens. The hydrostatic head above this lens is minute as compared with the hydrostatic head of the total water table.

## 6. Analytic Description of Interstitial Radon Concentrations During Mine Overpressure

The transport and distribution of a substance, moving within any medium by diffusion only, is described by Fick's first and second laws of diffusion (F-1, J-1):

$$J = -D \nabla C \quad (1)$$

$$\frac{\partial C}{\partial t} = D \text{ lap } C \quad (2)$$

where  $J \equiv$  flux of diffusing substance

$D \equiv$  diffusion coefficient of the substance within  
the medium

$C \equiv$  concentration of diffusing substance

$\nabla \equiv$  gradient operator

lap  $\equiv$  Laplacian operator

When relating flux to concentration gradient it is essential to maintain consistent units. If working with interstitial concentrations, one must use a flux across exposed interstices and not across total soil surface. If working with flux across a total surface, concentrations must be amount per volume of bulk soil and not per volume of interstices.

The situation in sandstone interstices is more complex than the above equations. The rock is Ra-bearing; Rn is therefore continuously formed throughout the medium. Radon is also continually removed from the interstitial gas by radioactive



decay at a rate proportional to its concentration.

$$\text{rate of Rn decay} = \lambda C \quad (3)$$

where  $\lambda$  = decay constant for Rn,  $\lambda = \ln 2/\text{half-period}$  of Rn.

Taking these factors into account Eq. (2) is enlarged to:

$$\frac{\partial C}{\partial t} = D \text{ lap } C + \varphi - \lambda C \quad (4)$$

where  $\varphi \equiv$  a term accounting for interstitial production of Rn [see Eq. (23)].

When a mine is overpressured, a term accounting for the convective flow of gases must be introduced. In a porous medium, the rate of change in concentration due to convection is (S-1)

$$\frac{\partial C}{\partial t} = - \frac{1}{S} \text{div } (qC) \quad (5)$$

where  $S \equiv$  the porosity of the medium, i.e., the ratio of void volume to total volume.

$q \equiv$  the convective velocity.

$\text{div} \equiv$  divergence; in the cartesian xyz coordinate

$$\text{system div} \equiv \frac{\partial}{\partial x} + \frac{\partial}{\partial y} + \frac{\partial}{\partial z}$$

Equation (5) may be combined with Eq. (4) to yield a statement which heuristically accounts for Rn diffusion, convection, production, and decay:

$$\frac{\partial C}{\partial t} = D \text{ lap } C - \frac{1}{s} \text{ div } (qC) + \varphi - \lambda C = 0 \quad (6)$$

Setting Eq. (6) equal to zero gives the steady state case.

It is necessary to develop an expression which will describe  $q$  as a function of location within the rock surrounding a mine.

Macroscopically, the viscous flow of a homogeneous fluid (either compressible or incompressible) through a porous medium is described by the differential form of Darcy's law (S-1, M-3):

$$q = - \nabla \left( \frac{k}{\mu} P \right) \quad (7)$$

where  $q \equiv$  velocity of fluid within the bed (cm/sec)

$P \equiv$  pressure (g/cm sec<sup>2</sup>)

$k \equiv$  permeability of the bed (cm<sup>2</sup>)

$\mu \equiv$  viscosity of the fluid (poise = g/sec cm)

$\nabla \equiv$  gradient operator; in the cartesian xyz coordinate system:

$\nabla \equiv \vec{i} \frac{\partial}{\partial x} + \vec{j} \frac{\partial}{\partial y} + \vec{k} \frac{\partial}{\partial z}$ , where  $\vec{i}$ ,  $\vec{j}$ , and  $\vec{k}$  are the unit vectors.

The viscosity of the air may be assumed to be constant for the experimental conditions of constant temperature and only slight variation in the total pressure. This allows  $\mu$  to be taken outside the differential operator. The permeability of the sandstone environment, while assumed to be fixed in a

given direction, is not independent of direction. In a stratified sandstone, permeability parallel to the plane of stratification is greater than the permeability perpendicular to the plane of stratification. This directional dependence of  $k$  requires that  $k$  be operated on by  $\nabla$ . Equation (7) may be expanded:

$$q = -\frac{1}{\mu} \left( \vec{i} k_x \frac{\partial P}{\partial x} + \vec{j} k_y \frac{\partial P}{\partial y} + \vec{k} k_z \frac{\partial P}{\partial z} \right) \quad (8)$$

The component velocities parallel to the major axes are:

$$q_x = -\frac{k_x}{\mu} \frac{\partial P}{\partial x}; \quad q_y = -\frac{k_y}{\mu} \frac{\partial P}{\partial y}; \quad q_z = -\frac{k_z}{\mu} \frac{\partial P}{\partial z} \quad (9)$$

From Eq. (9) it is noted that the resultant velocity at any point is not necessarily in line with the resultant pressure gradient at that point.

The equation of continuity for the steady-state case having neither sources nor sinks is (S-2):

$$\text{div} (\rho q) = 0 \quad (10)$$

where  $\rho \equiv$  fluid density.

Under normal atmospheric conditions, the behavior of air differs only slightly from that of an ideal gas (W-1). For the conditions of the experiment (isothermal and small total pressure changes), one may assume an ideal relationship between density and pressure:  $\rho = GP$ , where  $G$  is a constant. Substitution of this into the steady-state solution of Eq. (10) yields:

$$\text{div } (Pq) = 0 = \frac{\partial Pq_x}{\partial x} + \frac{\partial Pq_y}{\partial y} + \frac{\partial Pq_z}{\partial z} \quad (11)$$

Substitution of Eq. (9) into Eq. (11) yields:

$$0 = \frac{k_x}{\mu} \frac{\partial [P(\partial P / \partial x)]}{\partial x} + \frac{k_y}{\mu} \frac{\partial [P(\partial P / \partial y)]}{\partial y} + \frac{k_z}{\mu} \frac{\partial [P(\partial P / \partial z)]}{\partial z} \quad (12)$$

But  $P \frac{\partial P}{\partial x} = \frac{1}{2} \frac{\partial (P^2)}{\partial x}$ ; therefore Eq. (12) reduces to:

$$k_x \frac{\partial^2 P^2}{\partial x^2} + k_y \frac{\partial^2 P^2}{\partial y^2} + k_z \frac{\partial^2 P^2}{\partial z^2} = 0 \quad (13)$$

If the permeability were equal in all directions, i.e., if

$k_x = k_y = k_z$ , Eq. (13) would reduce to Laplace's equation.

It is in fact possible, through a transformation of coordinates,

to reduce Eq. (13) to Laplace's equation.

$$\text{Let } X = \frac{x}{\sqrt{k_x/k_y}}, \quad Y = y, \quad Z = \frac{z}{\sqrt{k_z/k_y}}; \quad (14)$$

$$\text{then } \frac{\partial^2 P^2}{\partial X^2} + \frac{\partial^2 P^2}{\partial Y^2} + \frac{\partial^2 P^2}{\partial Z^2} = 0 \quad (15)$$

The initially anisotropic system has been transformed into an isotropic medium. The permeability of this medium can be shown to be equal to  $k_y$ , the permeability measured in the y direction of the "real world environment".

Developments most common in mines are stopes and drifts. A stope may be approximated by an oblate spheroid. A drift is approximated by an infinitely long elliptic cylinder. The derivation of a theoretical analysis of Rn distribution in both cases is very similar. Because the field data were obtained primarily in drift type environments, further theoretical

derivation will relate to elliptic cylinders.

Working in the transformed (isotropic) system Eq. (7) is expanded to (M-2):

$$q = -\frac{k}{\mu} \left[ \frac{1}{a(\cosh^2 u - \cos^2 v)^{\frac{1}{2}}} \left( \frac{\partial P}{\partial u} \vec{u} + \frac{\partial P}{\partial v} \vec{v} \right) + \frac{\partial P}{\partial Z} \vec{z} \right] \quad (16)$$

where:  $a$  is the distance from the focii of the ellipse to the center of the ellipse

$u$  is a series of confocal ellipses.

$v$  is a series of hyperbolas and varies from 0 to  $2\pi$ .

The relationship between the transformed cartesian coordinates  $X$ ,  $Y$ , and the elliptical coordinates  $u$ ,  $v$ , is

$$X = a \cosh u \cos v$$

$$Y = a \sinh u \sin v$$

For a given value of  $u$  and  $v$ ,  $P$  is constant regardless of  $Z$ .

Pressure is constant on any given ellipse ( $u$ ), regardless of angle ( $v$ ). Thus  $P$  is independent of  $v$  and  $Z$  and the  $\frac{\partial P}{\partial v}$  and  $\frac{\partial P}{\partial Z}$  terms in Eq. (16) are equal to zero.

The value of  $\frac{\partial P}{\partial u}$ , derived from solution of Eq. (15), Laplace's equation, in elliptical coordinates is given in Eq. (17)

$$\text{lap } P^2 = 0 = \frac{1}{a^2(\cosh^2 u - \cos^2 v)} \left( \frac{\partial^2 P^2}{\partial u^2} + \frac{\partial^2 P^2}{\partial v^2} \right) \quad (17)$$

From Eq. (17)

$$P^2 = Au + B \quad (18)$$

$$\frac{\partial P}{\partial u} = \frac{A}{2P} = \frac{P_2^2 - P_1^2}{2P} \cdot \frac{1}{u_2 - u_1} \quad (19)$$

where A and B are constants

$P_1$  and  $P_2$  are pressures at  $u_1$  and  $u_2$  :

Since applied overpressure is only a small fraction of the total pressure of the system, Eq. (19) may be accurately approximated by

$$\frac{\partial P}{\partial u} = \frac{P_2 - P_1}{u_2 - u_1} = R \quad (20)$$

For a given overpressure, Eq. (20) is constant. Let that constant be equal to R. This completes the derivation of the statement for interstitial convective flow.

Placing D, the diffusion coefficient, outside of the Laplacian operator in Eq. (6) implies that D is independent of direction. This, of course, cannot be the case for both the untransformed (non-isotropic permeability) and the transformed (isotropic permeability) systems. In fact D is probably somewhat directionally dependent in the natural system though less than the permeabilities would indicate. As will be observed shortly, the solution of Eq. (6) is not significantly dependent upon the diffusion term. The solution is facilitated by keeping D out of the Laplacian.

Using Eq. (16) and Eq. (20), Eq. (6) may now be expanded into elliptical cylindrical coordinates:

$$\begin{aligned} & \frac{D}{a^2 (\cosh^2 u - \cos^2 v)} \left( \frac{\partial^2 C}{\partial u^2} + \frac{\partial^2 C}{\partial v^2} \right) + \\ & + \frac{k R}{s \mu a^2 (\cosh^2 u - \cos^2 v)} \frac{\partial C}{\partial u} + \varphi - \lambda C = 0 \end{aligned} \quad (21)$$

Note that while  $P$  does not have  $v$  dependence,  $C$  does have dependence on  $v$ .

The interstitial Rn production term,  $\varphi$ , is normally assumed to be constant and is conventionally measured by determining the interstitial Rn concentration in rock at depths where concentration becomes constant with depth (W-2). The Rn production is then just equal to the rate at which Rn is decaying.

$$\varphi = \lambda C_{\infty} \quad (22)$$

where  $C_{\infty}$  is the Rn concentration at large depths.

Actually the rate at which Rn emanates from the individual rock particles into the rock interstices appears to be a function of the Rn concentration in the interstices. Measurements of the Rn production rate in several rock samples taken from the test areas revealed that when the interstitial Rn concentration is maintained for long periods of time at a low level ( $< 10 \mu\mu\text{C/l}$  of pore), the interstitial production rate

of Rn is 2 to 3.7 times greater than the interstitial production rate when the Rn concentration approaches  $C_{\infty}$ .

The prolonged low interstitial Rn concentration was achieved by continually passing nitrogen ( $N_2$ ) through a rock sample. The velocity of the  $N_2$  within the rock was about 5 cm/min. Lower velocities were not used due to the difficulty in maintaining, at a constant value, sufficiently small pressure gradients across the rock samples. During 1.4 cm Hg overpressure in the foreman's room the velocity of the air as it flows through the surface layers of rock is about 3 cm/min. However this velocity rapidly decreases as the air flows further into the rock. If on the wall of a 10 ft. diameter tunnel the velocity of flow is 3 cm/min., 10 ft. into the wall the velocity is 1 cm/min., and 30 ft. into the wall the velocity is only 0.4 cm/min. or 0.8 ft/hr. Radon production in the low Rn environment was calculated as the Rn concentration in the effluent  $N_2$  times the volume rate at which the  $N_2$  was passing through the rock.

A high interstitial Rn concentration was achieved by sealing the rock and allowing Rn to accumulate until it reached near-equilibrium with its  $Ra^{226}$  parent. The interstitial gas was then sampled and the production rate estimated as production rate equaling decay rate [Eq. (22)].



That the interstitial production rate of Rn is higher in regions of low interstitial Rn concentration than in regions of high Rn concentration appears logical. When interstitial Rn concentration is high there is a smaller difference between the Rn concentration in the rock particle and the Rn concentration in the pore than when the interstitial Rn concentration is low. This implies a reduced Rn flux into the interstices from the particle, and hence a reduced interstitial Rn production rate, in regions of high Rn concentration.

A consideration of Fick's first law of diffusion (F-1, J-1), which states that the diffusion-driven flux is proportional to the concentration gradient in that region, indicates that a first approximation of this variable interstitial Rn production rate,  $\phi$ , is linearly dependent on the local interstitial Rn concentration,  $C$ . This approximation must fulfill the empirically determined boundary conditions: in regions of high Rn concentration  $\phi \rightarrow \lambda C_{\infty}$ ; and, in regions of low Rn concentration  $\phi \rightarrow E\lambda C_{\infty}$ , where  $E$  is the empirical constant, greater than 1, that states the increase of the interstitial production rate in low Rn regions over the production rate in high Rn regions. These requirements are met by:

$$\phi = \lambda [EC_{\infty} - (E - 1)C] \quad (23)$$

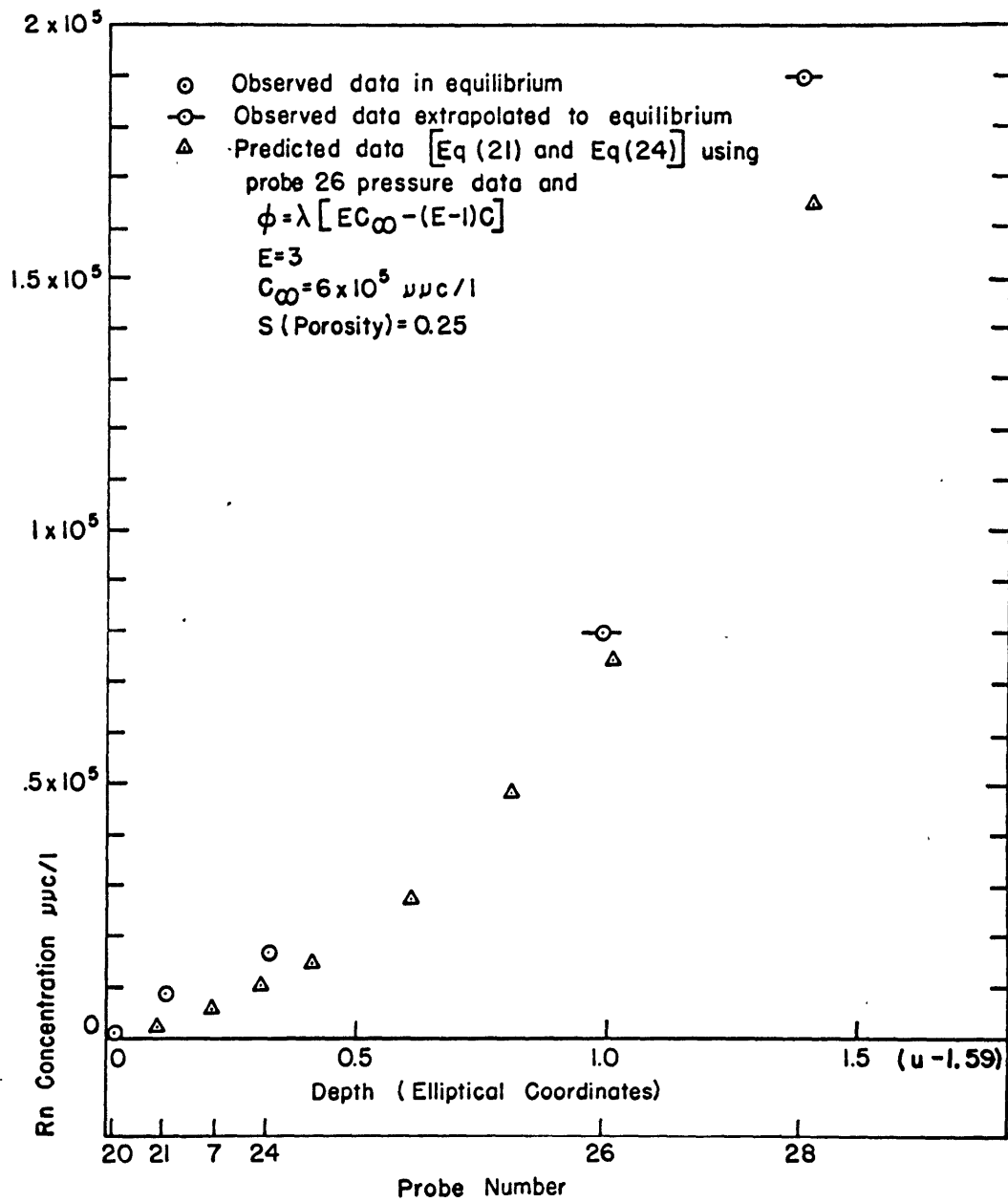
For rock types of the 5702 area and the foreman's room the value of  $E$  is between 2 and 3.7. Equation (23) may be substituted directly into Eq. (21).

Equation (21) does not have an analytic solution. Numerical solution demonstrates that omission of the diffusion term affects the value of the solution by less than 5% to depths greater than 16 feet within the wall. This is not surprising; diffusion transport is normally very small compared even to weak convective influences. Omitting the diffusion term in Eq. (21) allows this equation to be solved analytically. The solution is

$$C = C_{\infty} + F \exp \left[ \frac{\lambda s E}{k R} \mu a^2 \left( \frac{u}{2} + \frac{1}{4} \sinh 2u - u \cos^2 v \right) \right] \quad (24)$$

where  $F$  is a constant determined by the  $Rn$  concentration on the wall of the tunnel.

The solution to Eqs. (21) and (24) with  $E$  equal to 3 and the convective term based on pressure data observed during 0.9 cm Hg overpressure in the foreman's room is presented in Fig. 14. Included in this figure for comparison are interstitial  $Rn$  concentrations observed during 0.9 cm Hg overpressure. Similar data are presented in Fig. 15 for the case of 1.4 cm Hg overpressure. The agreement between theory and observed data is encouraging especially when one considers the many approximations necessary in relating an analytic solution to field data.



COMPARISON OF OBSERVED AND PREDICTED INTERSTITIAL RADON CONCENTRATIONS VS DEPTH, 0.9 cm Hg OVERPRESSURE, FOREMAN'S ROOM

FIGURE 14.

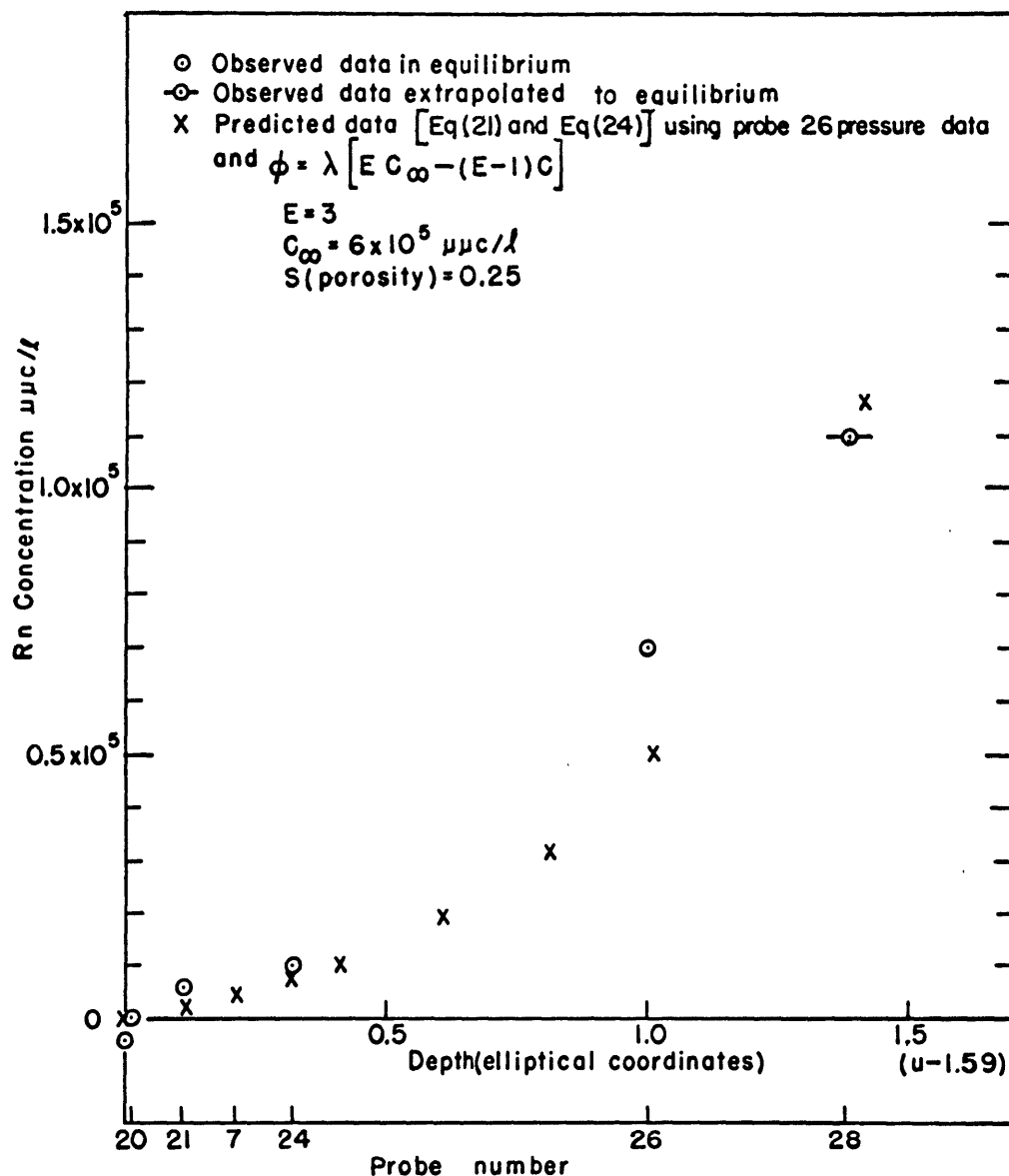


FIGURE 15. COMPARISON OF OBSERVED AND PREDICTED INTERSTITIAL RADON CONCENTRATIONS vs DEPTH ; 1.4 cm Hg OVERPRESSURE FOREMAN'S ROOM

It is noted that the theory tends to fall slightly below the observed points. An empirical factor is very probably necessary in the convective term of Eq. (6). At any given location the Rn concentration in the moving air is likely not the average Rn concentration of all interstitial air in that portion of rock. Although, on a microscale, flow through a porous medium is non-laminar, there still exists a stagnant layer of air surrounding each soil particle. It is in this very boundary layer that Rn is introduced into the system. In addition, the rate of purging flow through pores oriented perpendicularly to the mainstream will be small or nonexistent. Radon will leave these stagnant air bodies by diffusion into the moving air stream. As observed in the solution of Eq. (21), Rn transport by diffusion is much less effective than the convective transport. Thus a high Rn concentration is able to exist in these non-purged pores and the amount of Rn removed from a given volume of rock by purging air is actually less than the amount indicated by the convective term,  $\frac{1}{s} \text{div} (qC)$ , of Eq. (6) where C is the average interstitial Rn concentration.

Other workers (E-1, K-1) consistently report dispersion of concentration fronts passing through porous media. This is attributed to varying velocities of the moving stream within the porous medium. De Josselin de Jong (D-1) states that dispersion of a concentration front in the direction transverse

to the main flow may be 6 to 8 times smaller than dispersion in the longitudinal direction. This is indicative of greatly reduced flow through pores oriented perpendicularly to the general flow pattern.

Experiments in the laboratory have shown that the efficiency with which air flowing through the interstices of a rock removes  $R_n$  from these interstices decreases with increasing velocity. This indicates that, at any given velocity, the effectiveness with which the purging air removes interstitial  $R_n$  is less than the theoretical maximum.

Thus the heuristic approach of Eq. (6) appears to be inadequate. The variable approximation of the production term with  $E = 3$  partially satisfies the empirical data. A coefficient of about 0.9 modifying the convective term to account for the incomplete efficiency of the purging air will make the theory closely match the observed data.

## 7. BIBLIOGRAPHY

- B-1 Boyer, R.F., "Coal Mine Disasters, Frequency by Month", Science 144, 1447 (19 June 1964).
- C-1 Chamberlain, A.C., and E.D. Dyson, "The Dose to the Trachea and Bronchi from the Decay Products of Radon and Thoron", Brit. J. Radiol. 29, 317 (1956).
- D-1 de Josselin de Jong, G., "Longitudinal and Transverse Diffusion in Granular Deposits", Trans. Am. Geophys. Un. 39, 67 (1958).
- D-2 de Villiers, A.J., and J.P. Windish, "Lung Cancer in a Fluorspar Mining Community, I. Radiation, Dust, and Mortality Experience", Brit. J. Ind. Med., 21, 94 (1964).
- E-1 Eriksson, E., "A Note on the Dispersion of a Salt-Water Boundary Moving through Saturated Sand", Trans. Am. Geophys. Un. 39, 937 (1958).
- E-2 Evans, R.D., H.W. Kraner, and G.L. Schroeder, Edgerton, Germeshausen and Grier, Inc., Report B-2516, 6 December 1962.
- F-1 Fick, A., Pogg. Ann. 94, 59 (1855).
- H-1 Holaday, D.A., D.E. Rushing, R.D. Coleman, P.F. Woolrich, H.L. Kusnetz, and W.F. Bale, "Control of Radon and Daughters in Uranium Mine and Calculations on Biologic Effects", U.S.P.H.S. Publication 494 (1957).
- H-2 Hosler, Charles L., "Atmospheric Surface Pressure Related to Coal Mine Explosions", Trans. Am. Geophys. Un. 29, 607 (1948).
- J-1 Jost, W., Diffusion in Solids, Liquids, Gases, Academic Press, New York, 1960.
- K-1 Kaufman W., and G. Orlob, "An Evaluation of Ground Water Tracers", Trans. Am. Geophys. Un. 37, 297 (1956).
- K-2 Kraner, H.W., G.L. Schroeder, R.D. Evans, and A.R. Lewis, "Large Volume Scintillation Chamber for Radon Counting" Rev. Sci. Instr. 35, 1259 (1964).

- M-1 McIntosh, C.B., "Atmospheric Conditions and Explosions in Coal Mines", Geograph. Rev. 47, no. 2, 155 (1957).
- M-2 Moon, P., and D.E. Spencer, Field Theory Handbook, Springer-Verlag, Berlin, 1961.
- M-3 Muskat, M., Flow of Homogeneous Fluids Through Porous Media, McGraw-Hill Book Co., New York, 1937.
- N-1 New York Times, "249 German Miners Dead, 146 Missing in a Blast", 8 February 1962, p. 1, col. 8.
- S-1 Scheidegger, A.E., The Physics of Flow Through Porous Media, Macmillan Co., New York, 1960.
- S-2 Sokolnikoff, I.S., and R.M. Redhaffer, Mathematics of Physics and Modern Engineering, McGraw-Hill Book Co., New York, 1958.
- W-1 Waller, W.H., W.K. Lewis, W.H. McAdams, and E.R. Gilliland, Principles of Chemical Engineering, McGraw-Hill Book Co., New York, 1937.
- W-2 Wilkening, M.H., and J.E. Hand, "Radon Flux at the Earth-Air Interface", J. Geophys., 65, no. 10, 3367 (1960).



## APPENDIX

## 8. Experimental Installations

Figures 16-19 and Table 2 describe the location in the two test areas of the sampling probes not shown in the main body of this work. Experiments in the foreman's room were performed with two sets of sampling probes. The set shown in Fig. 16 and described in Table 2 was used in the first experiment (June 1963); the second experiment (August 1963) employed the probes shown in Figs. 1 and 17.

Figures 3, 18, and 19 are detailed areas of locations included in Fig. 2, a general description of the 5702 area. Note that in both areas sampling probes are located in several directions with respect to the test area. This permitted a measure of the effect which the bedding planes have on the motion of purging air and thus on the final distribution of Rn within rock adjacent to the test area.

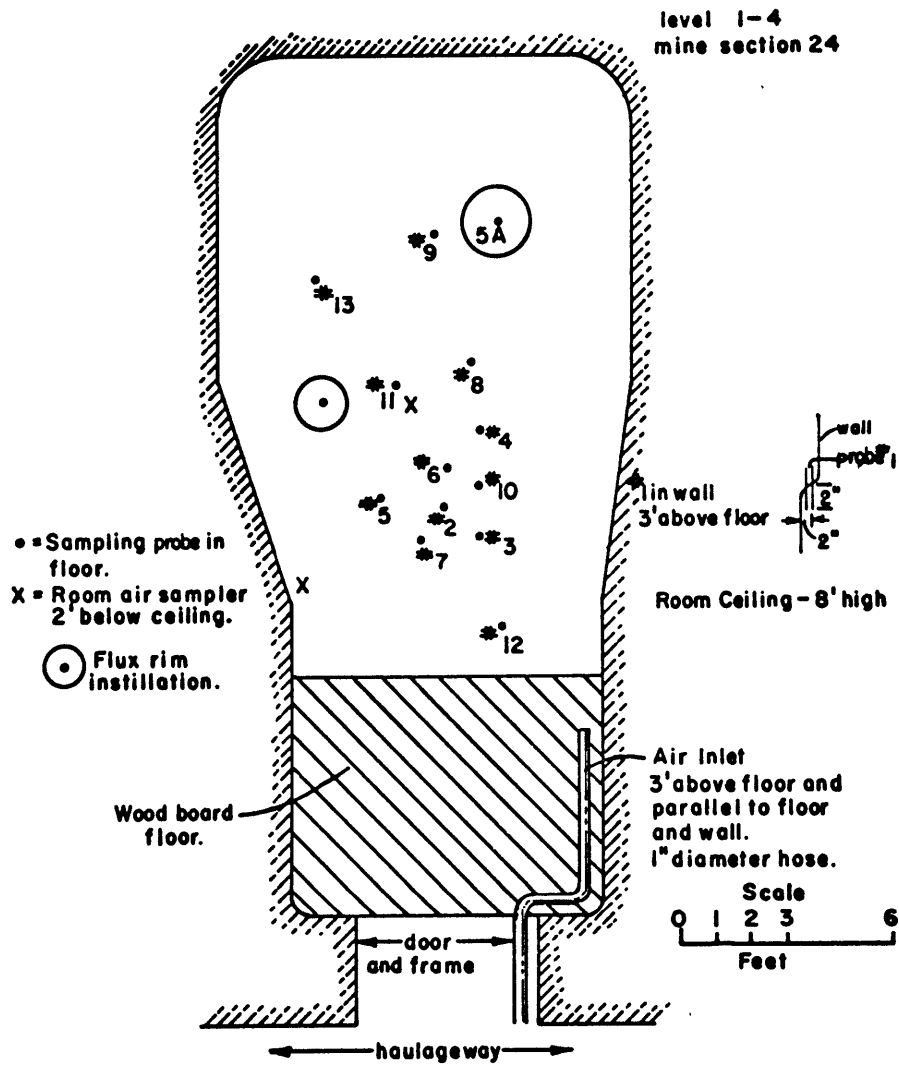


FIGURE 16. PLAN VIEW OF SAMPLING INSTALLATION AT FOREMAN'S ROOM

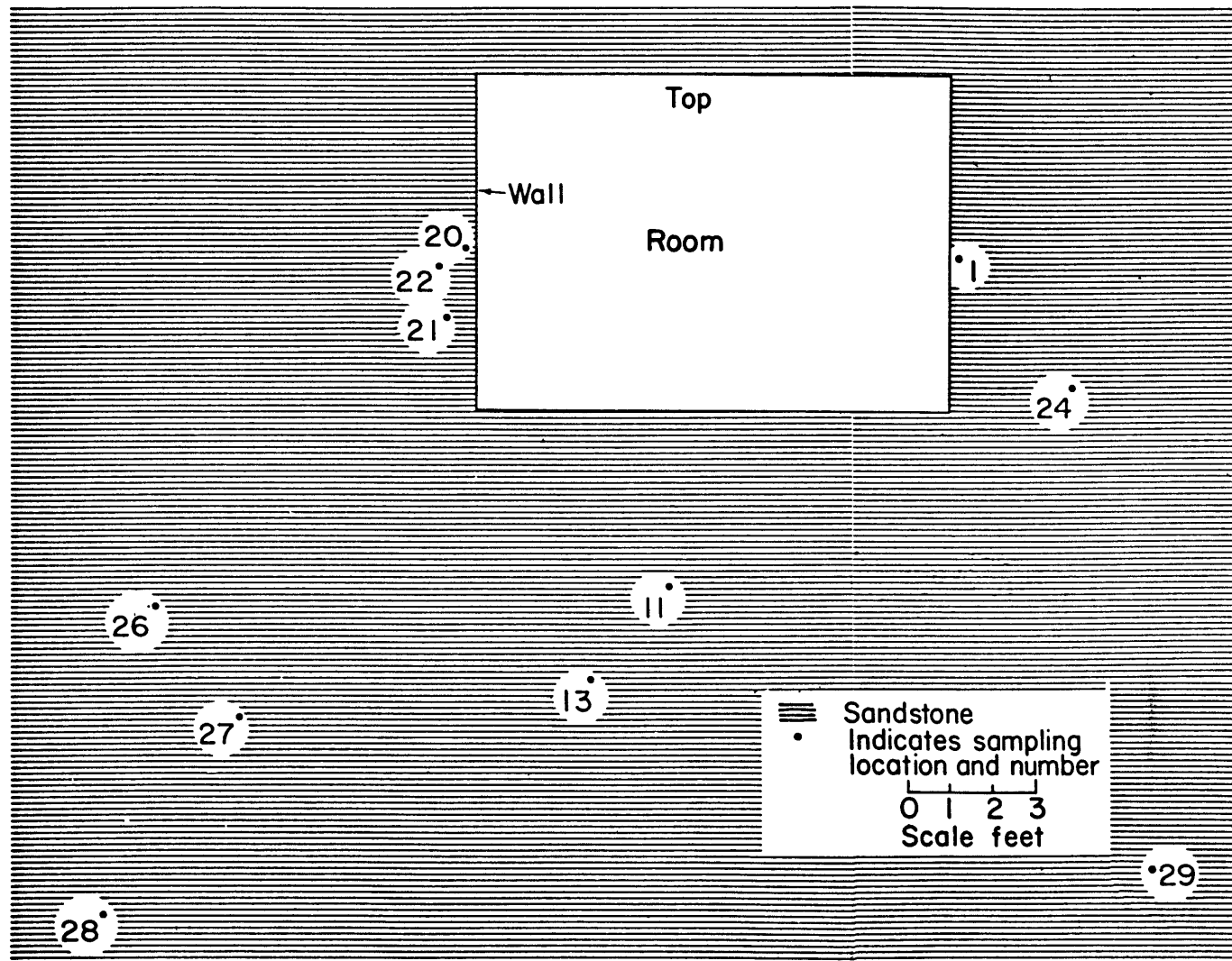


FIGURE 17. PROFILE OF SAMPLING INSTALLATION, FOREMAN'S ROOM

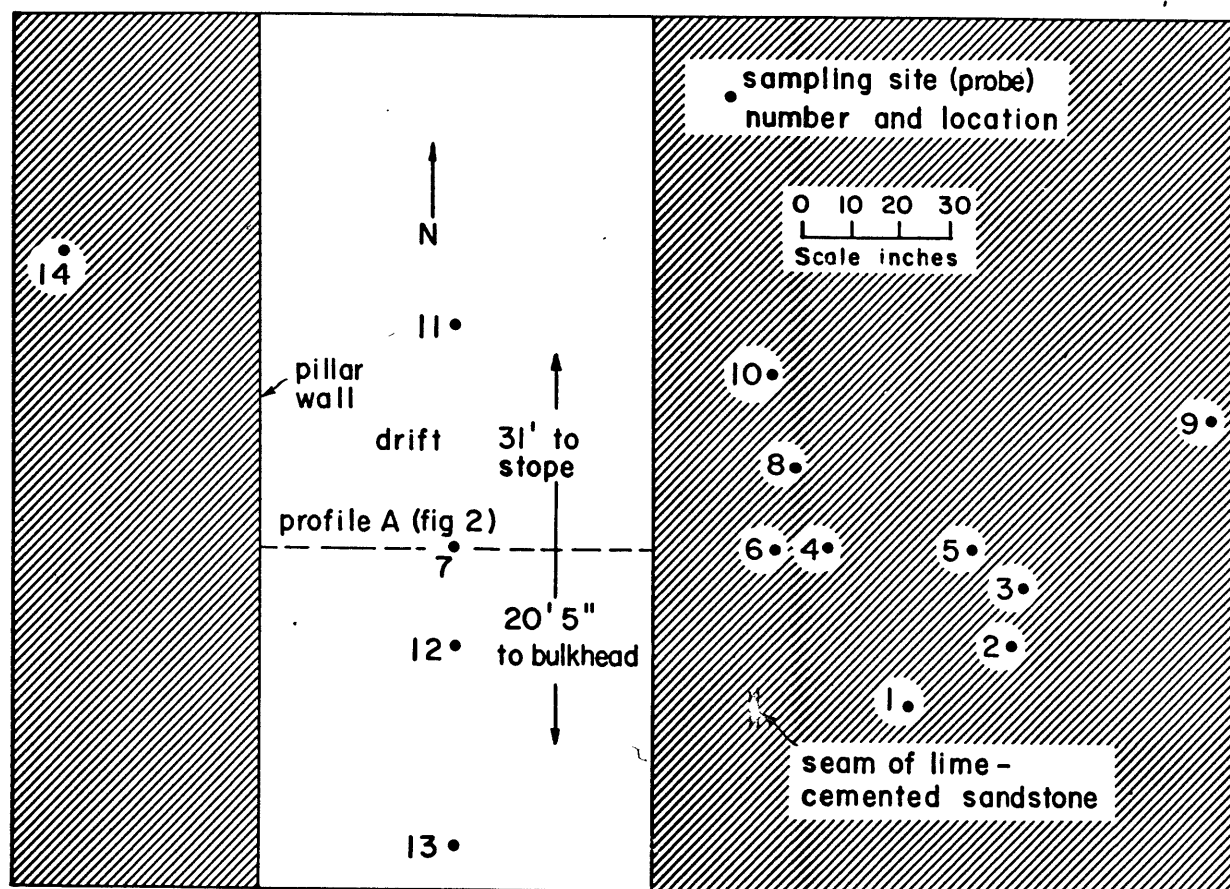


FIGURE 18. PLAN VIEW OF SAMPLING SITES IN DRIFT OF 5702 TEST AREA

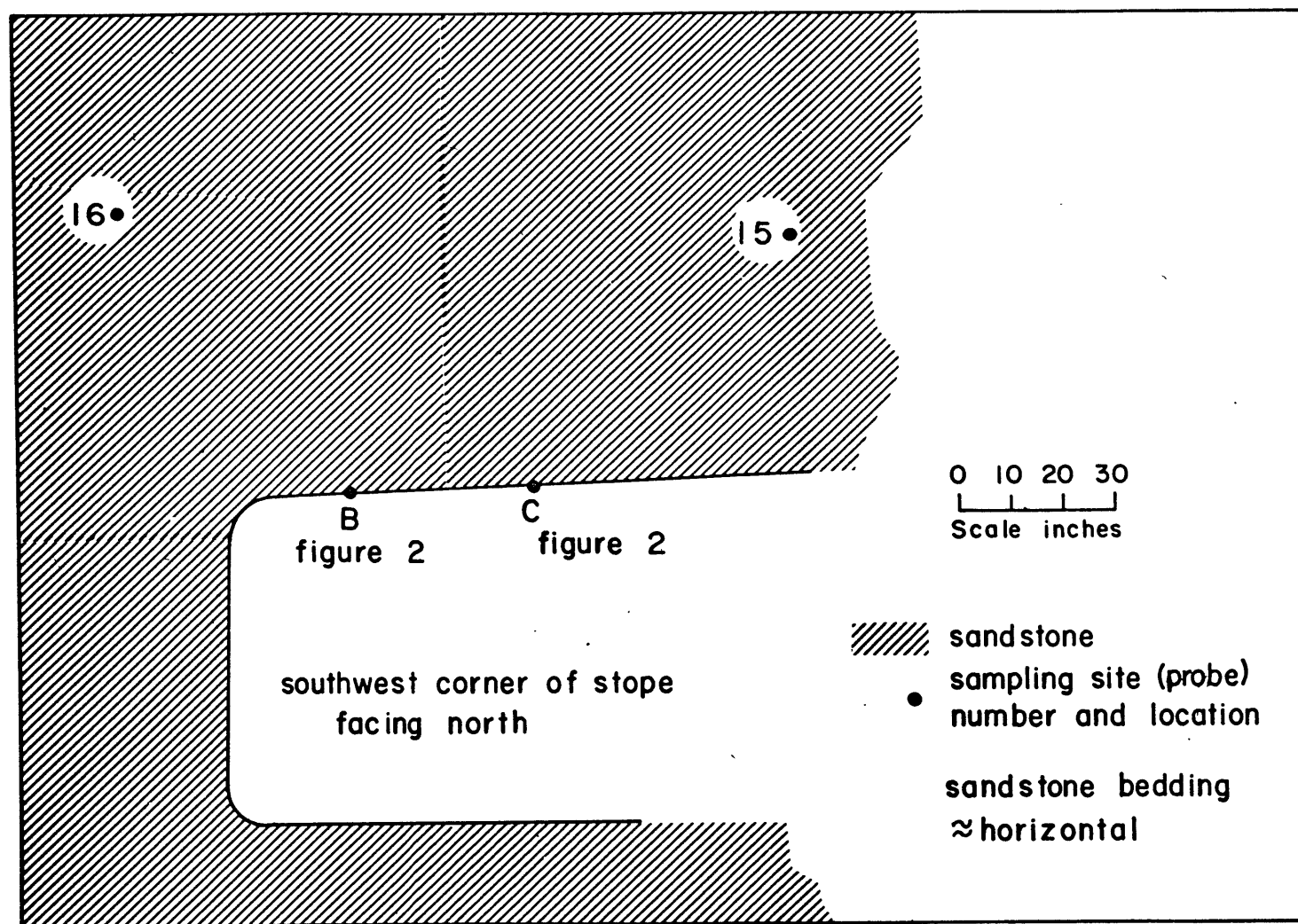


FIGURE 19. PROFILE OF SAMPLING SITES IN STOPE OF 5702 TEST AREA

TABLE 2.

Sampling Probes in Foreman's Room, June 1963

<u>Probe no.</u>	<u>Sampling depth (in.)</u>	<u>Depth of crushed rock packing above sampling level prior to epoxy seal (in.)</u>
1	2	1
2	2	no epoxy
3	5	1½
4	6	2
5	9	2½
6	10	3
7	14	3
8	15	?
9	22	5
10	24	10
11	50	3
12	75	26
13	77	6½

---

Probe no. 1 is in the wall of the room; all other probes are in the floor of the room.

## 9. Experiments

Several experiments were performed at each of the two areas. The general scope of each experiment is listed here in chronological order of the experiments.

June 1963: 3.3 to 3.8 cm Hg overpressure for 68 hrs., foreman's room.

This experiment, the first of the series, was to determine whether overpressure would actually reduce the Rn flux into a mine and, if it did, whether this reduction could be maintained continuously for several days. Interstitial gas and room air sampling were started shortly after the application of overpressure in order to determine the rate at which any induced changes occur. Two Rn flux measurements were made in the floor of the room prior to and immediately after the overpressure period. No provision for sampling Rn daughter products was made. Interstitial gas samples were taken during the 24 hrs. following the termination of overpressure.

August 1963: Overpressure varied in stages from 0.5 cm Hg to 3 cm Hg, foreman's room.

The previous experiment indicated that Rn concentrations in the surface 3 ft. of rock attain equilibrium conditions for a given overpressure within the initial 20 hrs. of the overpressure. This suggested that the Rn flux into an area would



also equilibrate in this period. In order to learn the empirical relationship of Rn flux to applied overpressure in the foreman's room, the room was held at the following overpressures for 24-hr. periods (cm Hg): 1.0 to 0.9, 1.4, 2.2, 3.0. During this time interstitial gas and room air samples were taken. Air input was monitored. After this sequence of overpressure, the air seal on the room was improved and the following overpressures were established for periods of several hours each (cm Hg): 1.2, 1.8, 3.0, 0.5, 0.2. Air input to the room was monitored.

December 1963: 21 days of continual overpressure 1.0 cm Hg, 5702 area.

It was still necessary to determine whether a moderate overpressure could maintain a reduced Rn flux into a large mining area for an extended period of time. The possibility existed that in time the air occupying the interstices of rock adjacent to the test area would attain a pressure equal to that of the test area. In this case flow from the test area would cease. The 21 days of overpressure were conducted to define this point. Interstitial gas and room air samples were taken; humidity, air consumption, and interstitial pressures were measured.

January, February 1964: Ventilation of test area with about 100 ft<sup>3</sup>/min. of dilution air, no overpressure, 5702 area.

To demonstrate that ventilation by overpressure provides a more efficient use of air than ventilation by dilution, the room air of the 5702 area was diluted with no overpressure (air was allowed to vent freely); the same volume input rate of air (about 100 ft<sup>3</sup>/min.) required to maintain the 1 cm Hg overpressure during the December 1963 test was used. The resulting room air Rn concentrations were compared with the room air Rn concentrations experienced during 1 cm Hg overpressure. The January experiment lasted 7 days; air input rate was 107 ft<sup>3</sup>/min., room air Rn concentrations were measured. The February experiment lasted 4 days; air input rate was 102 ft<sup>3</sup>/min., room air Rn and Rn daughter-product concentrations were measured.

26 February - 10 March 1964: Overpressure varied in stages from 0.6 cm Hg to 1.0 cm Hg, 5702 area.

This test was to demonstrate that the flux into the 5702 area was a function of applied overpressure. To this end, it was similar to the August 1963 overpressure experiments in the foreman's room. The bulkhead seals had deteriorated and some air loss around the seals occurred. This created the effect of limited dilution accompanying the overpressure. The extent of air loss by leakage could be estimated from air con-

sumption measurements made during previous tests when the air seals were more effective; room air and interstitial gas samples were taken. A duct was installed through the air seals to permit the measure of Rn daughter-product concentrations without the need of opening the bulkheads.

30 March - 15 April 1964: Ventilation by dilution plus 1.0 cm Hg overpressure, 5702 area.

Since mines are required by law to maintain the Rn daughter-product concentration below a specific level it was interesting to determine if the addition of diluting air to the overpressured area does reduce the Rn daughter concentration in proportion to the increased consumption of air. Dilution air, allowed to exhaust from the test area through a regulated vent, was supplied by fan at rates of 300, 800, and 1200 ft<sup>3</sup>/min. Overpressure was held at 1 cm Hg by regulating the exhaust vent. Room air and interstitial gas were sampled. Radon daughter-product concentrations were measured.

May 1964: 0.43 and 0.26 cm Hg underpressure, 5702 area.

Mines are often ventilated by upcasting air through an exhaust hole that extends to ground surface. This requires that air be pulled into the mine at another surface shaft under the influence of the partial vacuum created by the exhaust fan. A result is that the mine air is underpressured with respect to air pressures experienced in the rock interstices prior to

the start of ventilation. This underpressure will initially cause of flow of Rn-rich interstitial air from the rocks into the mine. If a negative pressure gradient between interstitial air and mine air persists then flow will continue from the rock interstices into the mine.

In this test the vacuum was established by an exhaust fan installed in a bulkhead. An 0.43 cm Hg underpressure was maintained for 7 days; 0.26 cm Hg underpressure was maintained for 5 days. Interstitial gas, room air, and exhaust air were sampled; Rn daughter-product concentrations were measured. Air pressures in the interstices of rock adjacent to the test area and the volume of air exhausted were monitored.

#### 10. Radon Concentrations in Interstitial Gas

The 21 day, 1 cm Hg overpressure experiment, 5702 area, demonstrated that at least in this experimental area, an extended period of overpressure is effective in continually maintaining a decreased Rn flux into the pressured region. Figures 20-24 clearly show that once overpressure conditions are established no varying trends in interstitial gas concentrations are observed. Figures 20-24 include descriptions of the orientation of each sampling probe with respect to the mine and the stratifications of the sandstone in which the mine is located. Since stratification is nearly horizontal, all probes entering the rock perpendicular to the mine walls (ribs) locate the sampling probes in such a manner that air passing from the mine into the rock may reach the probe site by traveling parallel to the layers of stratification. Probes entering the rock perpendicular to the mine floor or ceiling locate the sampling probes such that air passing from the mine reaches the probe by traveling perpendicularly to the layers of stratification.

Figures 20-24 indicate that to the greatest depth studied the total change in interstitial Rn concentration induced by overpressure occurs in less than 4 days after the start of pressure; the major portion of this change occurs in the first 24 hrs. of overpressure. The rate of depletion of interstitial Rn at the start of overpressure and the final total fractional change in Rn concentration is greater at probes located parallel

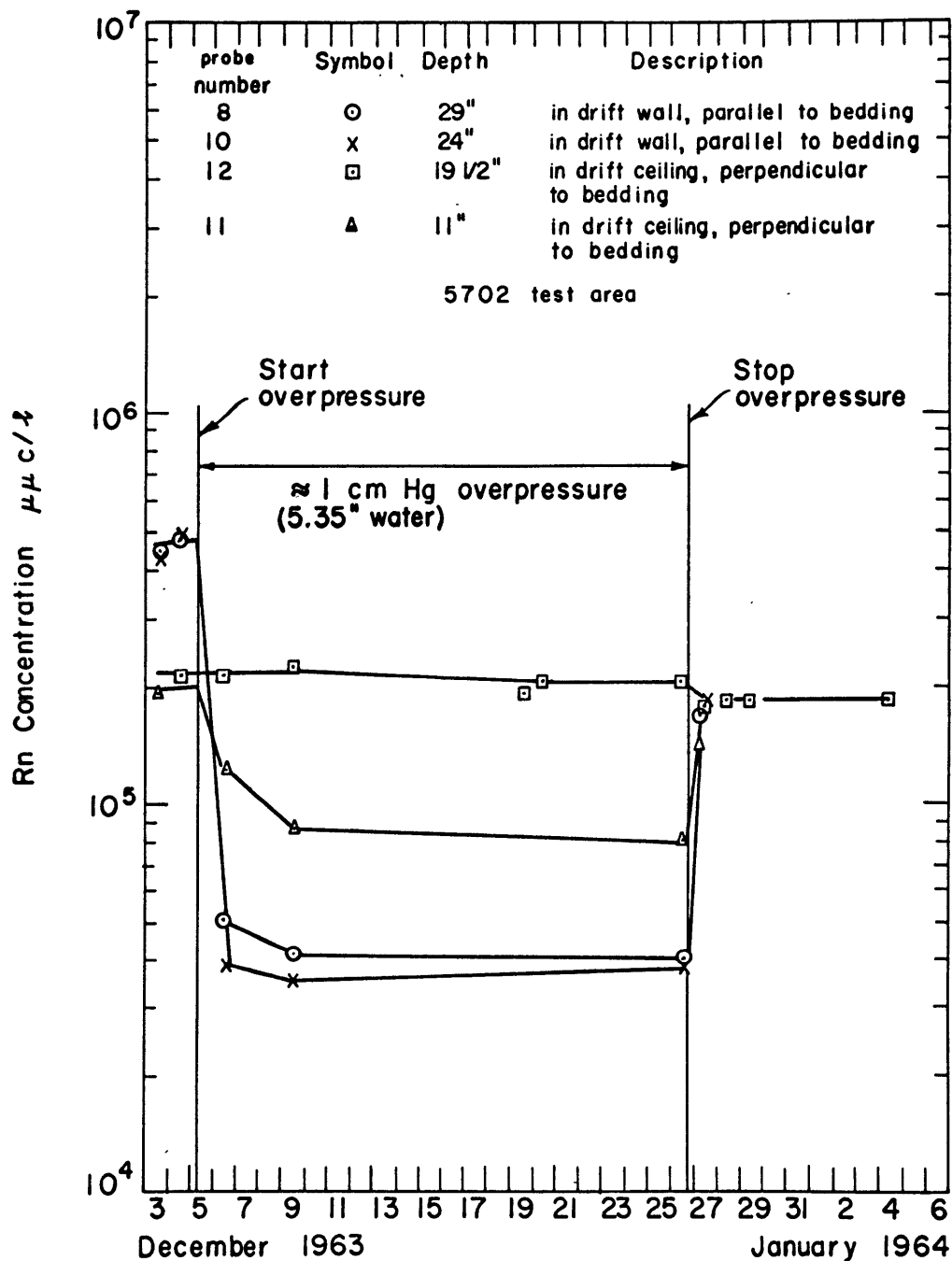


FIGURE 20. INTERSTITIAL RADON CONCENTRATION VS. TIME  
21 Day overpressure test, 5702 area

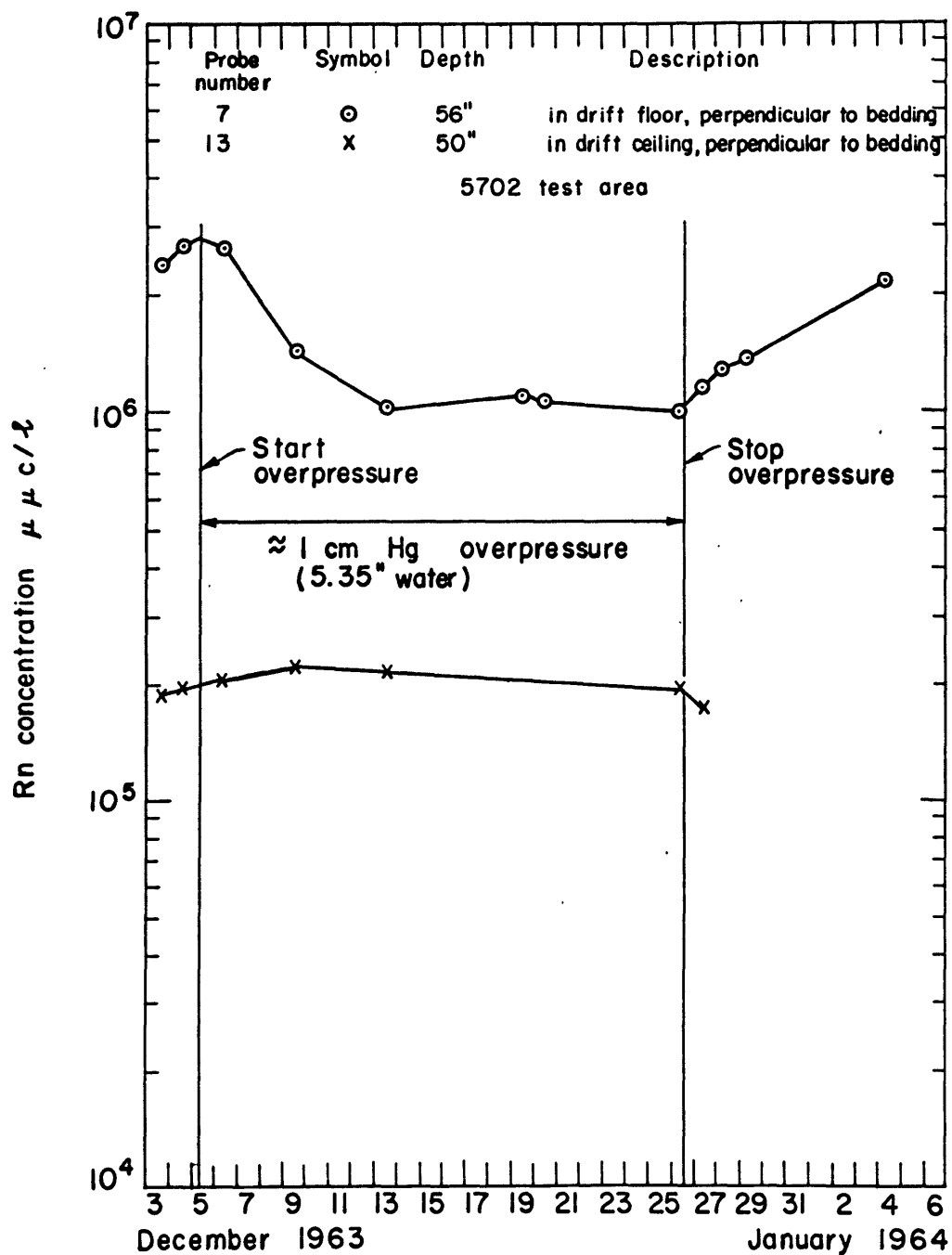


FIGURE 21. INTERSTITIAL RADON CONCENTRATION VS. TIME  
21 Day overpressure test, 5702 area

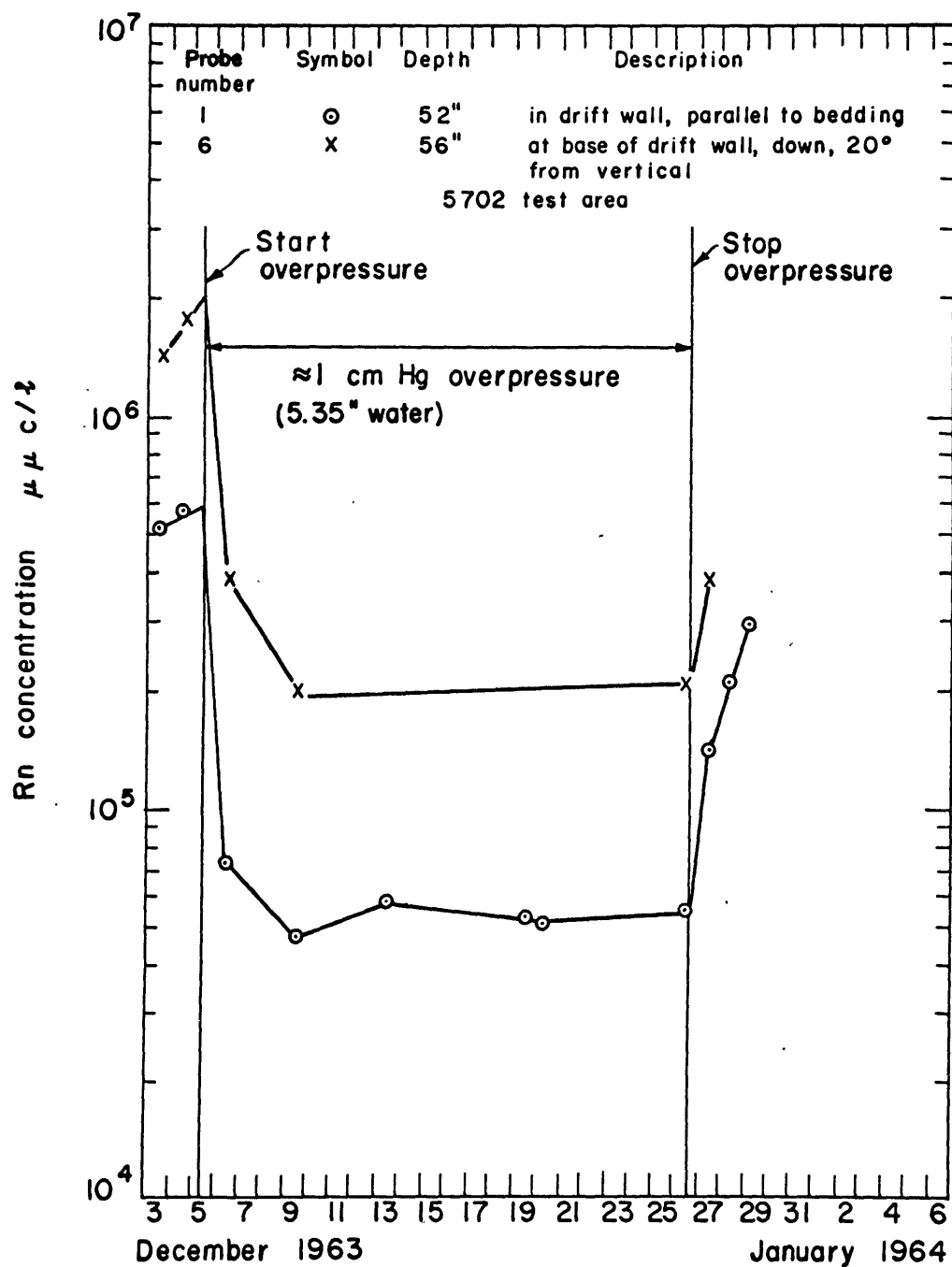


FIGURE 22. INTERSTITIAL RADON CONCENTRATION VS. TIME  
21 Day overpressure test, 5702 area



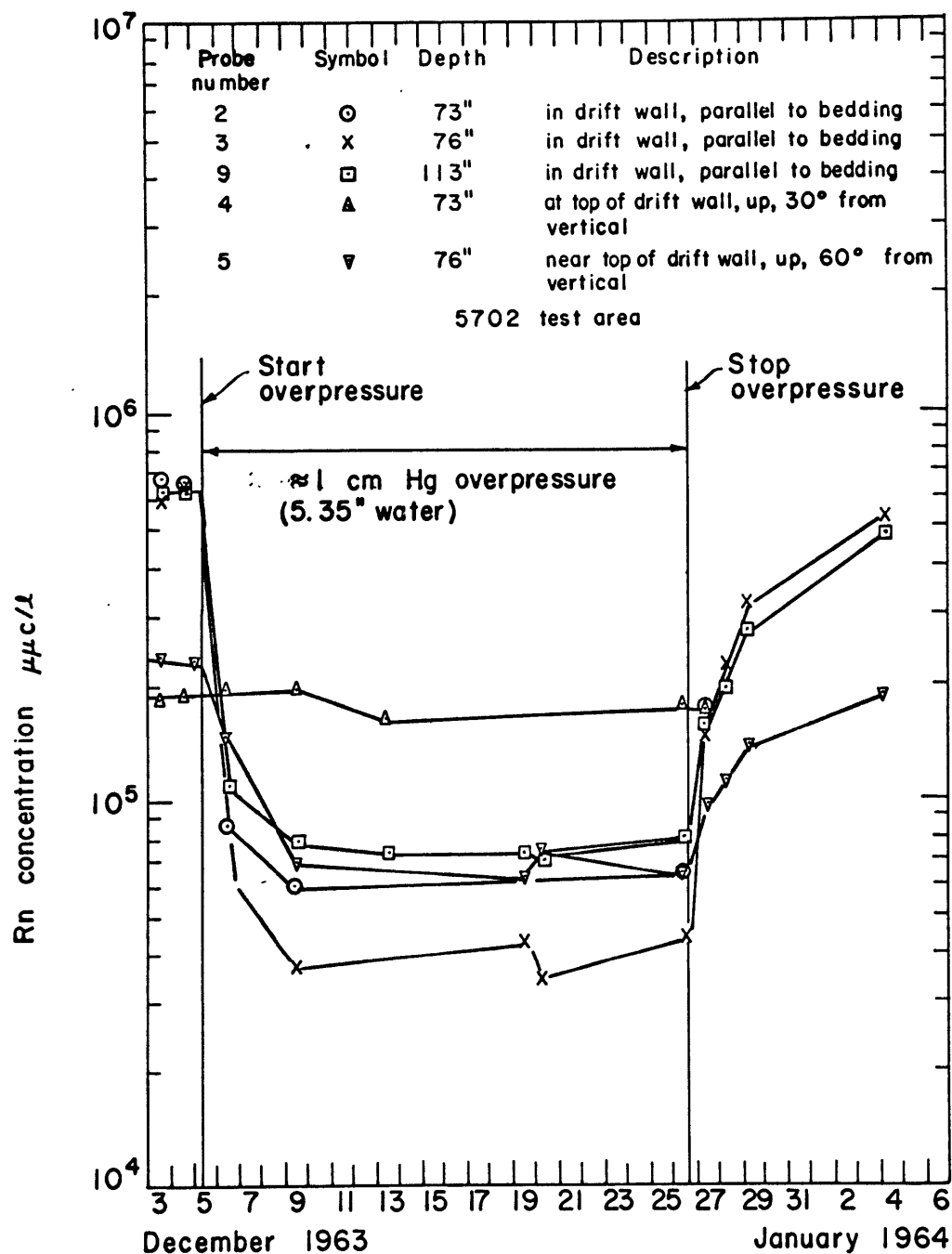


FIGURE 23. INTERSTITIAL RADON CONCENTRATION VS. TIME  
21 Day overpressure test, 5702 area

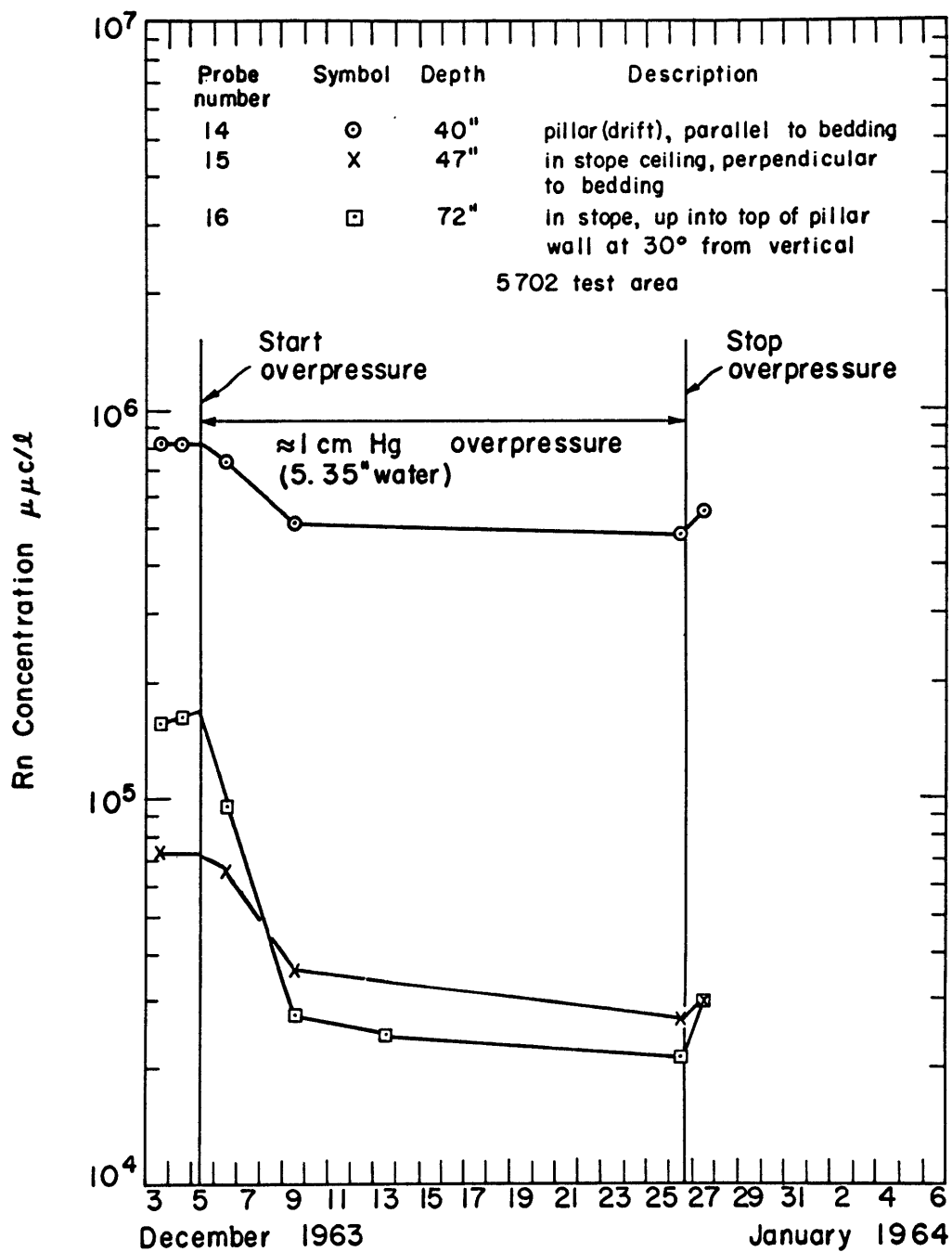


FIGURE 24. INTERSTITIAL RADON CONCENTRATION VS. TIME  
21 Day overpressure test, 5702 area

to rock stratification with respect to the mine than at probes located perpendicular to the stratifications (e.g., probe 7, Fig. 21, as compared with probe 2 and 3, Fig. 23). Just as in the rock surrounding the foreman's room, the air passes more readily parallel to stratifications (the direction of high permeability) than across stratifications (low permeability). The purging of Rn by air traveling outward from the pressurized area is therefore not equally efficient in all directions but is maximum in a direction parallel to the layering of the rock medium.

At the end of the overpressure portion of the test, interstitial Rn concentrations only gradually return to the pre-overpressure values.

Figures 25-27 present the interstitial Rn concentration data observed during underpressure tests in the 5702 area. At the start of underpressure there appears to be a transient effect. This will be discussed later. Once what appear to be the equilibrium conditions for the test are established, the Rn concentrations follow predictable trends<sup>1</sup>. Deep probes retain their overpressure concentrations (c.f., Fig. 25, probes 2, 3, 9; Fig. 26, probes 6, 7) since interstitial gas moving toward the test area from greater depths contains Rn concentrations similar to the concentration normally observed at these deep areas. Only one shallow probe was sampled several days

<sup>1</sup>Due to exceptionally difficult operating conditions during this experiment some samples were mislabeled. Several such cases have been worked out between field and laboratory and corrected. The anomalies in Fig. 26 would be alleviated if samples from holes 6 and 1 on 30 April were reversed and the sample attributed to hole 6 on 7 May was, in reality, from either hole 12 or hole 13.

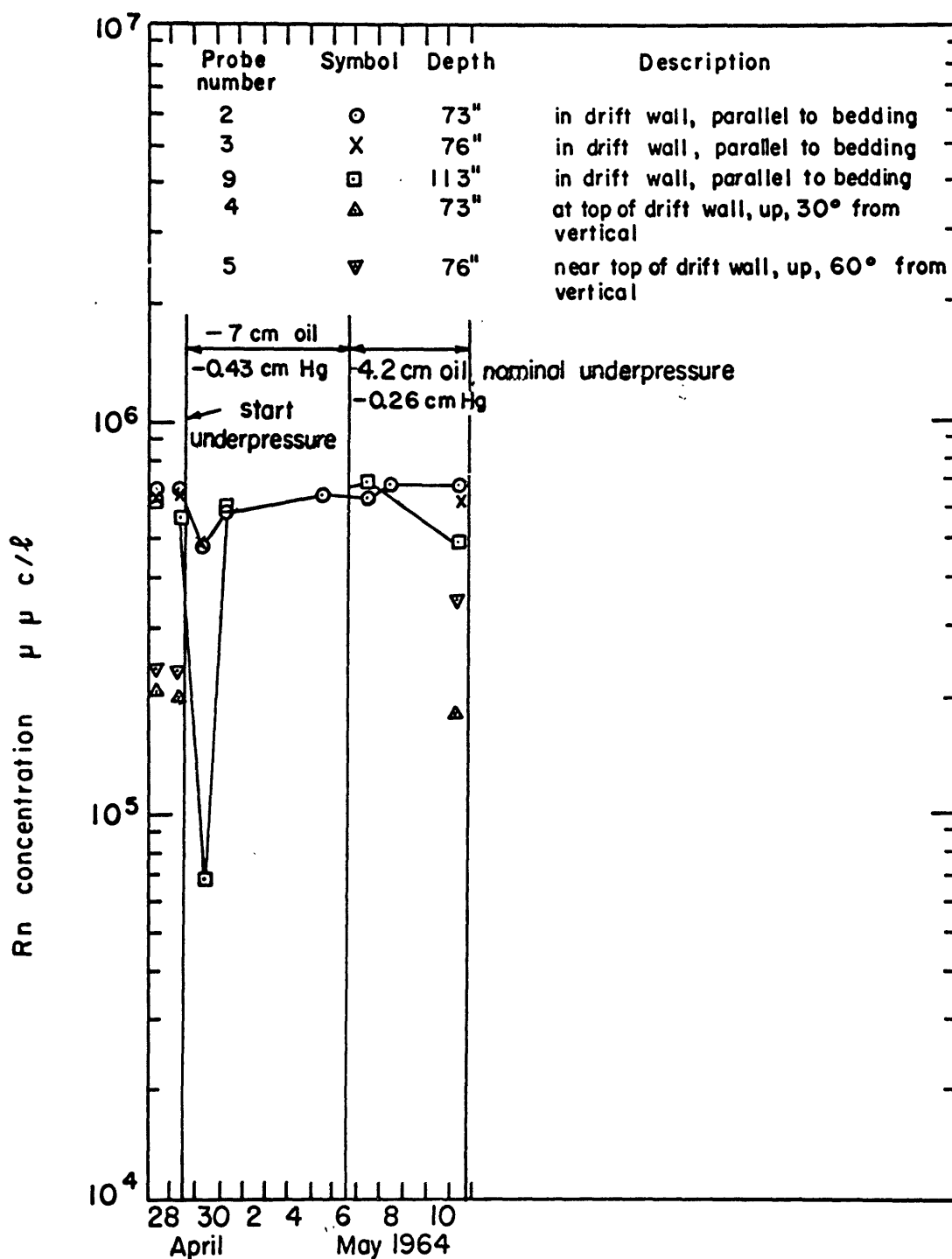


FIGURE 25. INTERSTITIAL RADON CONCENTRATION VS. TIME  
underpressure experiment 5702 area

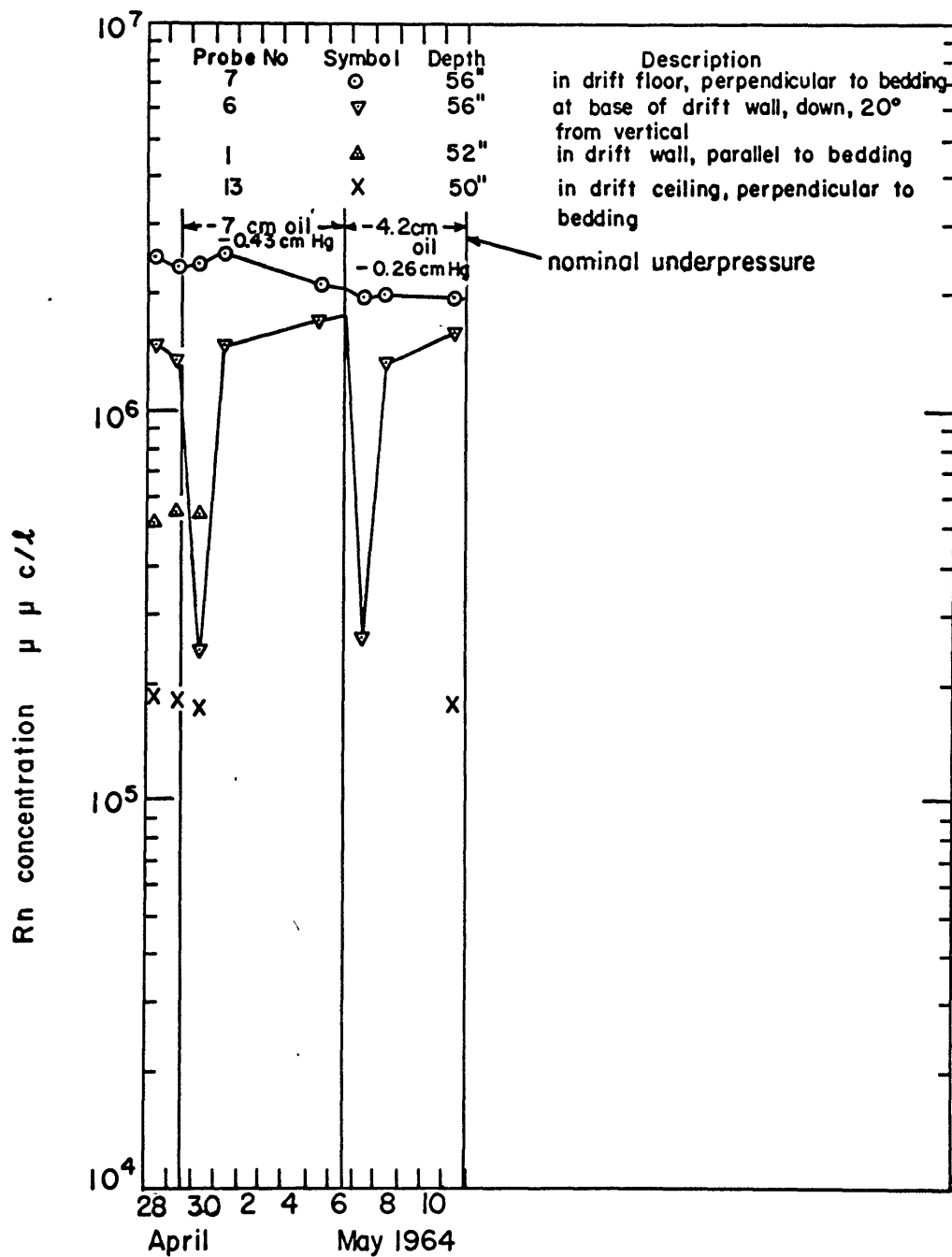


FIGURE 26. INTERSTITIAL RADON CONCENTRATION VS. TIME  
 underpressure experiment, 5702 area

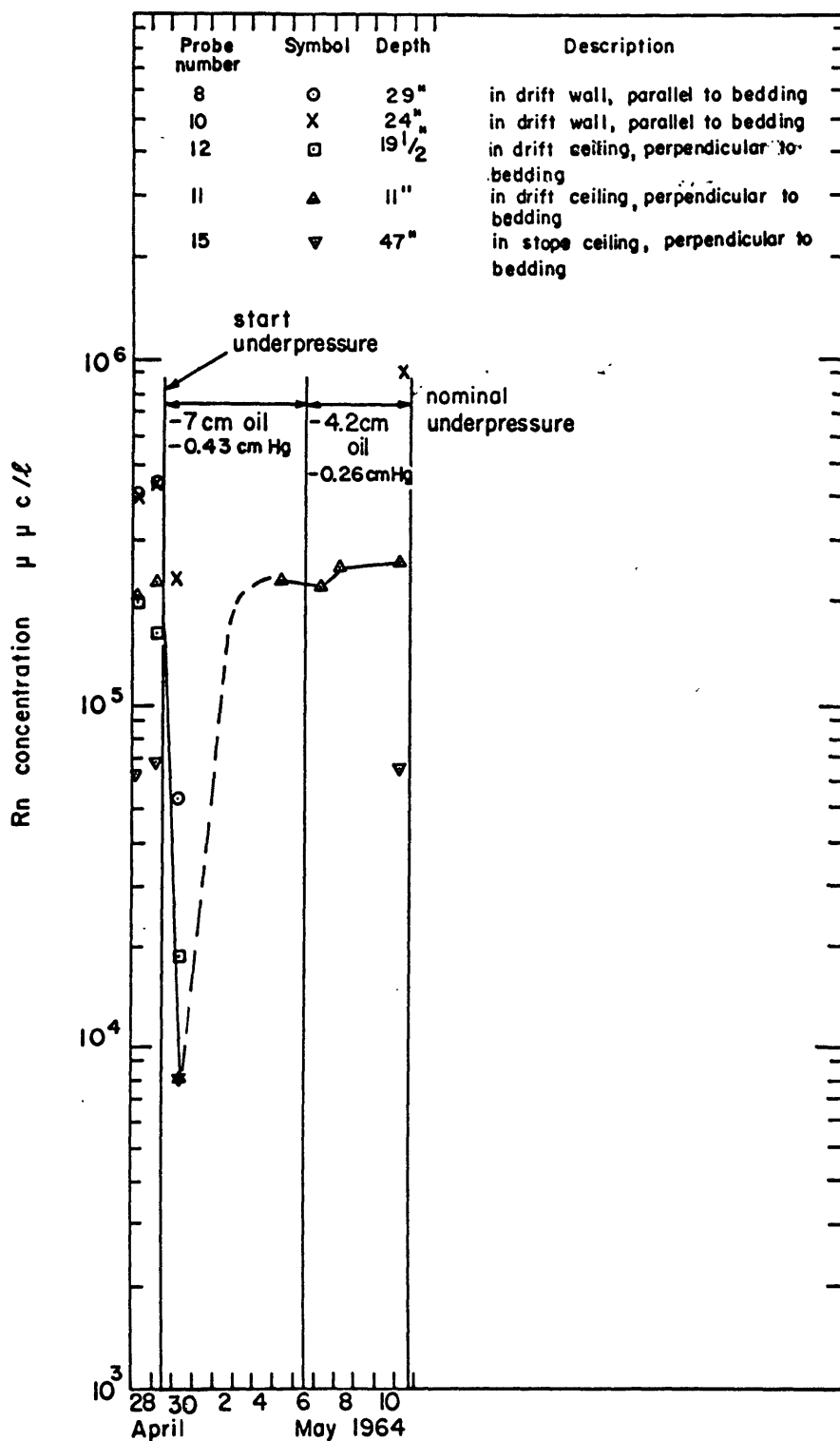


FIGURE 27. INTERSTITIAL RADON CONCENTRATION VS. TIME  
underpressure experiment 5702 area

after the start of underpressure. As would be expected, this site, probe 10 (Fig. 27), showed a significant increase in Rn concentration. Data from probe 5 (Fig. 25) follow a trend similar to that of probe 10. This site is located 76" into the drift wall and at an elevation slightly above that of the drift ceiling. The shale lens, which overlies the 5702 area causes the Rn concentration in the vicinity of probe 5 to be depleted below concentrations normally observed at such depths (compare pre-overpressure data probe 5 with probes 2 and 3). With underpressure, horizontal flow towards the test area from greater depths (higher Rn concentrations) passes probe 5 and increases the Rn concentration in this area. The significant pressure difference between probe 5 and the test area (Fig. 11) and also between probe 10 and the test area demonstrates the existence of air motion.

Note that sampling probes located above the drift ceiling of the 5702 area show little or no change in Rn concentration during underpressure as compared with pre-underpressure conditions. As stated in the text, this is the result of the low permeability shale lens overlying much of the test area. This lens blocks air motion from depth toward the test area.

The origin of the drop in interstitial Rn concentrations experienced at the start of underpressure at most of sampling probes is uncertain. It would be expected that with the establishment of underpressure, flow into the test area from the rock interstices would begin. This would have the effect of

increasing Rn concentrations in regions where diffusion had depleted the concentration during non-pressured periods. The initial drop in concentration may indicate a flow of low Rn air originating in a tunnel outside the test area. The closest non-underpressured mine area is greater than 50 feet from the sampling probes. The Rn concentration in this non-pressured area is believed to be nominally 6000  $\mu\text{mc}/\text{l}$ .

Interstitial Rn concentrations observed during non-pressure periods are not necessarily directly related to depth within the wall. Factors such as local Ra enrichment or varying porosity affect the concentrations. The very low Rn concentration measured at probe 28, foreman's room, is possibly the result of a deficiency of Rn parents in the vicinity of the sampling area. From Fig. 17, it is seen that probe 28 is remote from the main ore body. Probe 26 of the foreman's room may be situated in the vicinity of an enrichment of ore. This would account for the high Rn concentration experienced at this location. The site of probe 15, 5702 area (52 in. deep, ceiling of stope, area C, Fig.2) had an exceptionally low pre-overpressure Rn concentration which was further depleted during overpressure. The location may have been distant from the main ore body; the hole is in a corner of the stope.

For probe 27, foreman's room, the pre-overpressure Rn concentrations shown are believed to be lower than the normal values of this site. The hole in which this probe was placed was filled only 2 hrs. prior to the sampling at 1000 hrs., 10 August 1963.



## 11. Radon Flux Measurements

Total Rn flux into a given area during overpressure is calculated from measurements of room-air Rn concentrations and total air passing through the test area. When the room-air concentration comes into equilibrium with the surrounding rock during the dynamic conditions of a period of overpressure, the Rn concentration within the room becomes fairly uniform and constant. At this time, the quantity of Rn diffusing into the room per unit time is just equal to the amount of Rn decaying per unit time, plus the amount of Rn removed by convection. The loss by decay is calculated as total Rn in the room [ (amount of Rn per liter) x (volume in liters of the room)] multiplied by the Rn decay constant. The Rn removed by convection is estimated from air consumption. In a period of constant overpressure, the rate at which air enters the room equals the rate at which air leaves the room; by monitoring air input to the room, a direct measure is obtained of the rate at which air leaves the room. It is assumed that air leaving the room has the same Rn concentration as the air which remains in the room. The validity of this assumption is indicated by the extreme uniformity of air Rn concentrations within an overpressured area. At equilibrium, then, the rate at which Rn is removed by convection is equal to the air input rate to the room times the Rn concentration in the room.

With the establishment of what appear to be equilibrium conditions for each underpressure period it is possible to estimate the Rn flux into the area. Knowledge of interstitial

pressures in rock surrounding the test area allows a prediction of the rate at which interstitial gas flows into the 5702 area from the adjacent rock. Since, at equilibrium, pressure in the 5702 area remains constant, room air must be exhausted at a rate equal to the rate of interstitial gas introduction. The rate of Rn removal by convection is then (room air Rn concentration) x (volume exhaust rate of air from 5702 area). The total rate at which Rn is removed from the 5702 area is this convection depletion plus the total Rn decay rate within the area. At equilibrium the Rn flux into the 5702 area equals the rate at which Rn is removed. Due to bulkhead leakage, direct measure of the net volume of air removed from the 5702 area during underpressure was not possible.

Interstitial pressure data observed during 0.43 cm Hg underpressure indicate a flow of about  $30 \text{ ft}^3/\text{min}$  of soil gas into the test area (compare this with  $100 \text{ ft}^3/\text{min}$  flowing into the rock during 1 cm Hg overpressure). During this underpressure room air Rn concentration is about  $1.7 \times 10^5 \mu\mu\text{c}/\text{l}$ . The volume of the test area is  $150,000 \text{ ft}^3$ . These data, by the previously described method, indicate a total Rn flux into the test area of  $4 \times 10^{-6} \text{ c}/\text{sec}$ . A check on this value is to assume that the  $30 \text{ ft}^3/\text{min}$  of interstitial gas entering the area has a Rn concentration of about  $3 \times 10^5 \mu\mu\text{c}/\text{l}$ . This rate of Rn introduction plus the normal rate diffusion into the area equals a total of  $6 \times 10^{-6} \text{ c}/\text{sec}$  Rn entering the 5702 area. The agreement between the two flux predictions is good; if the

interstitial gas drawn into the test area by influence of the underpressure has a Rn concentration of  $2 \times 10^5 \mu\mu\text{c/l}$  the two predictions agree at  $4 \times 10^{-6} \text{ c/sec}$  Rn flux into the 5702 area. Even at the lower flux value, the underpressure flux is 3 times the  $1.25 \times 10^{-6} \text{ c/sec}$  Rn flux observed during no pressurization of the area.

Similar arguments for the 0.26 cm Hg underpressure indicate an underpressure Rn flux into the 5702 area of about twice the normally observed value, with about  $15 \text{ ft}^3/\text{min}$  of interstitial gas entering the area.

## 12. Room Air Radon Concentrations

Figure 28 presents room air Rn concentration as a function of time during overpressure tests in the foreman's room. The times of sealing the room and applications of overpressure are indicated. Also shown for each overpressure are the rates of air input to the room in cubic feet per minute. Part of this air entered the interstices of the rock environment and part left the room through leaks and through the rock immediately surrounding the door to the room. The room air Rn concentration data are most meaningful when used in conjunction with the rate of air input to the room to obtain the total Rn flux into the test area. Since overpressures greater than 1 cm Hg produce about a 20-fold decrease in the Rn flux into the foreman's room, the room air Rn concentrations presented in Fig. 28 are of the order of 5 percent of the Rn concentrations which would be achievable using the same volume of air for ventilation by dilution (i.e., no overpressure).

Figure 29 shows the room air Rn concentration observed during a 21-day period of 1 cm Hg overpressures in the 5702 area. Three widely separated locations were sampled. Air consumption during this period averaged about  $100 \text{ ft}^3/\text{min}$ . After 2 to 3 days of overpressure the Rn concentration equilibrated at about  $4500 \text{ } \mu\mu\text{c/l}$ . Figure 30 presents room air Rn concentrations experienced in the 5702 area while the area was ventilated by dilution (no overpressure) at a rate of 107 and  $102 \text{ ft}^3/\text{min}$ .

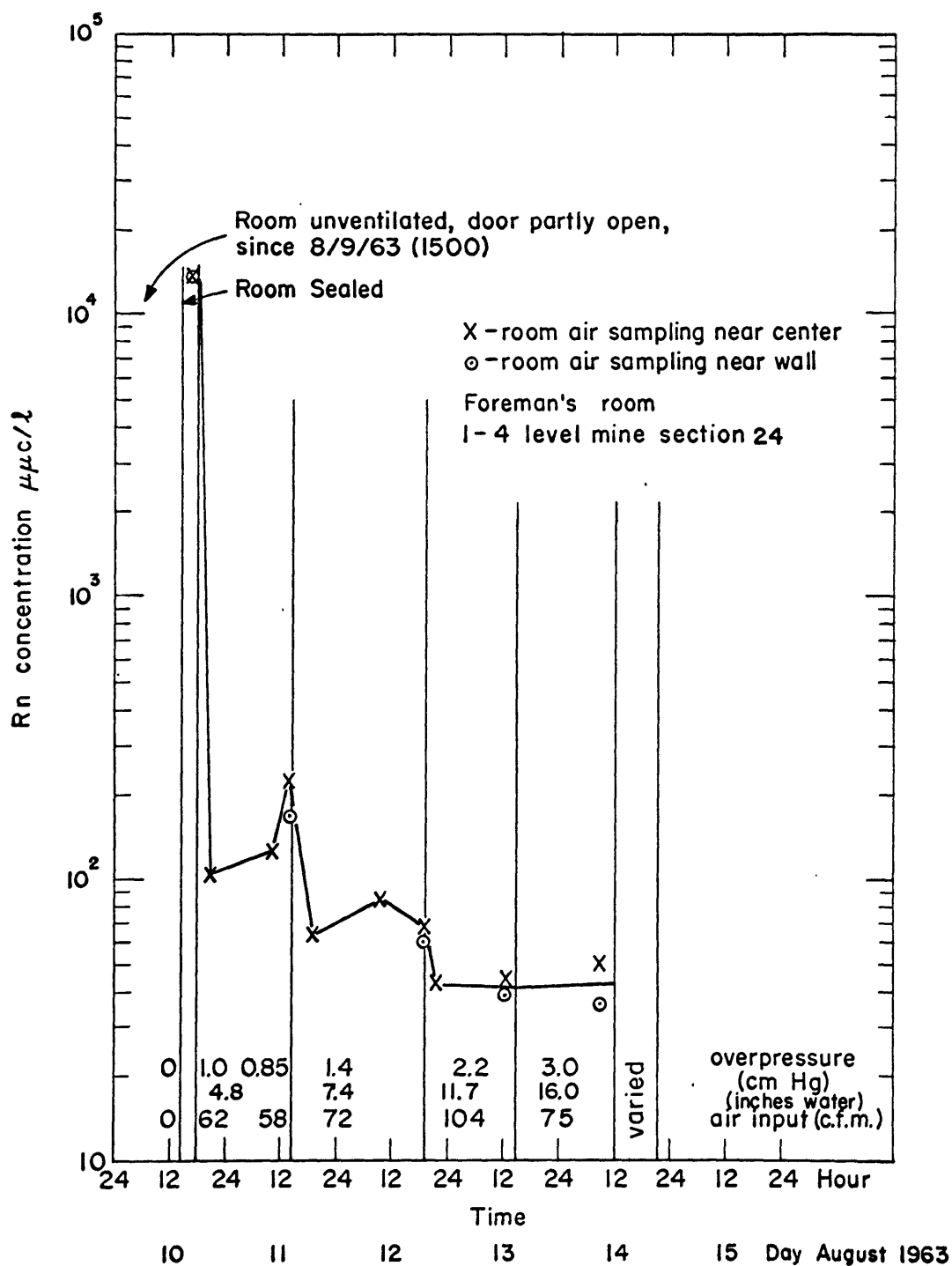


FIGURE 28. ROOM AIR RADON CONCENTRATION VS. TIME,  
VARIED OVERPRESSURE TEST, FOREMAN'S  
ROOM

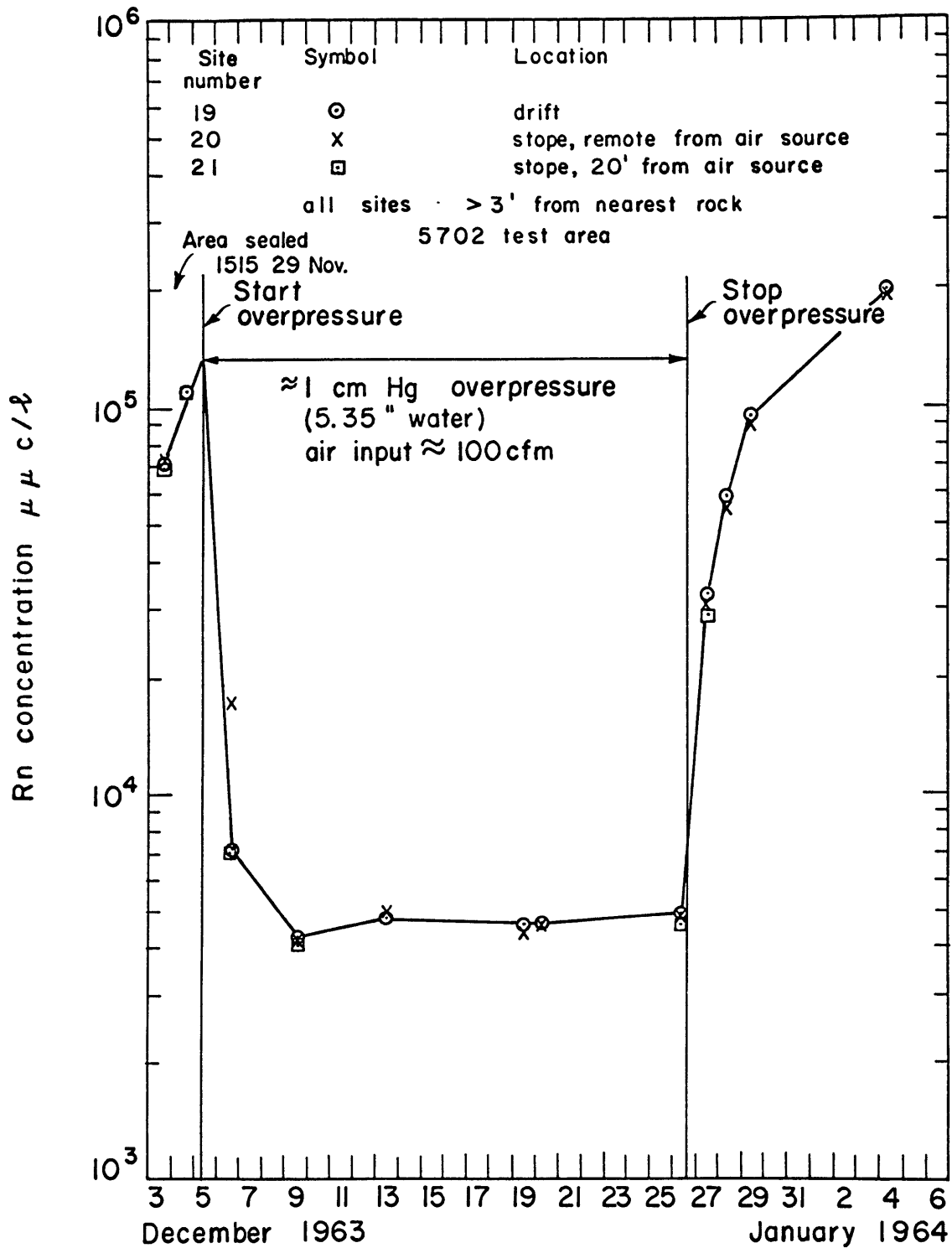


FIGURE 29. ROOM AIR RADON CONCENTRATION VS. TIME  
21 DAY OVERPRESSURE TEST, 5702 AREA

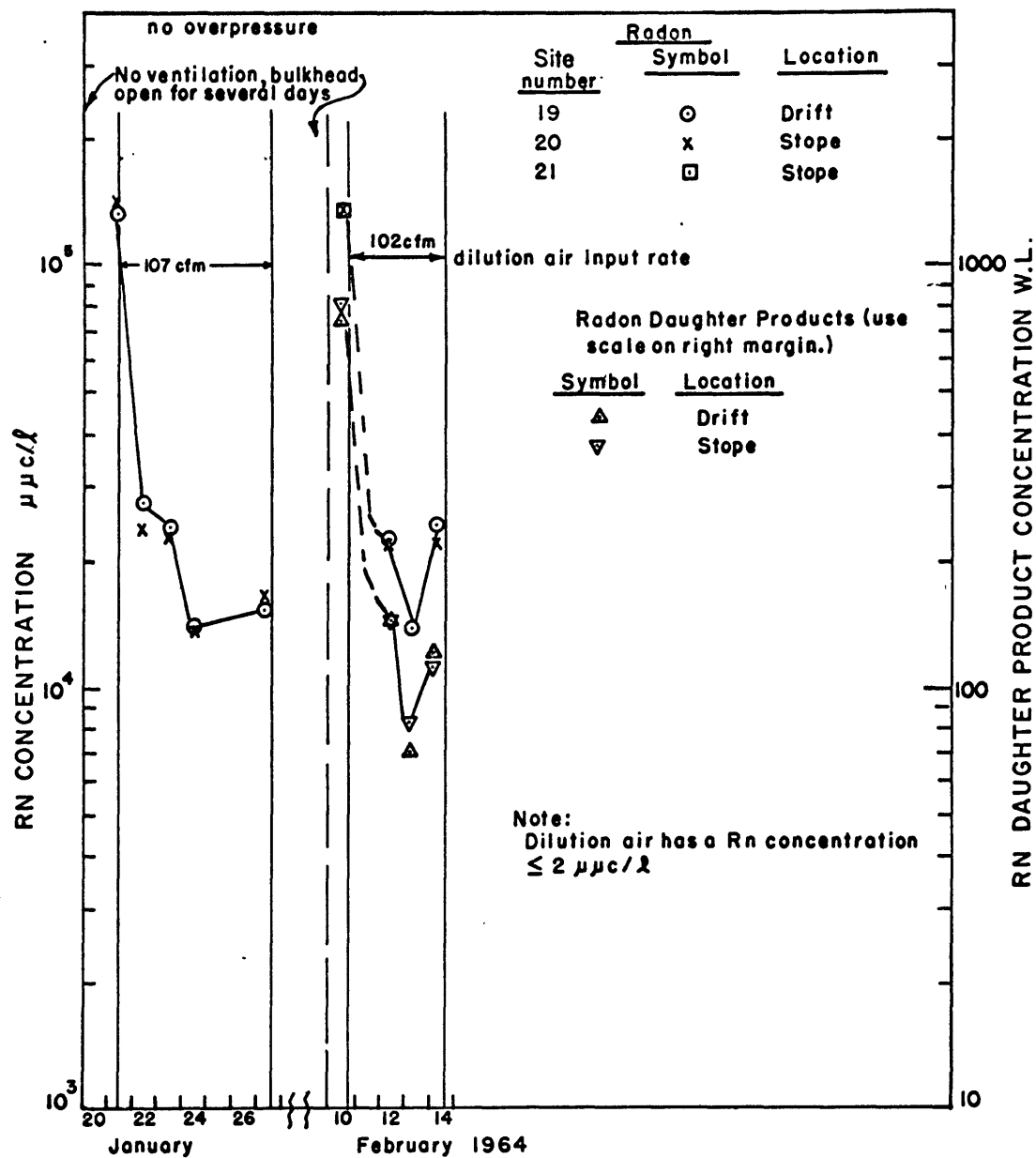


FIGURE 30. ROOM AIR RADON AND RADON DAUGHTER PRODUCT CONCENTRATIONS DURING STATED AIR DILUTION CONDITIONS vs. TIME, 5702 AREA.

The equilibrium Rn concentration is slightly greater than 20,000  $\mu\mu\text{c}/\text{l}$ , a concentration almost five times that obtained during overpressure.

Figure 31 presents room-air Rn concentrations and Rn daughter working levels observed in the 5702 area during the overpressure and air consumption conditions stated in the figure. These data were used for calculations of Rn flux into the 5702 area during the indicated overpressure.

Figure 32 shows the room air Rn concentrations observed in the 5702 area during the underpressure tests. The 35 percent increase in Rn concentration (from  $1.7 \times 10^5 \mu\mu\text{c}/\text{l}$  28-29 April, to  $2.3 \times 10^5 \mu\mu\text{c}/\text{l}$  30 April) observed on the first day of underpressure is likely associated with the decrease in interstitial Rn concentrations observed at this same time. It demonstrates the effectiveness with which interstitial gas is drawn into an underpressured area. The  $2.3 \times 10^5 \mu\mu\text{c}/\text{l}$  room air Rn concentration, 30 April, is the highest room air Rn value measured in the 5702 area.

The  $1.7 \times 10^5 \mu\mu\text{c}/\text{l}$  air Rn concentration of 28-29 April is higher than the  $1.4 \times 10^5 \mu\mu\text{c}/\text{l}$  observed in the 5702 area when the area is sealed and not ventilated. This high value is attributed to a sharp drop in barometric pressure on the morning of 28 April.

Prior to underpressure the Rn daughter-product concentration was 1200 WL. During the first days of underpressure, the daughter-product concentration was 1440 WL. This increase



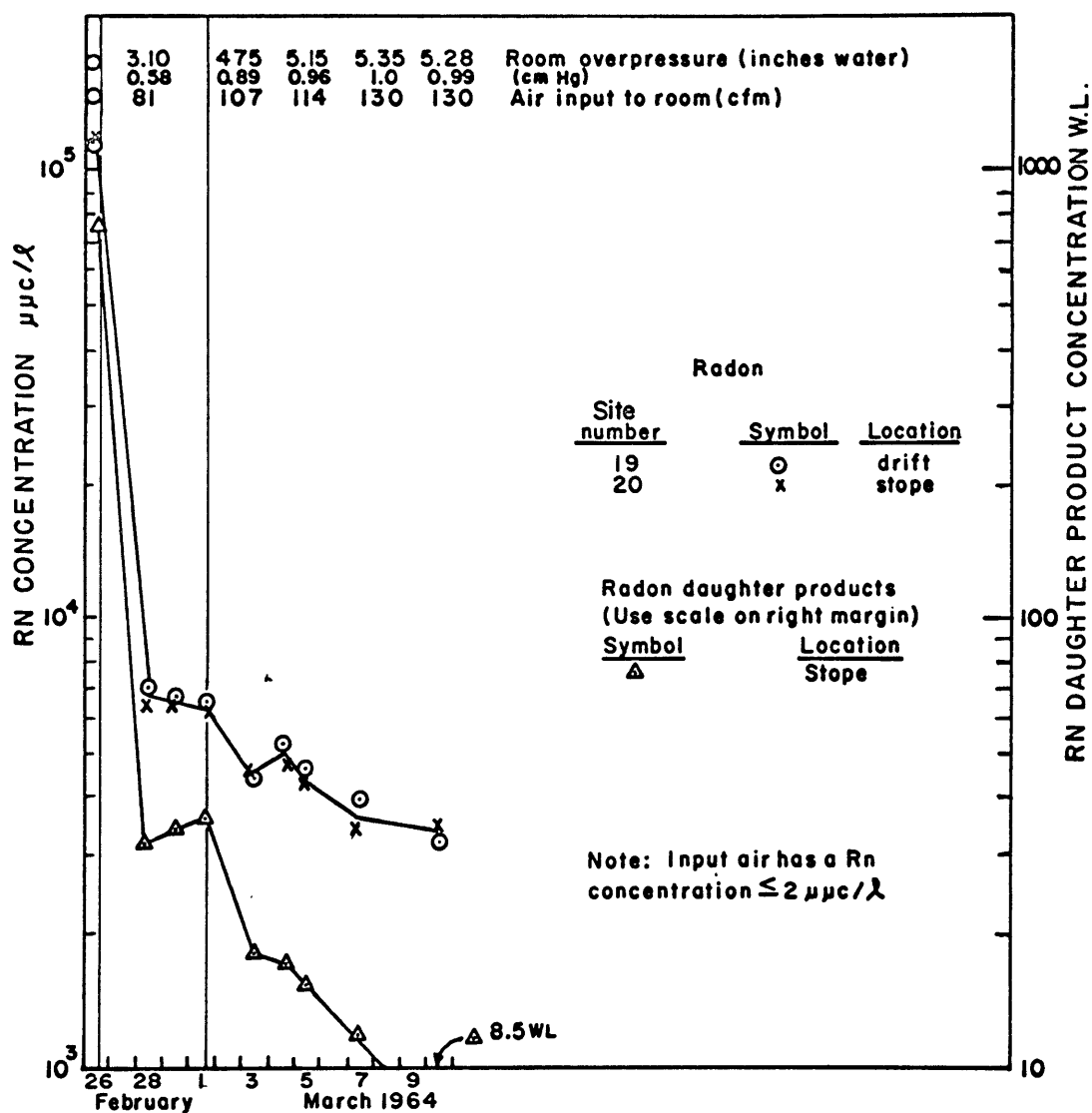


FIGURE 31. ROOM AIR RADON AND RADON DAUGHTER PRODUCT CONCENTRATIONS DURING STATED OVERPRESSURE CONDITIONS vs. TIME, 5702 AREA.

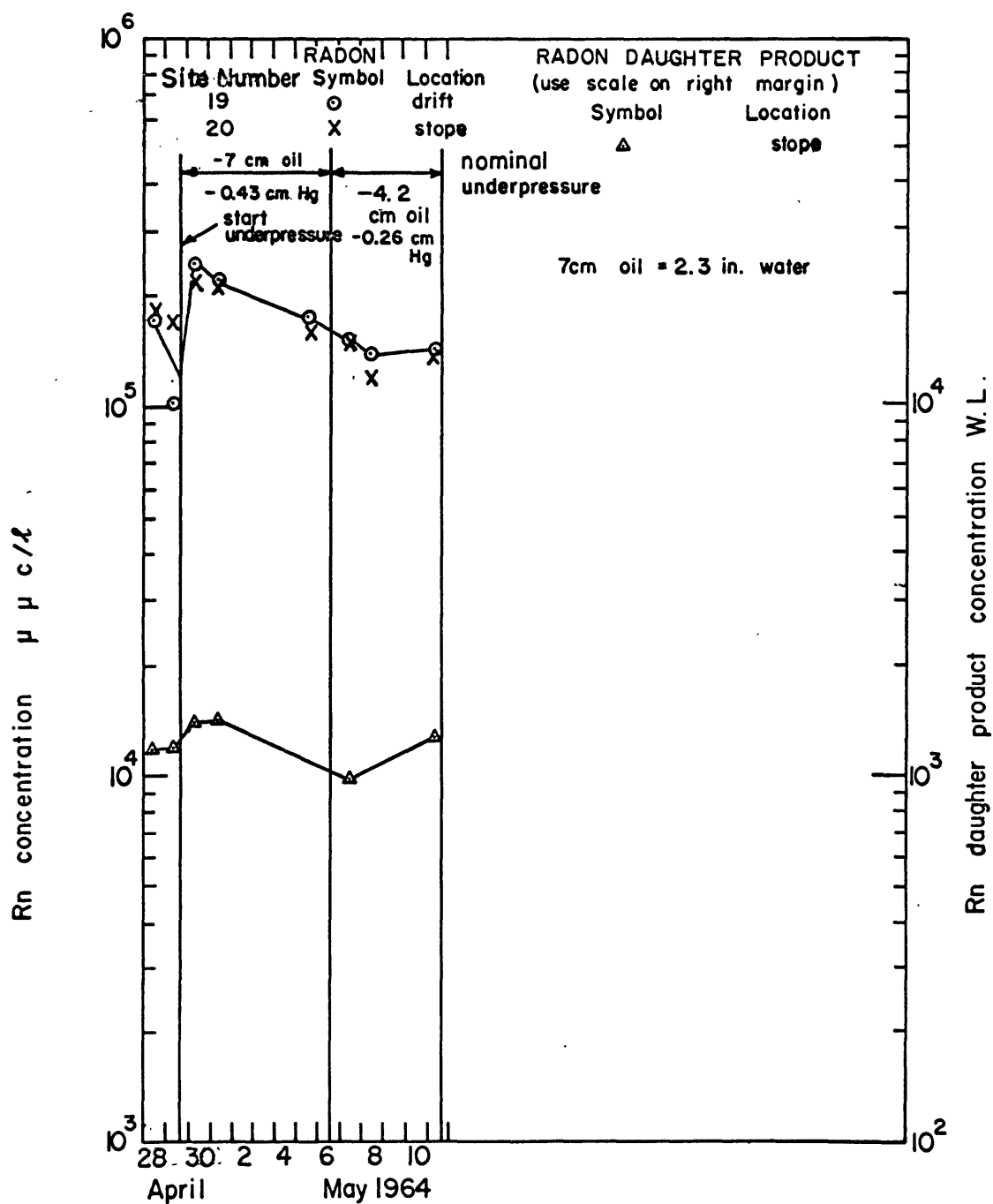


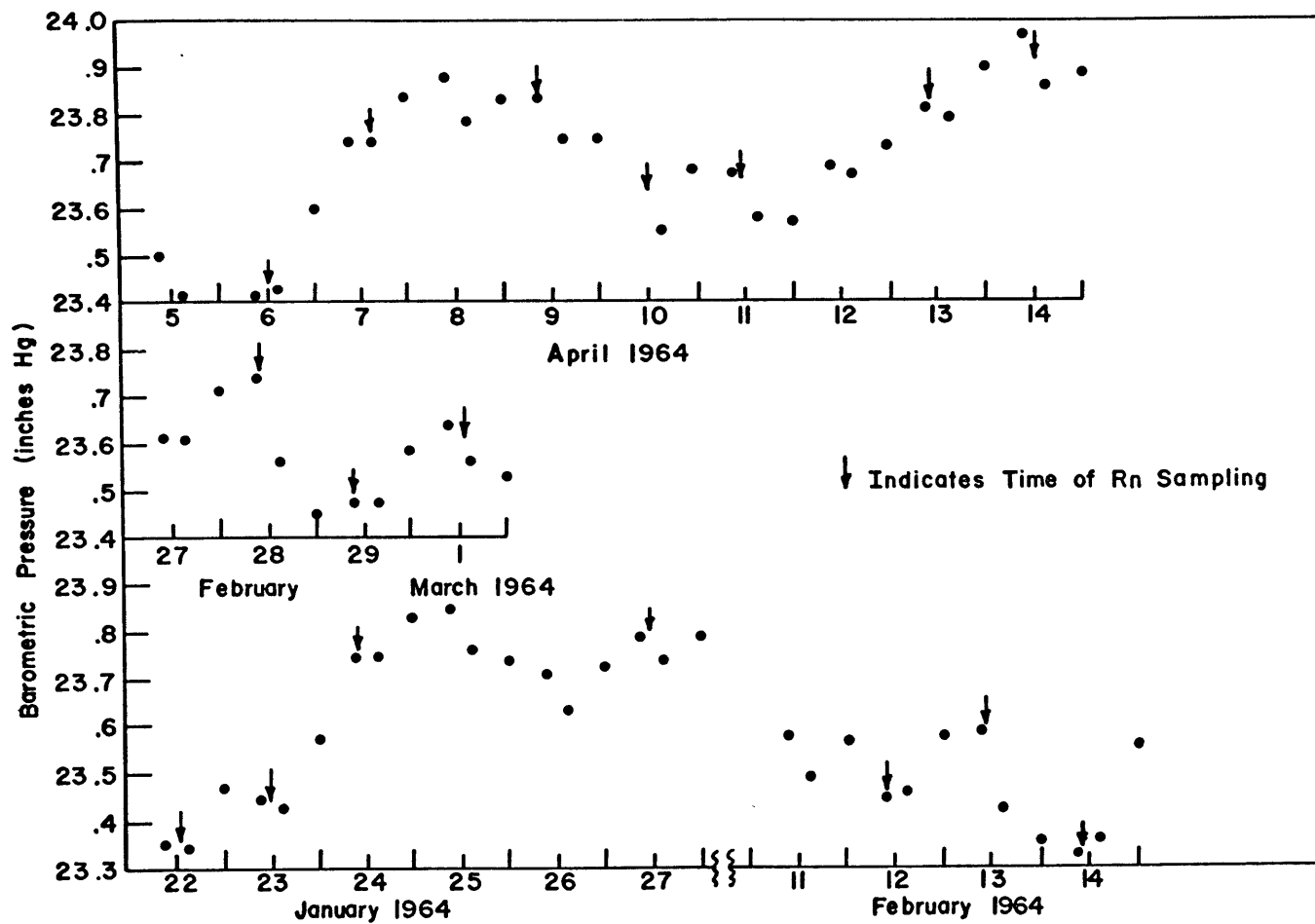
FIGURE 32. ROOM AIR RADON AND RADON DAUGHTER  
PRODUCT CONCENTRATION VS. TIME  
underpressure experiment, 5702 area

occurs with the rise in air Rn concentration observed shortly after the start of underpressure.

The low Rn concentrations experienced on 24 and 27 January, and 13 February, 1964, (Fig.30), appear to be the result of rising barometric pressure prior to Rn sampling (Fig. 33). The effect that barometric pressure changes have on Rn flux and hence on Rn concentrations was described in the text. Summarily, barometric pressure changes may be viewed as a short term over- or underpressuring of the mine.

With conventional mine ventilation (dilution), changes in barometric pressure experienced above ground are also observed within the mine, however the magnitude of the change below ground may be different from that at ground surface. Alterations of the rate of dilution ventilation produce within the mine, pressure variations similar to those variations resulting from barometric pressure changes.

Results of an attempt to combine large volume dilution with overpressure in the 5702 area are presented, in part, in Fig. 34. The area was held at about 1 cm Hg overpressure during the entire test; the volume of dilution air was varied. Because the air volume requirement was great, dilution air was supplied by fan from poorly ventilated air outside the 5702 area. The Rn concentration in this diluting air was high. This masked convincing results, since one must deal with a small difference between two large numbers. As stated in the text, the increased turbulence resulting from this flow of air



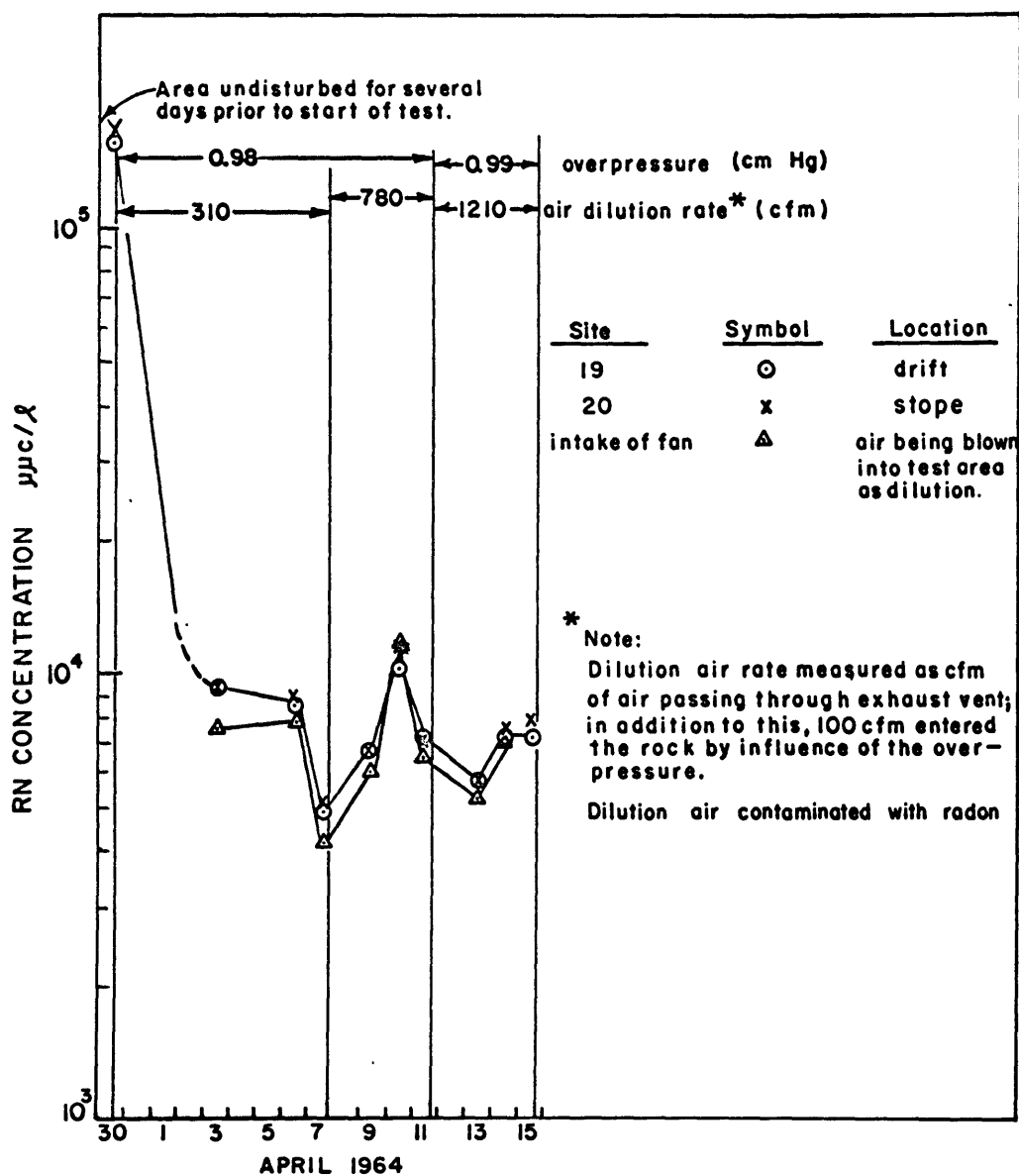


FIGURE 34. AIR RADON CONCENTRATION FOR STATED DILUTION AND OVERPRESSURE CONDITIONS vs. TIME, 5702 AREA.

did not increase the Rn flux above the normal 1 cm Hg overpressure value.

The time period encompassed by the test represented in Fig. 34 was an active one barometrically. Excursions by Rn concentrations from what appear to be stable values for each dilution period are clearly accompanied by opposite trends in barometric pressure as shown by a comparison of data in Fig. 33 and Fig. 34. Calculations of the amount of Rn entering the 5702 area by diffusion may be performed by solution of a steady-state material balance: Rn into 5702 by convection plus Rn in by diffusion equals Rn out of 5702 by convection plus Rn decay. All factors except diffusion are known. Results indicate that diffusion of Rn into the 5702 area remains fairly constant at about  $2.5 \times 10^{-7}$  c/sec during the entire 1 cm Hg overpressure period. The variations in observed Rn concentrations in the 5702 area are the result of barometrically induced changes in the Rn concentration of the large volume of air entering the test area as dilution air. Such changes in the Rn concentration of this air are to be expected. The air originates in a non-overpressured area of the mine ventilated by dilution and, hence, its Rn content is subject to barometric influences. The high Rn concentration in this dilution air measured on 10 April 1964 is the result of a drop in barometric pressure during the hours prior to sampling. The pressure falls more rapidly in the mine tunnel than in the interstices of rock surrounding the tunnel. A pressure gradient is established

which induces flow of interstitial gas, rich in Rn, from the rock into the mine area. The result is as if the mine had been underpressured. Calculation of the diffusion-induced Rn flux from 5702 area rock into the 5702 area during this same period does not show a corresponding increase. Again, overpressuring is seen to decrease the effects which changes in barometric pressure have on the flux of Rn into a mine area.

During the 21-day overpressure test, air Rn concentrations remained remarkably constant (Fig. 29) and yet barometric pressure changes were of the same magnitude and frequency as during these other tests.

On 6 April (1 cm Hg overpressure, 310 ft<sup>3</sup>/min dilution) during a period of stable barometric conditions, the diffusion-produced flux of Rn into the 5702 area was  $2.6 \times 10^{-7}$  c/sec. This is just the flux that was observed during the 21-day, 1 cm Hg, overpressure test. The dilution air was carrying into the test area six times more Rn than that which diffused into the area from the surrounding rocks. Had the diluting air been free of Rn, the equilibrium Rn concentration in the 5702 area would have been approximately 1/4 of the Rn concentration attained during the 21-day test<sup>2</sup>. The Rn daughter-product concentration would have been about 3 WL (25 percent equilibrium between Rn and daughters). That dilution plus overpressure

<sup>2</sup>The factor of 1/4 is obtained from the ratio of air volumes consumed in the tests. In each 1 cm Hg overpressure period 100 ft<sup>3</sup>/min entered the rock surfaces under the influence of the pressure gradient. In the dilution test an additional 310 ft<sup>3</sup>/min were added:  $100/410 \approx 1/4$ .

is effective in reducing the Rn concentration was demonstrated when during a period of 1 cm Hg overpressure in the 5702 area, 130 ft<sup>3</sup>/min total air input (100 ft<sup>3</sup>/min into the rock plus 30 ft<sup>3</sup>/min dilution) reduced the Rn daughter concentration to 8.5 WL (Fig. 31, 10 March 1964).



### 13. Diffusion Coefficient of Radon in Sandstone

From equilibrium interstitial Rn concentration gradients observed in rock surrounding an overpressured area, the observed Rn flux into the overpressured area, and the measured surface area of the room, it is possible to estimate an approximate value for the diffusion coefficient of Rn in sandstone using Fick's first law of diffusion [ Eq.(1) ] .

To facilitate calculations of D, several simplifications were made. The porosity<sup>3</sup> of the rock was assumed to be uniformly 25 percent. Reported porosity values for rocks taken from this mine actually have a wide range but tend to cluster between 20 and 33 percent for rocks similar to those of the foreman's room (L-1). D was assumed to be independent of direction. There may in fact be a directional dependence of D resulting from the layering of the sandstone just as there is a directional dependence of permeability to convective flow in this rock.

These assumptions and the consistent sampling techniques may introduce systematic errors into the results. Values of D estimated from data observed in the foreman's room (Figs.4,5) are presented in Fig. 35. Measurements of D for Rn in other porous media have been performed and the following results were obtained: alluvial flat  $0.036 \text{ cm}^2/\text{sec}$ , glacial debris  $0.02 \text{ cm}^2/\text{sec}$  (S-2). The agreement between these results and the general value of  $0.03 \text{ cm}^2/\text{sec}$  observed in the overpressure experiments

<sup>3</sup>Porosity is the ratio of void volume to total volume of rock (i.e., volume of solids plus voids).

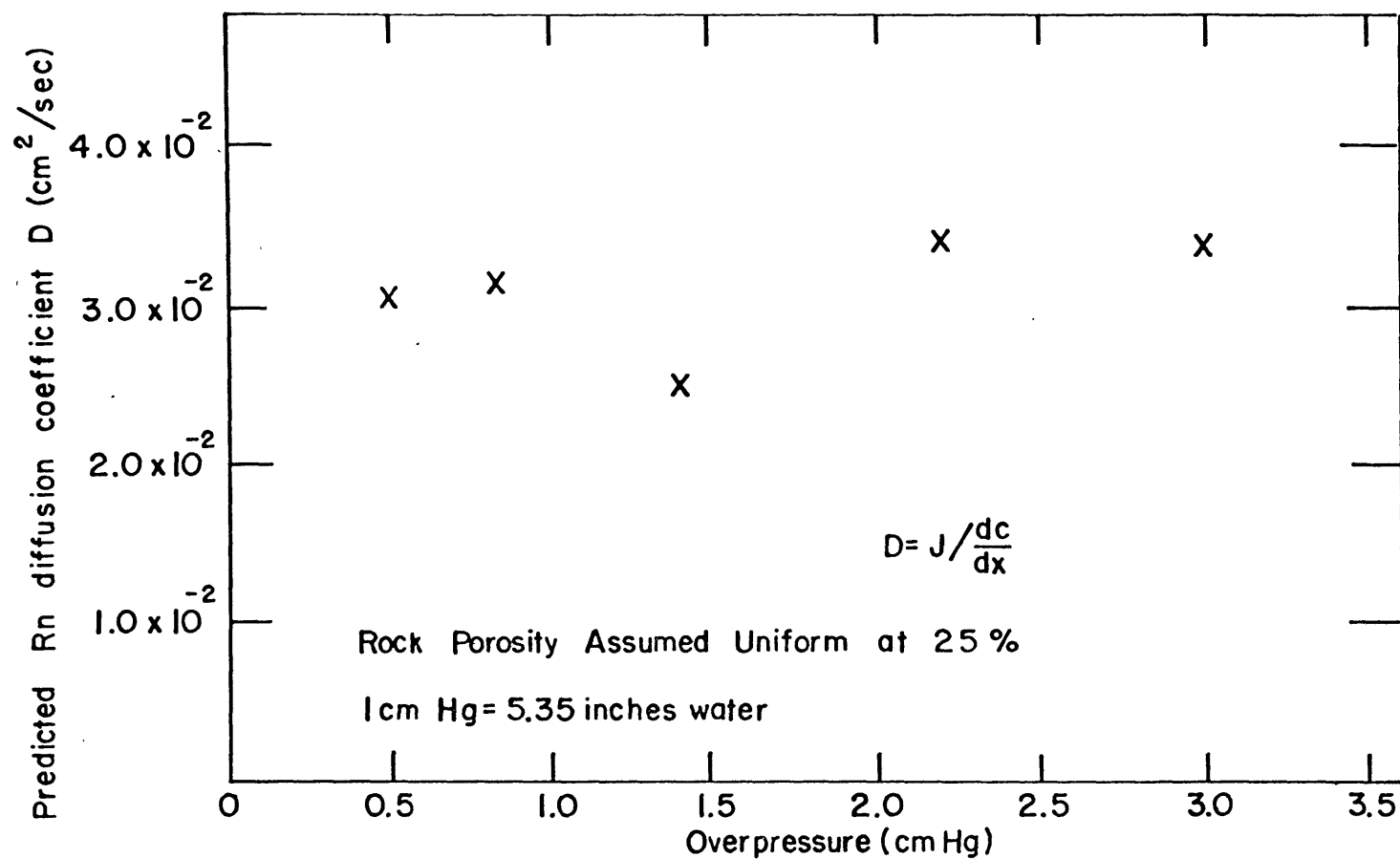


FIGURE 35. RADON DIFFUSION COEFFICIENT ( $D$ ) AS PREDICTED FROM INTERSTITIAL RADON CONCENTRATION GRADIENT ( $\frac{dc}{dx}$ ) IN BULK ROCK AND OBSERVED RADON FLUX ( $J$ ) ACROSS TOTAL ROCK SURFACE VS. OVERPRESSURE, FOREMAN'S ROOM

tends to indicate the validity of the initial assumption that diffusion acts independently of convection once an overpressure concentration gradient is established.

#### 14. Permeability of Test Site Environment

Samples of sandstone and shale were taken from the 5702 area and the foreman's room in order to determine the permeability of the rock environment of these areas. Rock specimens were sealed in plastic to preserve their in-situ moisture content and were then shipped to M.I.T. for permeability analysis. Figure 36 schematically describes the apparatus used for permeability measurement. In Fig. 36,  $P_1$ ,  $T_1$ , and  $P_2$ ,  $T_2$  represent the pressure and temperature of the nitrogen measured at the indicated points. The pressure measurements taken on manometers determined the pressure gradient across the rock sample. The pressure and temperature of the nitrogen determine its viscosity. In practice, the three indicated temperature probes showed the same temperature to within  $1^\circ\text{C}$ . The downstream pressure,  $P_2$ , was held to within 0.5 cm of water of atmospheric pressure. The volume rate of gas flow was monitored on the indicated wet-test meter.

The formula describing permeability for a compressible fluid is:

$$k = -\frac{Q}{a} \frac{\mu L^2 P_o}{(P_L^2 - P_o^2)} \quad (25)$$

where  $k \equiv$  permeability coefficient of the porous medium ( $\text{cm}^2$ )

$Q \equiv$  volume flow rate of gas ( $\text{cm}^3/\text{sec}$ ) at  $P_o$

$L \equiv$  length of the rock sample (cm)

$P_o \equiv$  pressure on the upstream side of the rock sample  
( $\text{g/cm sec}^2$ )

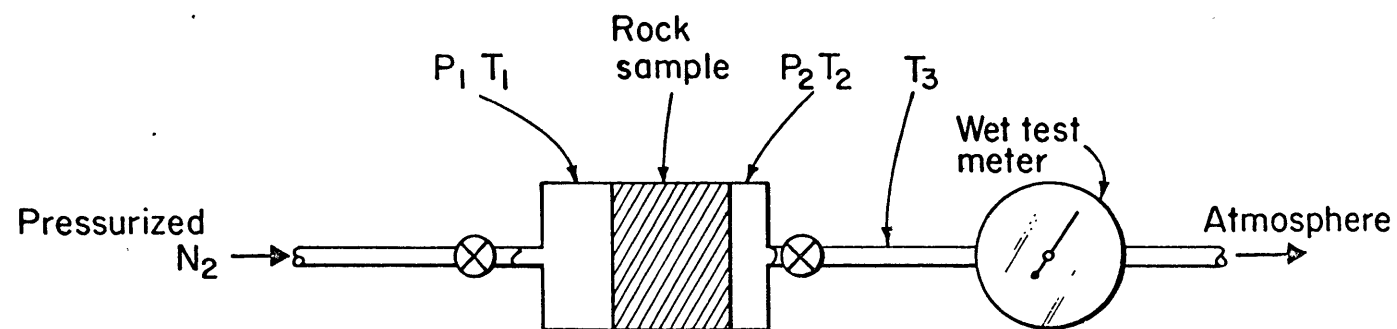


FIGURE 36. APPARATUS FOR DETERMINATION OF PERMEABILITY OF ROCK SAMPLES

$P_L \equiv$  pressure on the downstream side of the rock  
sample ( $\text{g/cm sec}^2$ )

$\mu \equiv$  viscosity of the gas (poise =  $\text{g/sec cm}$ )

$a \equiv$  cross sectional area of the rock ( $\text{cm}^2$ )

The metric units of the components of Eq. (25) are stated. Note that in essence the permeability coefficient is an empirical proportionality factor relating the quantity of gas flowing through a given porous medium to the flow-inducing pressure gradient across the porous medium.

Table 3 lists measured permeabilities of samples from the 5702 area and the foreman's room. The variation of permeability among the samples and the consistently lower permeability in the direction perpendicular to the planes of stratification as compared with permeability parallel to planes of stratification for a given sample are common for sandstone.

TABLE 3.

Permeability of Sandstone from Foreman's Room and 5702 Area

<u>Sample No.</u>	<u>Origin</u>	<u>Description</u>	<u>Permeability (cm<sup>2</sup>)</u>	
			<u>Parallel to bedding</u>	<u>Perpendicular to bedding</u>
1	foreman's room	gray sandstone	$22.0 \times 10^{-9}$	$14.5 \times 10^{-9}$
6*	5702 area	gray sandstone	$27.8 \times 10^{-9}$	$26.3 \times 10^{-9}$
6*	5702 area	gray sandstone		$26.2 \times 10^{-9}$
3	5702 area	gray sandstone	$54.6 \times 10^{-9}$	$33.2 \times 10^{-9}$
5	5702 area	black-green sandstone, strongly cemented	$78.2 \times 10^{-9}$	$61.2 \times 10^{-9}$

Shale was tested but yielded no measurable flow of gas with pressure gradients up to 8 cm Hg per cm of shale.

\*The bedding planes on this sample were extremely undefined; all other samples had obvious markings.

# 15. Permeability of the Mathematically Transformed Mine Environment

The coordinate transformation, Eq. (14), which converts Eq. (13) into Laplace's equation also reduces the real world system of anisotropic permeability to an isotropic system (see main text). The permeability of this isotropic system can be shown to be  $k_y$ .

The coordinate transform was:

$$X = \frac{x}{\sqrt{k_x/k_y}}; \quad Y = y; \quad Z = \frac{z}{\sqrt{k_z/k_y}} \quad (14)$$

Let velocities in the transformed system be denoted by  $Q$  and velocities in the untransformed system by  $q$ .

$$Q_X = \frac{\partial X}{\partial t} = \frac{\partial x}{\partial t} \sqrt{\frac{k_y}{k_x}} = q_x \sqrt{\frac{k_y}{k_x}} \quad (26)$$

Also

$$Q_X = -\frac{k_X}{\mu} \frac{\partial P}{\partial X} \quad (\text{Darcy's Law}) \quad (27)$$

and

$$\frac{\partial P}{\partial X} = \frac{1}{\sqrt{k_y/k_x}} \frac{\partial P}{\partial x} \quad (28)$$

Thus

$$Q_X = -\frac{k_X}{\mu} \frac{1}{\sqrt{k_x/k_y}} \frac{\partial P}{\partial x} \quad (29)$$

$$q_x = -\frac{k_x}{\mu} \frac{\partial P}{\partial x} \quad (\text{Darcy's Law}) \quad (30)$$



Recalling Eq. (26), we have

$$Q_X = -\frac{k_X}{\mu} \frac{1}{\sqrt{k_Y k_X}} \frac{\partial P}{\partial x} = -\frac{k_X}{\mu} \sqrt{\frac{k_Y}{k_X}} \frac{\partial P}{\partial x} \quad (31)$$

Solving for  $k_X$

$$k_X = k_Y$$

Similar arguments for the Y and Z directions show that the system is of isotropic permeability.

# 16. Comparison of Observed and Predicted Rates of Air Consumption in the Foreman's Room

Figure 37 presents pressures observed in the interstices of rock surrounding the foreman's room during overpressure experiments. Applying the geometric approximation of the foreman's room shown in Fig. 38 and using these pressure data, in conjunction with the theoretical statement of the convective flow into the walls of an elliptical tunnel, Eq. (16), the volume flow rate into the walls of the foreman's room may be predicted. To predict the flow into the planar ends of the area, a form of Eq. (25) is used (S-1):

$$Q_o = -\frac{k}{u} \frac{(P_L^2 - P_o^2)}{L} \cdot \frac{a}{2P_o} \quad (32)$$

where  $a$  = area of flow

$P_o$  = total room pressure

$P_L$  = total pressure observed at depth  $L$  within the rock.

The total air flow will be approximated by the sum of the flow through the ends and walls of the room. Figure 39 shows the observed air consumption as a function of overpressure, for several sealings of the room and the predicted air consumption. The predicted consumption shown is based on pressure data observed at probe 26. Predictions by data from other probes

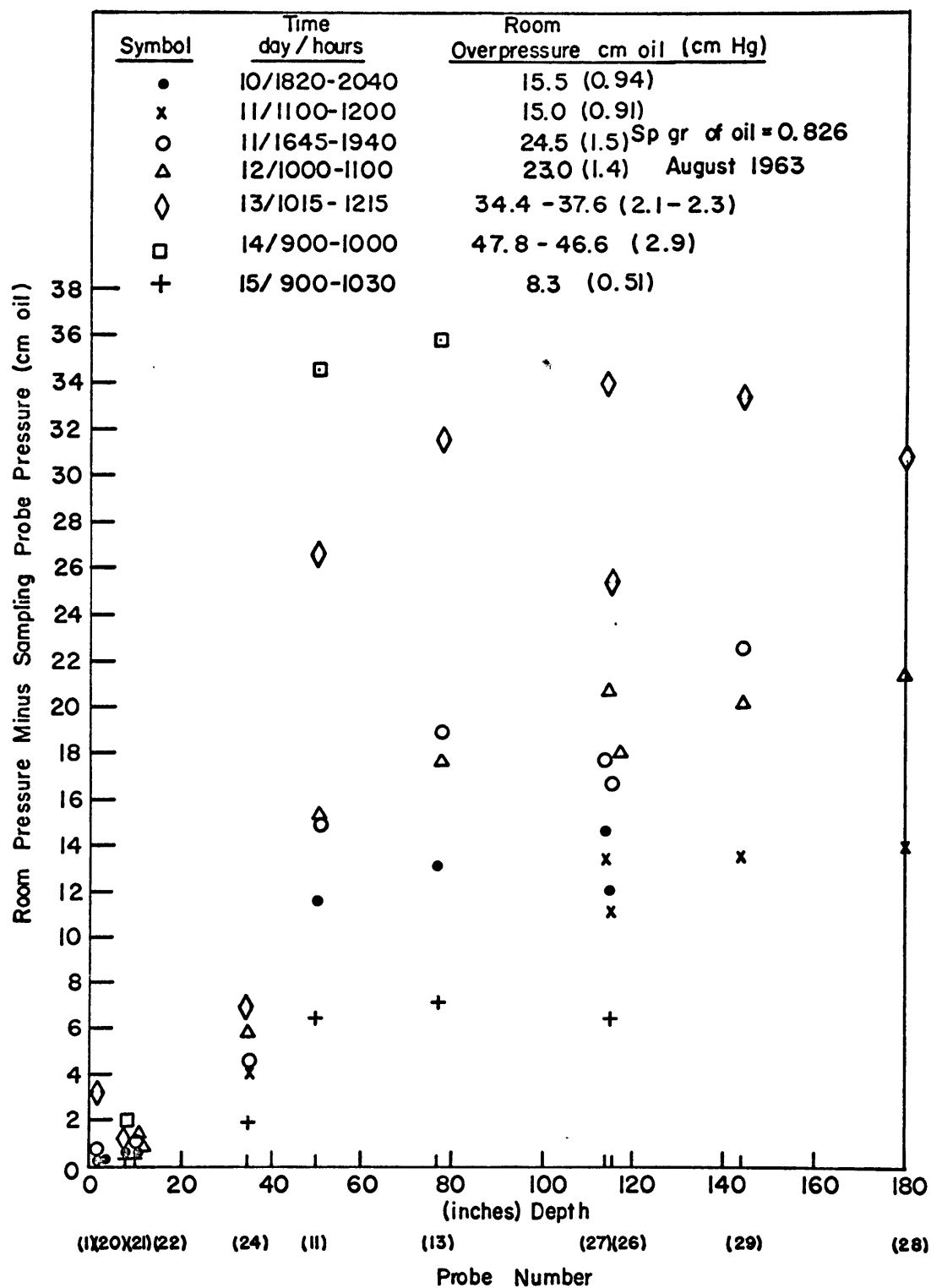


FIGURE 37. PRESSURE DIFFERENCE BETWEEN SAMPLING PROBE AND TEST AREA FOR STATED OVERPRESSURE VS. DEPTH, FOREMAN'S ROOM

- Profile of Foreman's, level 1-4, mine section 24
- Approximation of cross section of Foreman's Room

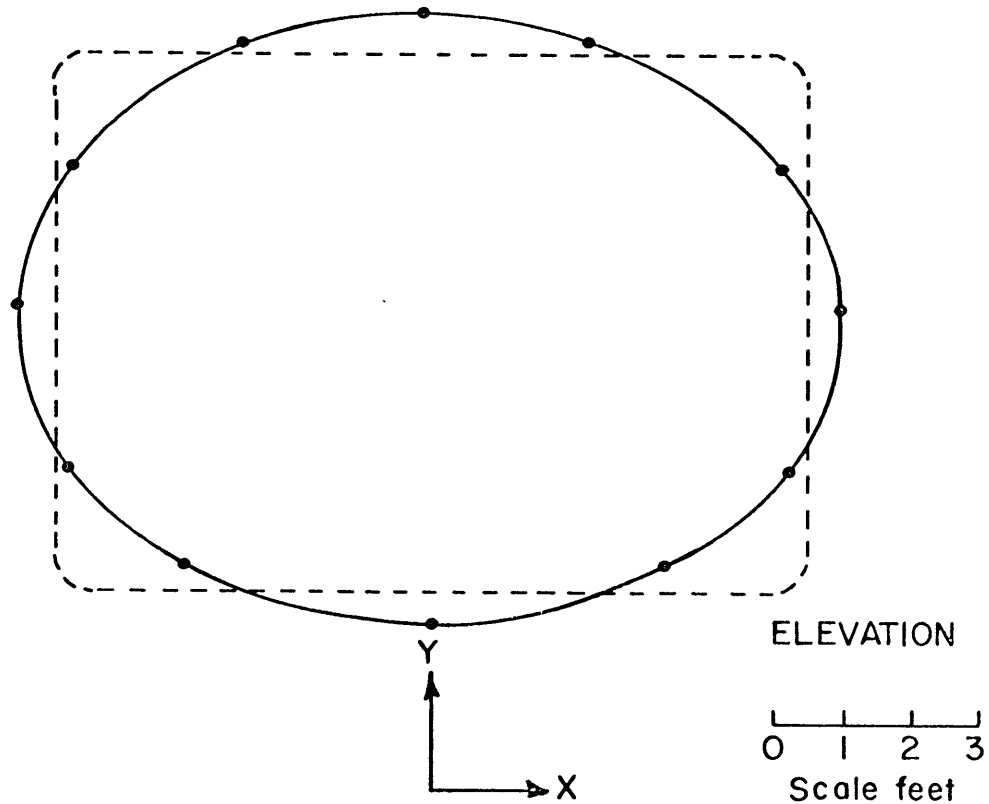


FIGURE 38. APPROXIMATION OF THE PROFILE OF FOREMAN'S ROOM

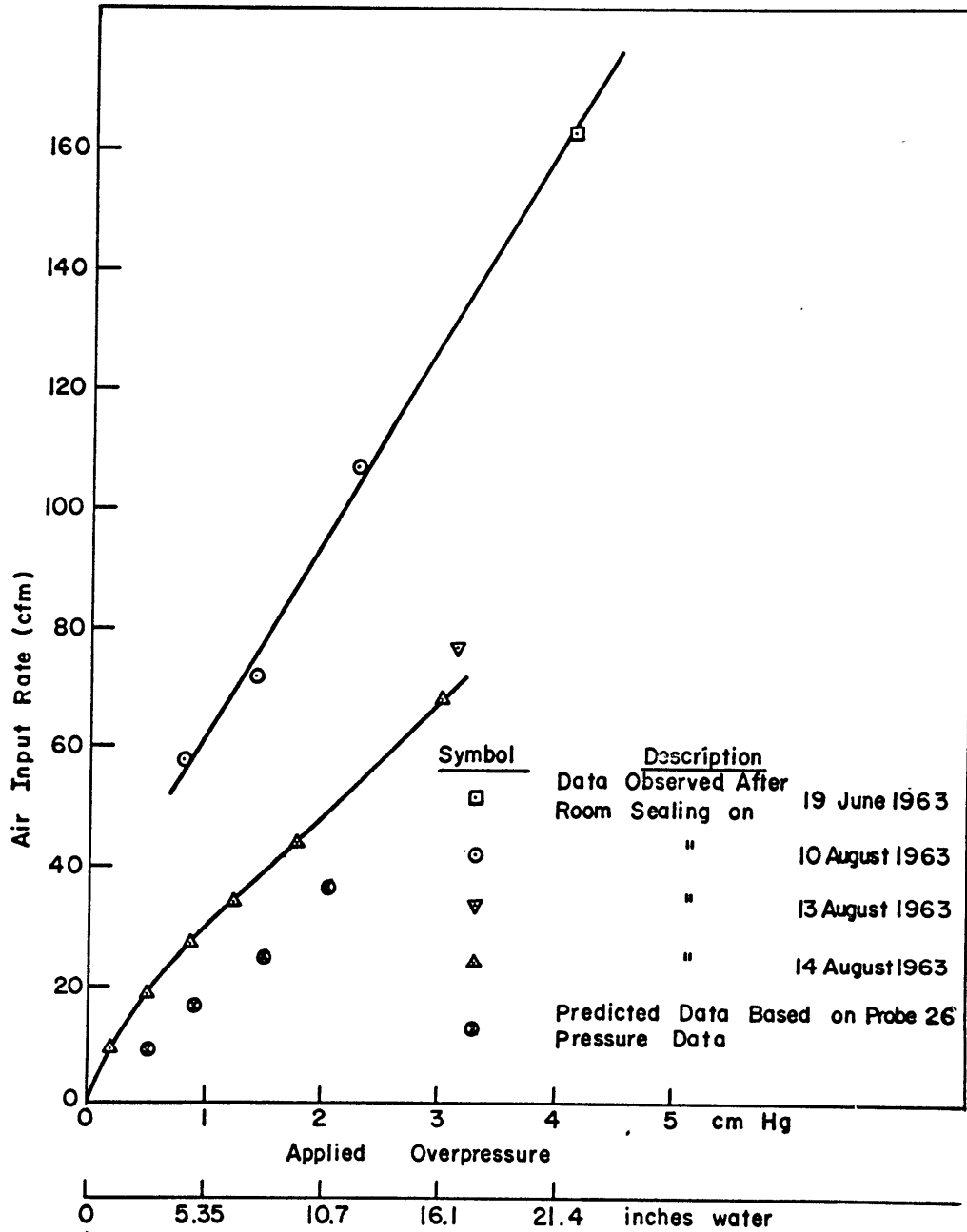


FIGURE 39. OBSERVED AND PREDICTED AIR INPUT RATE TO FOREMAN'S ROOM DURING OVERPRESSURE VS. APPLIED OVERPRESSURE

(excluding the very shallow probes where the elliptical approximation of the room is invalid) yield air consumptions that fall between the probe 26 predicted data and the data observed for the final sealing of the room. The effect of the several resealings of the room is evident from the decrease in air consumption with subsequent sealings. Note that there was only slight reduction in air consumption between the last two sealings. Most of the leaks had been removed.

17. Theoretical Description of Interstitial Radon  
Concentrations in Rock Adjacent to a Mine Tunnel  
During Non-pressure Conditions

A theoretical statement of the steady-state Rn concentrations within the wall surrounding a non-pressured mine is given by Eq. (4):

$$\frac{\partial C}{\partial t} = 0 = D \text{ lap } C + \varphi - \lambda C \quad (4)$$

Recall that the Rn production term has the value

$$\varphi = \lambda [EC_{\infty} - (E - 1)C] \quad (23)$$

Expanding the lap C for the case of an infinite cylinder (a long tunnel) and introducing into Eq. (4), Eq. (23) for  $\varphi$  yields

$$0 = D \frac{\partial^2 C}{\partial r^2} + \frac{D}{r} \frac{\partial C}{\partial r} - \lambda C + \lambda [EC_{\infty} - (E - 1)C] \quad (33)$$

where  $r$  = radius.

Multiplying Eq. (33) by  $r^2/D$  and simplifying gives:

$$0 = r^2 \frac{\partial^2 C}{\partial r^2} + r \frac{\partial C}{\partial r} + r^2 \left( \frac{\lambda EC_{\infty} - \lambda EC}{D} \right) \quad (34)$$

The homogeneous form of Eq. (34) is obtained by substitution of  $C = C' + C_{\infty}$ .

$$r^2 \frac{\partial^2 C'}{\partial r^2} + r \frac{\partial C'}{\partial r} - r^2 \frac{\lambda E}{D} C' = 0 \quad (35)$$

This equation is satisfied by the Bessel function of zero order (H-1):

$$C' = Z_0 \left( i \sqrt{\frac{\lambda E}{D}} r \right) = A I_0 \left( \sqrt{\frac{\lambda E}{D}} r \right) + B K_0 \left( \sqrt{\frac{\lambda E}{D}} r \right) \quad (36)$$

where  $Z_0$  ( $i \sqrt{\lambda E/D} r$ ),  $I_0$  ( $\sqrt{\lambda E/D} r$ ), and  $K_0$  ( $\sqrt{\lambda E/D} r$ ) are conventional notations for Bessel functions of zero order, and A and B are constants.

Reintroducing C for C', Eq. (36) becomes:

$$C = \left[ A I_0 \left( \sqrt{\frac{\lambda E}{D}} r \right) + B K_0 \left( \sqrt{\frac{\lambda E}{D}} r \right) \right] + C_\infty \quad (37)$$

By nature of the particular Bessel functions (H-1, W-1)

$$I_0 \left( \sqrt{\frac{\lambda E}{D}} r \right) \rightarrow \infty \text{ as } r \rightarrow \infty$$

$$K_0 \left( \sqrt{\frac{\lambda E}{D}} r \right) \rightarrow 0 \text{ as } r \rightarrow \infty$$

Boundary conditions of the physical conditions within the mine environment are

$$C \rightarrow C_0 \text{ at } r = r_0$$

where  $r_0$  = radius of the tunnel

$C_0$  = Rn concentration in the surface layer of the rock

and

$$C \rightarrow C_\infty \text{ as } r \rightarrow \infty$$

where  $C_\infty$  = constant Rn concentration measured at great depths in the rock interstices.

Substituting the second boundary condition into Eq. (37) and



considering the nature of  $I_0 (\sqrt{\lambda E/D} r)$  and  $K_0 (\sqrt{\lambda E/D} r)$ , we find that  $A = 0$  since  $C$  does not become infinite at great depths.

From the above

$$C = BK_0 \left( \sqrt{\frac{\lambda E}{D}} r \right) + C_\infty \quad (38)$$

Substituting the first boundary condition,  $C \rightarrow C_0$  at  $r = r_0$ , into Eq. (38):

$$B = (C_0 - C_\infty) \left[ \frac{1}{K_0 (\sqrt{\lambda E/D} r_0)} \right] \quad (39)$$

and introducing this value of  $B$  into Eq. (38) gives

$$C = (C_0 - C_\infty) \frac{K_0 (\sqrt{\lambda E/D} r)}{K_0 (\sqrt{\lambda E/D} r_0)} + C_\infty \quad (40)$$

Equation (40) is the theoretical non-overpressure, steady-state solution of the Rn concentration gradient in rock surrounding a cylindrical tunnel located in a rock uniform in Rn diffusion and Ra characteristics.

Figure 40 shows the function generated by Eq. (40) for an environment that approximates the foreman's room. Included in the figure are interstitial Rn concentrations observed in the rock surrounding the foreman's room. The agreement between data and theory is fairly good. That the observed data lie

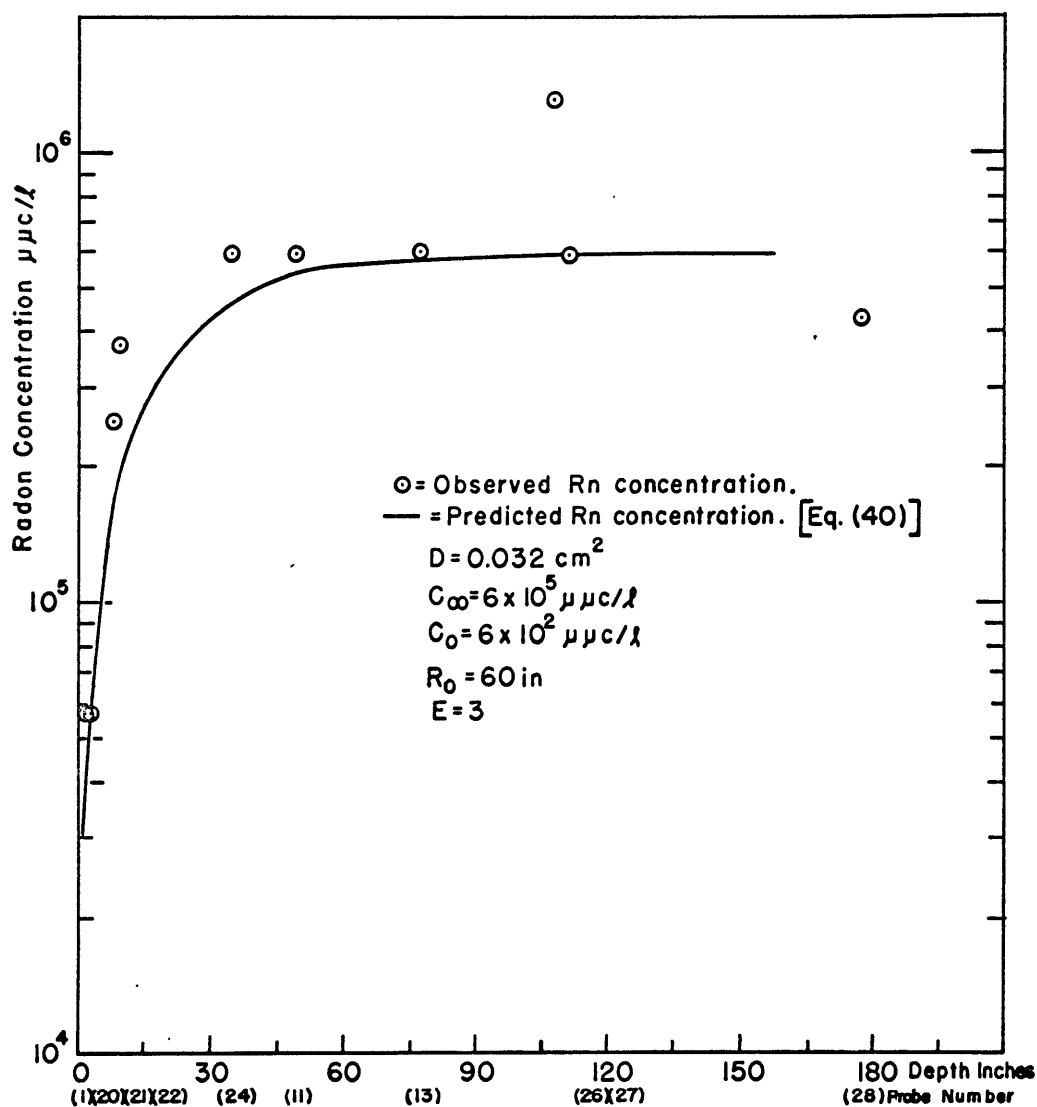


FIGURE 40. THEORETICALLY PREDICTED INTERSTITIAL CONCENTRATIONS IN ROCK SURROUNDING A 10 FOOT DIAMETER TUNNEL AND INTERSTITIAL RADON CONCENTRATIONS OBSERVED IN ROCK ADJACENT TO FOREMAN'S ROOM vs DEPTH; NORMAL PRESSURE.

above the prediction may, in fact, be indicative of an under-pressure in the area. The mine, at the time of sampling, was being ventilated by use of an exhaust fan at a shaft distant from the foreman's room. Such a system of ventilation requires by its very principle of operation that the pressure within the mine be less than local barometric pressure.

18. Derivation of Equation (24), an Analytic Description of Interstitial Radon Concentrations in Rock Surrounding an Overpressured Area.

The theoretical description of the interstitial Rn concentration in rock surrounding an overpressured area is given by Eq. (21) (see main text):

$$\begin{aligned} & \frac{D}{a^2 (\cosh^2 u - \cos^2 v)} \left( \frac{\partial^2 C}{\partial u^2} + \frac{\partial^2 C}{\partial v^2} \right) + \\ & + \frac{k}{s\mu a^2 (\cosh^2 u - \cos^2 v)} \frac{\partial C}{\partial u} + \varphi - \lambda C = 0 \end{aligned} \quad (21)$$

This equation does not have an analytic solution; however, a study of the numerical solution will show that certain simplifications can be justified.

Substituting Eq. (23),  $\varphi = \lambda[EC_\infty - (E-1)C]$ , into Eq. (21) yields

$$\begin{aligned} & \frac{D}{a^2 (\cosh^2 u - \cos^2 v)} \left( \frac{\partial^2 C}{\partial u^2} + \frac{\partial^2 C}{\partial v^2} \right) + \\ & + \frac{k}{s\mu a^2 (\cosh^2 u - \cos^2 v)} \frac{\partial C}{\partial u} - \lambda EC + \lambda EC_\infty = 0 \end{aligned} \quad (41)$$

The term  $\lambda EC_\infty$  is constant. The homogeneous form of Eq. (41) is obtained by setting  $C = C^* + C_\infty$ :

$$\frac{D}{a^2 (\cosh^2 u - \cos^2 v)} \left( \frac{\partial^2 C^*}{\partial u^2} + \frac{\partial^2 C^*}{\partial v^2} \right) + \frac{k R}{s_\mu a^2 (\cosh^2 u - \cos^2 v)} \frac{\partial C^*}{\partial u} - \lambda E C^* = 0 \quad (42)$$

Equation (42) is separable into two equations dependent upon  $u$  and  $v$  respectively.

$$\text{Letting } C^*(uv) = \sum U(u) V(v) \quad (43)$$

and multiplying by  $a^2 (\cosh^2 u - \cos^2 v)$ :

$$DU'' V + DV'' U + \frac{kR}{s_\mu} U' V - \lambda E a^2 (\cosh^2 u - \cos^2 v) UV = 0 \quad (44)$$

Separating Eq. (44)

$$DU'' + \frac{kR}{s_\mu} U' - (\lambda E a^2 \cosh^2 u + K) U = 0 \quad (45a)$$

$$DV'' + (\lambda E a^2 \cos^2 v + K) V = 0 \quad (45b)$$

where  $K$  is the separation constant.

Neither Eq. (45a) nor (45b) are solvable in analytic form. Equation (45b) has for its solution a Mathieu function (M-1) which, for the parameters obtained from a mine problem, is similar to, but is not exactly, a cosine. As  $v$  varies from 0 to  $\frac{\pi}{2}$  the function will experience its full range of values. The first term of the series of Mathieu functions that will comprise the final solution [indicated by  $\sum$  in Eq. (43)] is equal to one, the second term has a maximum variation of less than 5 percent. This indicates the very slight angular ( $v$ ) dependence of  $C^*$ , and hence  $C$ , in the transformed (isotropic

permeability) system when one studies this system in elliptical coordinates.

Equation (45a) is not described by any well-known function. Figure 41 presents the numerical solution to Eq. (45a), obtained on an analog computer, and based on the geometry, rock, and pressure environment of the foreman's room during 1.4 cm Hg overpressure. Three solutions to Eq. (45a) are presented for the identical conditions of 1.4 cm Hg overpressure but using 3 values of  $D$ : 0.03, 0.1, and 1.0  $\text{cm}^2/\text{sec}$ . The value of 0.03  $\text{cm}^2/\text{sec}$  is believed to be the most accurate estimate; the other values are used for comparison.  $E$  is taken as equal to one for this comparison since this will emphasize the significance of the diffusion term with respect to the contribution of the production term. It is at once evident that the solution to Eq. (45a) is not very sensitive to changes in  $D$ . A 3.3-fold increase in  $D$  from the estimated true value produces essentially no change in the solution. A 33-fold increase in  $D$  produces only a slight change in the curve. Since the diffusion term contributes little to the solution, Eq. (6) and Eq. (41) may be simplified by removing this term. Equation (41) becomes

$$\frac{k}{s\mu a^2} \frac{R}{(\cosh^2 u - \cos^2 v)} \frac{\partial c}{\partial u} - \lambda EC + \lambda EC_{\infty} = 0 \quad (46)$$

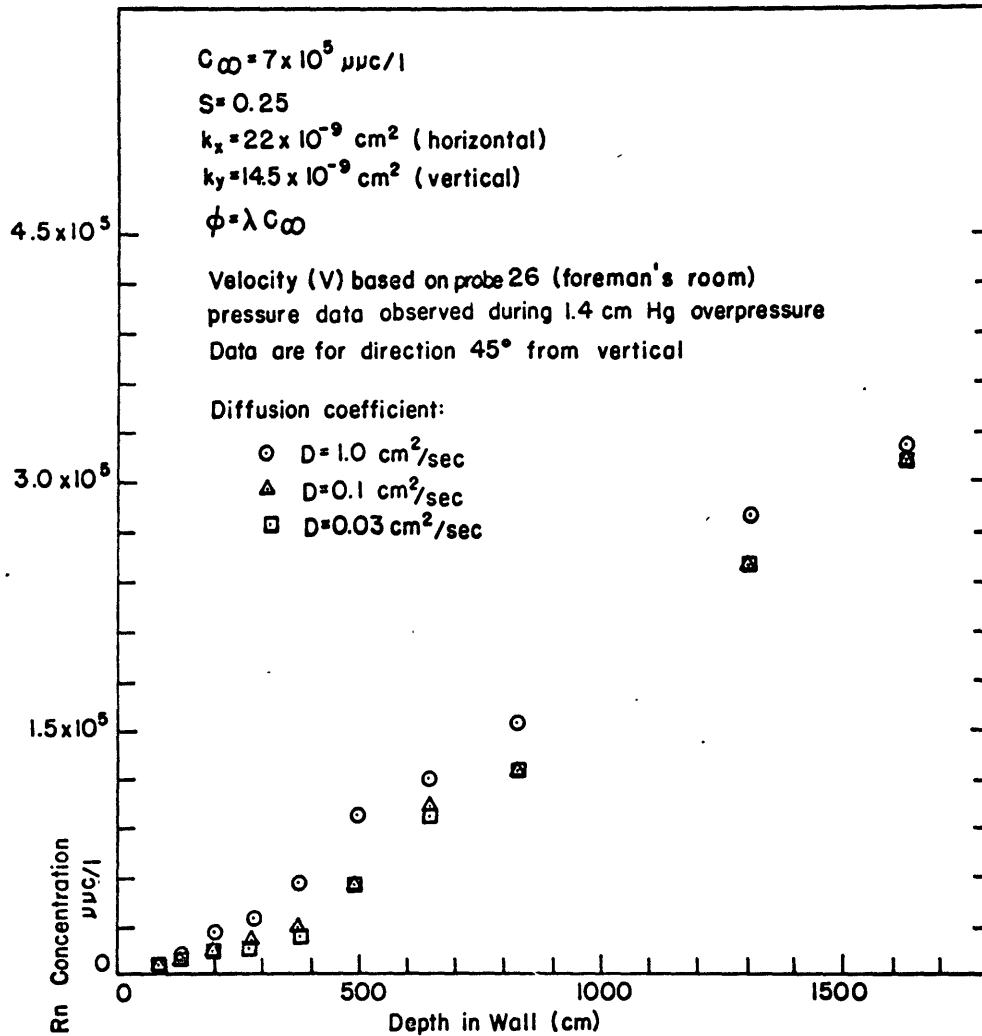


FIGURE 41: SOLUTIONS OF  $D \nabla^2 C - \frac{1}{S} \text{div}(VC) + \phi - \lambda C = 0$  USING STATED PARAMETERS

Equation (46) has the analytic solution

$$C = C_{\infty} + F \exp \left[ \frac{\lambda s E}{k R} \mu a^2 \left( \frac{u}{2} + \frac{1}{4} \sinh 2u - u \cos^2 v \right) \right] \quad (24)$$

where  $F$  is a constant determined by the  $Rn$  concentration on the wall of the tunnel.

Figure 42 presents the solution of Eq. (41), the complete statement, and Eq. (46), the simplified statement, for conditions of 1.4 cm Hg overpressure in the foreman's room. The concentrations are those predicted for a  $45^\circ$  angle with respect to the plane of sedimentation and for  $D = 0.03 \text{ cm}^2/\text{sec}$ . To a depth of 500 cm (16.4 ft) the two equations yield similar results. Because Eq. (46) has an analytic solution it is desirable to work with it in comparing predicted and observed data.



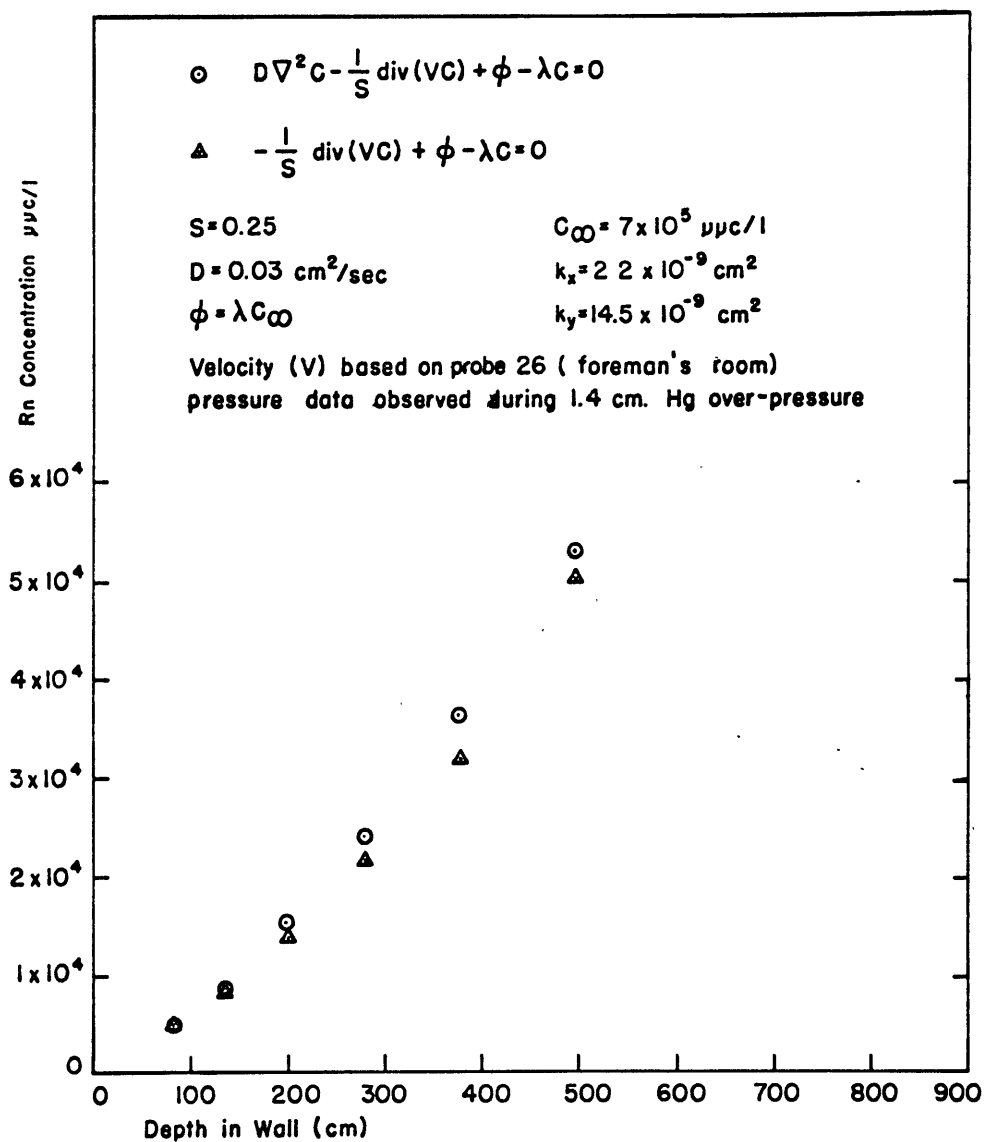


FIGURE 42. SOLUTIONS OF  $D \nabla^2 C - \frac{1}{S} \text{div}(VC) + \phi - \lambda C = 0$   
AND  $-\frac{1}{S} \text{div}(VC) + \phi - \lambda C = 0$

## 19. Determination of Interstitial Radon Production Rate in Rocks for Low and High Interstitial Radon Concentrations

The use of Eq. (23),  $\phi = \lambda[EC_{\infty} - (E - 1)C]$ , requires an empirical determination of the value of  $E$ , the ratio of interstitial Rn production rate in regions of low interstitial Rn concentrations to the production rate in regions of high Rn concentrations. Interstitial Rn production rate in a high Rn atmosphere was measured by allowing sealed rock specimens to accumulate Rn for periods of time that would indicate near equilibrium in Rn growth. The interstitial gas of the rock was then sampled and the production rate estimated using Eq. (22),  $\phi = \lambda C_{\infty}$ . The rate of Rn production is just equal to the rate of decay.

The interstitial Rn production rate in regions of low Rn concentration was determined by purging the rock samples for long periods of time with Rn-free nitrogen and measuring the flow rate and Rn concentration in the effluent stream. The production rate,  $\phi$ , = curies Rn/liter in effluent stream x liter/sec purge rate. Purge rate was measured on a calibrated wet test meter.

Values of  $E$  are listed in table 4. Each determination was carried out at least 3 times. It was necessary to purge the samples for greater than 15 hours to be certain that the

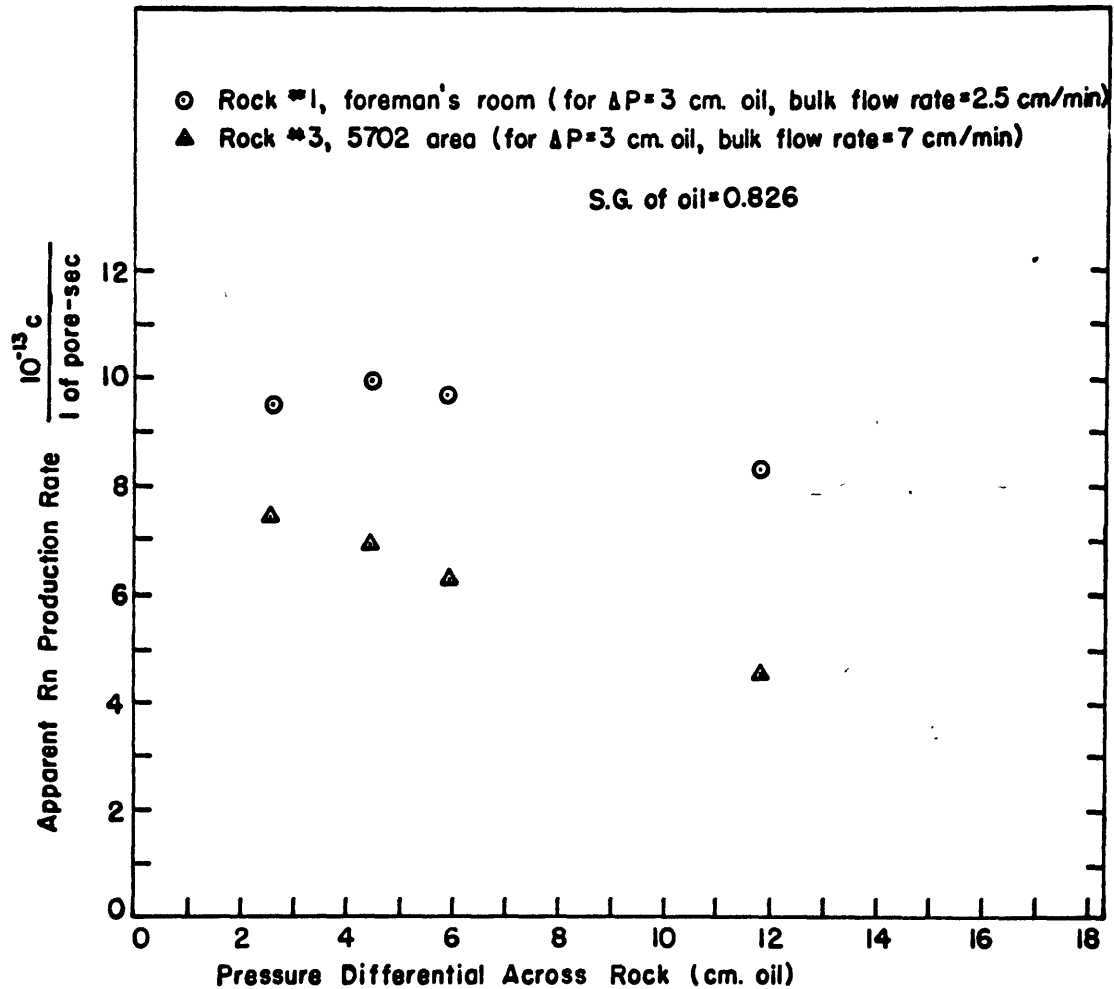
production rate had equilibrated. This indicates the time required for Rn in a particle of rock to come into equilibrium with the interstitial Rn surrounding that particle.

TABLE 4.

Values of E: Ratio of Interstitial Radon Production Rate in Low Radon Atmosphere to Interstitial Production Rate in High Radon Atmosphere.

<u>Rock Sample</u>	<u>Origin</u>	<u>E</u>
1	Foreman's room	3.7
3	5702 area	2.2
6	5702 area	2.0

It is of interest to note that the Rn production rate during purging appeared to be a function of the pressure difference across the rock. The velocity of the purging gas is directly proportional to the pressure difference. The negative trend of the apparent production rate with increasing pressure difference seen in Fig. 43 indicates that at any given purge rate the efficiency of the gas is less than the theoretical maximum. In determining E the production rate measured during the slowest flow, usually about 5 cm/min. linear bulk flow rate, was used.



APPARENT INTERSTITIAL RADON PRODUCTION RATE AS  
 DETERMINED BY PURGING VS PRESSURE DIFFERENTIAL  
 ACROSS ROCK SAMPLE

FIGURE 43

## 20. Radon and Radium in Mine Recycle Waters

The concentrations of Rn and Ra in recycle waters were measured in water samples from the 09 and 02 drifts, mine section 24, and from the 57 drift in the vicinity of the 57-02 raise, mine section 26. Recycle water is that water which is pumped through the interstices of low-grade U-bearing sandstone in an attempt to leach U from the stone. Determination of the Rn content of the water is of interest since this water may be a significant source of Rn in the mine atmosphere. The Ra may be an indicator of the dissolved U content of the water.

As the recycle water percolates through the rock interstices prior to entering the mine it is in intimate contact with the Rn-rich interstitial gas occupying these interstices. At 60<sup>0</sup>F. the Rn distribution coefficient between water and air is about 0.3. Thus significant quantities of Rn may dissolve in the water. This Rn will be liberated when the water enters the less Rn-rich gas of the rock immediately surrounding a mine and of the mine itself.

Figure 44 is a plan view of one of the two areas in which water was sampled. Figures 45 and 46 show Rn and Ra concentrations in the water samples taken in this area. Figure 47 shows the Rn concentration in the air immediately above this water. In all the measured cases, the ratio of the concentrations of Rn in water to Rn in the air above the water is greater than

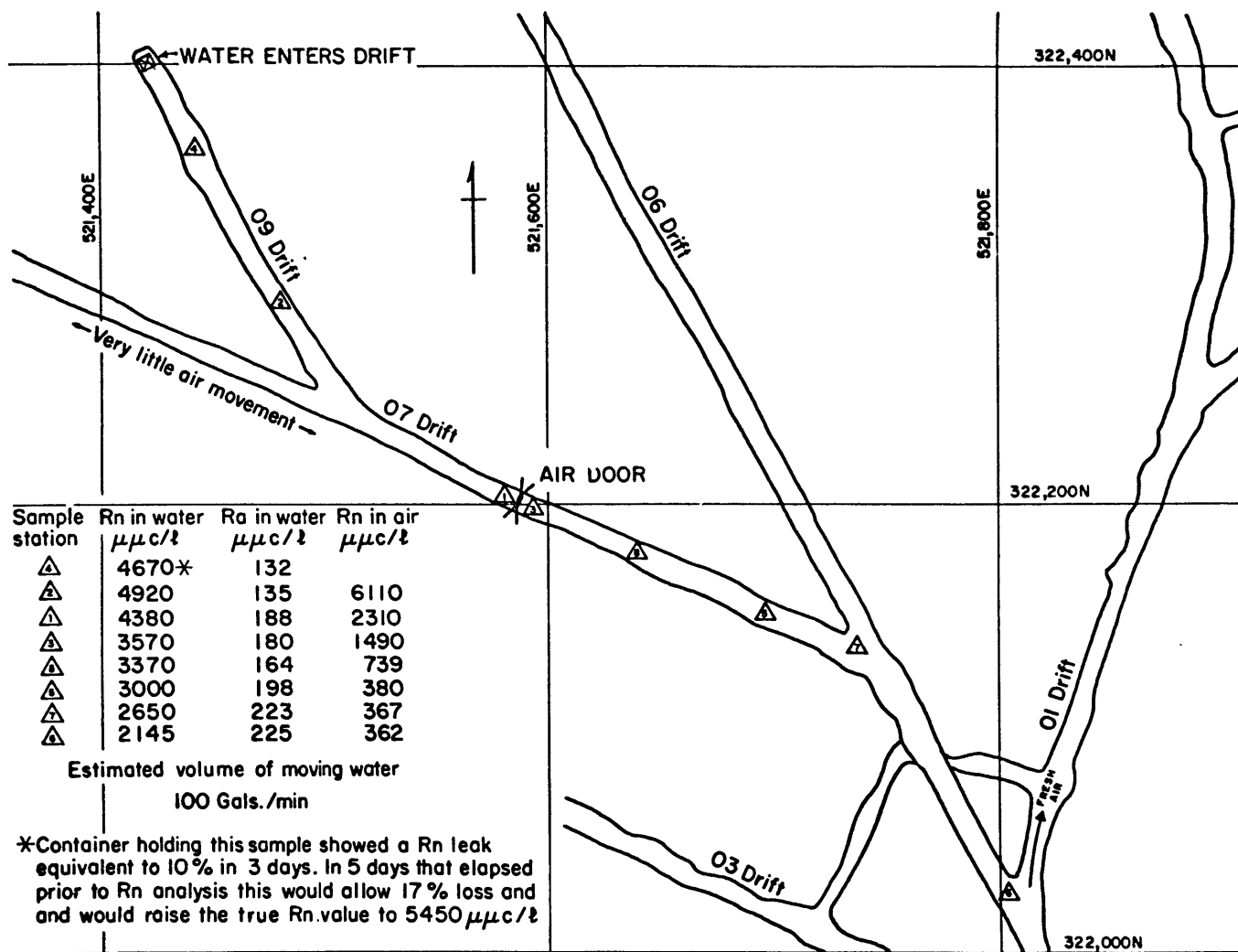


FIGURE 44. PLAN VIEW OF WATER AND AIR SAMPLING AREA  
20 SEPTEMBER, 1963

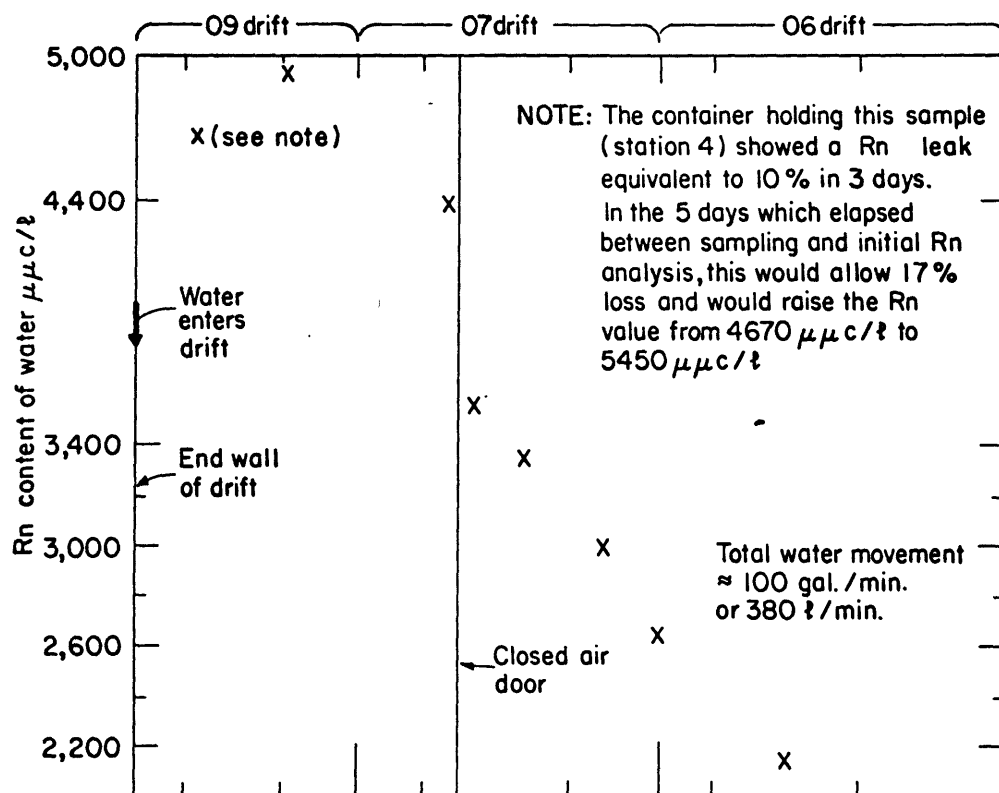


FIGURE 45. RADON CONTENT OF WATER VS. DISTANCE OF FLOW IN DRIFT

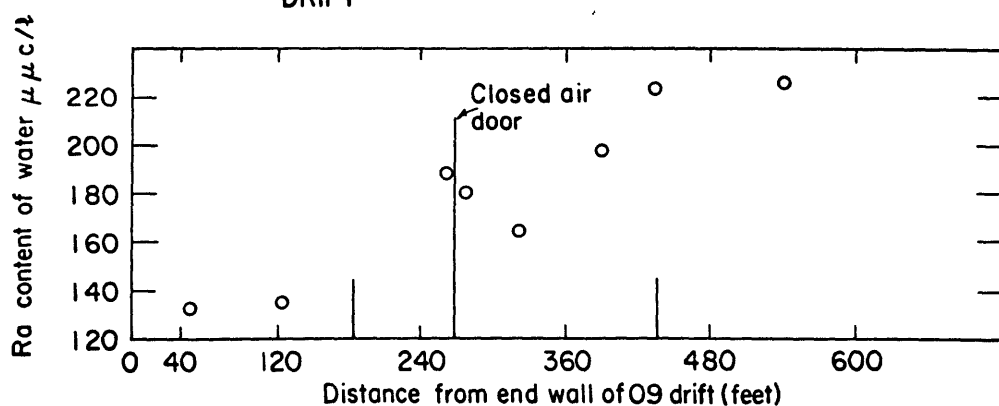


FIGURE 46. DISSOLVED RADIUM CONTENT OF WATER VS. DISTANCE OF FLOW IN DRIFT

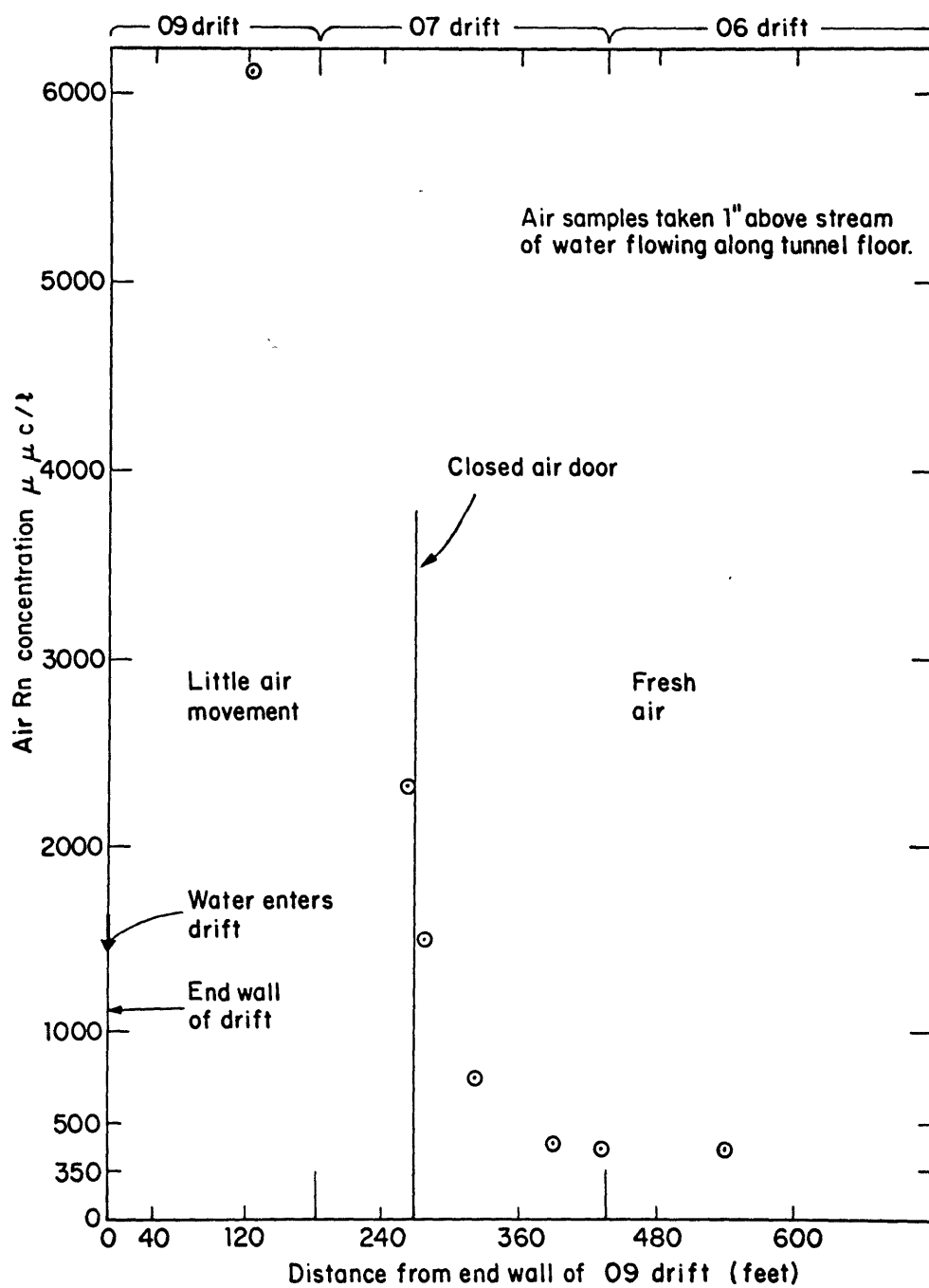


FIGURE 47. RADON CONCENTRATION IN AIR VS. DISTANCE FROM END OF 09 DRIFT



the distribution coefficient for Rn between water and air will allow (compare Fig. 45 and Fig. 47). As the water flows along the drift floor it gives up Rn to the atmosphere in an attempt to come into Rn equilibrium. This accounts for the continual decrease of the Rn concentration in the water.

The estimated flow of water within the tunnel is 100 gal/min. (380 l/min.). If the Rn, which leaves the water as the water flows through the tunnel, enters the tunnel atmosphere (as is probable), then this water adds approximately  $1.1 \times 10^6$   $\mu\text{c/min.}$  of Rn to the air of the studied portion of the tunnel. Estimating the surface area of the stream to be  $1.76 \times 10^6 \text{ cm}^2$ , the average flux of Rn from the water into the air is  $1 \times 10^{-14} \text{ c/cm}^2 \text{ sec.}$  The Rn flux from sandstone into the mine atmosphere measured in the 1-4 level foreman's room in June 1963 was  $4.0 \times 10^{-14} \text{ c/cm}^2$ . These two values are considered very similar.

Figure 46 presents the dissolved Ra content of the water samples as a function of distance from the end of the 09 drift. The values are believed to be accurate to within 10 percent. There is a definite increase in the Ra content of the water with increased distance of flow in the drift. This may be attributable to the haulage of ore along the 07 drift in past years. The water, as it flows along this tunnel floor, may dissolve Ra from previously spilled ore. Note also that while

flowing in the 07 drift the water increases its Ra concentration by about  $188 - 136 = 52 \mu\mu\text{c Ra/l}$ . Per day this amounts to about  $28 \mu\text{c Ra}$ , or the amount of Ra which would be in radioactive equilibrium with about 86 g of uranium. As the water enters the test area the concentration,  $130 \mu\mu\text{c/l}$ , is equivalent to  $1.3 \times 10^{-7}$  ppm of Ra.

From data included in Fig. 48, a plan view of the second water sampling area, it is seen that the Rn content of waters sampled in the 57 drift remained fairly constant with the exception of 465K. The very high Rn content of this sample,  $18300 \mu\mu\text{c/l}$ , is indicative of the high Rn concentration that the water has while it is within the rock interstices. This water was flowing rapidly from a drill hole and therefore still retained much of the "in-rock" Rn. The remaining samples have Rn concentrations that are close to being in equilibrium with the Rn in the atmosphere above the water (this section of the mine was poorly ventilated at the time of the experiment). Because of this equilibrium there is no tendency for the Rn to leave the water. Had the Rn concentration in the mine atmosphere been lower, the water would have shown a progressive depletion in Rn content.

The Ra concentration in this water is low and shows no clear trend. Because small aliquots of water (100 ml) were

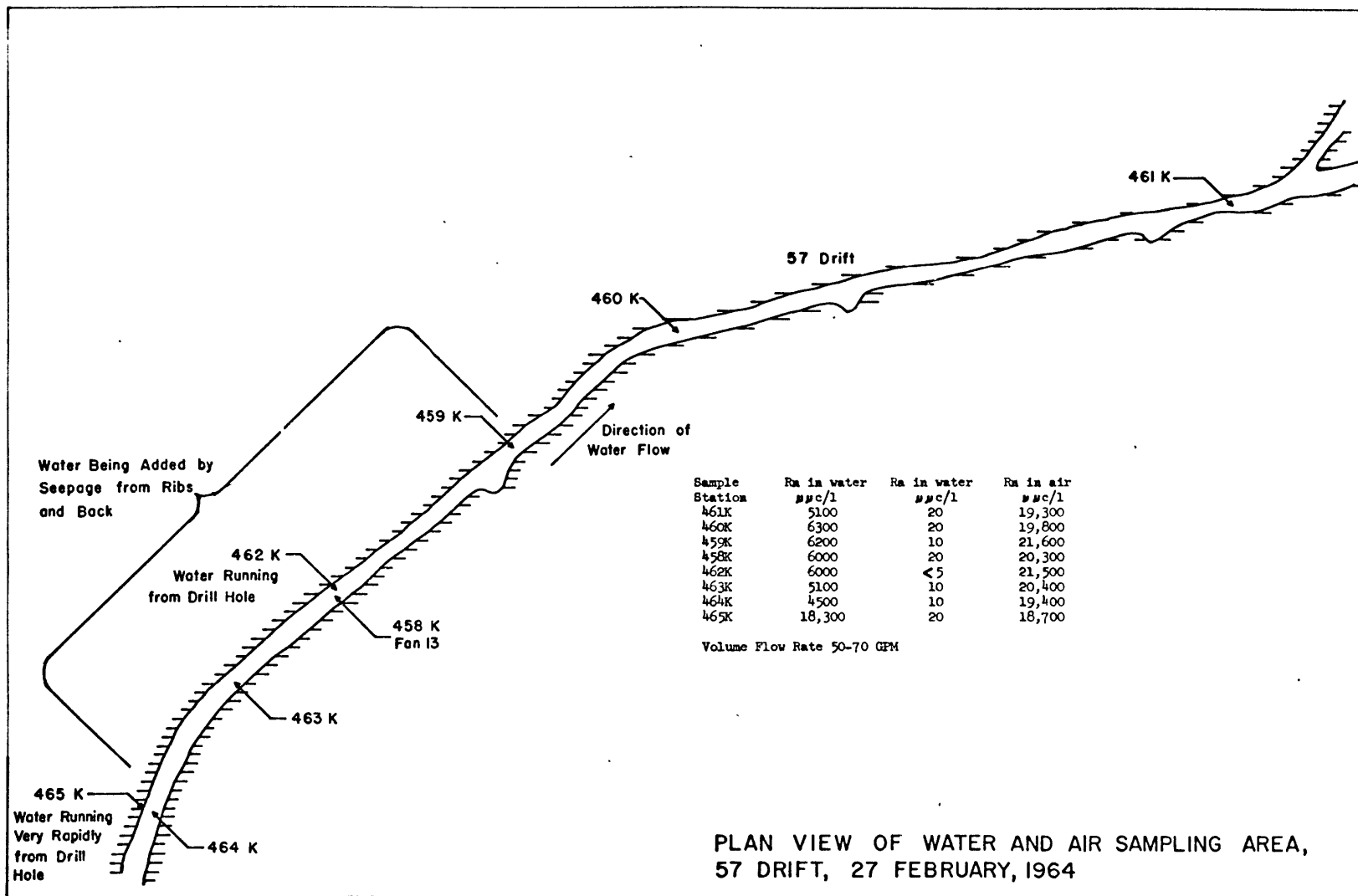


FIGURE 48

analyzed for the Ra (by milking the generated Rn) and because it is difficult to accurately differentiate between fine suspended particles and true dissolved substances, the Ra values might be assumed constant at about  $15 \mu\mu\text{c/l}$  or  $1.5 \times 10^{-8}$  ppm of Ra.

Both sampling experiments indicate that recycle water is capable of adding Rn to the mine atmosphere in significant quantities. Water samples must be taken at the point at which water enters the mine if an exact determination of the amount of Rn introduced by the water is to be obtained. The fact that samples 465K and 462K, both water samples from drill holes, had vastly different Rn contents indicates that the history of the water within the rock, especially the rate of travel, is a determining factor in the amount of Rn that the water will directly admit into a mine.

It is possible that overpressuring an area in which water is entering a mine may reduce the amount of Rn admitted to the mine by the water. If the interstices of the rock are not entirely filled with the water, then purging air will flow counter to the flow of water and will reduce the Rn concentration in the interstitial gas with which the water is in contact. Hence, the water will be able to retain less Rn prior to its entrance to the mine.

## 21. BIBLIOGRAPHY TO THE APPENDIX

- H-1 Hildebrand, F. B., Advanced Calculus for Engineers,  
Prentice-Hall, New York, 1950.
- L-1 Lane, William, Kermac Nuclear Fuels Corporation,  
private communication.
- M-1 Moon, P. and D. E. Spencer Field Theory Handbook,  
Springer-Verlag, Berlin, 1961.
- S-1 Scheidegger, A. E., The Physics of Flow Through Porous  
Media, Macmillan Co., New York, 1960.
- S-2 Schroeder, G. L., H. W. Kraner, and R. D. Evans,  
"Diffusion of Radon in Several Naturally Occurring  
Soil Types", to be published J. Geophys. Res.,  
January 1965.
- W-1 Watson, G. N., A Treatise on The Theory of Bessel  
Functions, Cambridge University Press, Cambridge,  
England, 1952.

## ACKNOWLEDGEMENTS

I thank Professor Robley D. Evans for his continual advice and enthusiastic encouragement in all phases of this work. The help of Marie Costello and Joseph Annis in the reduction of data, of James Morris and Marcel Semo in the maintenance of the electronic equipment, and of Mary Margaret Shanahan and the Radioactivity Center staff in the preparation of the many interim reports is appreciated.

I also wish to express my gratitude to the Kermac Nuclear Fuels Corporation for offering its time and the use of portions of its mining facilities as test areas. This cooperation was essential for the performance of these studies. In particular, thanks are extended to William Lane who personally helped in the design and performance of the experiments; to Marion Bolton, Jack Robison, and Milton Ward whose interest in and agreement with this work was a necessity; and to Leo Komar who acted as liaison for Kermac during the initial weeks of the study.

This work was supported in part by contract AT(30-1)-952 with the Division of Biology and Medicine, U. S. Atomic Energy Commission.

## BIOGRAPHICAL NOTE

Gerald Schroeder, born 20 February 1938, lived his childhood in Brookville, New York. He was graduated from the Avon Old Farms School in Avon, Connecticut in 1955. He attended the Massachusetts Institute of Technology from September 1955 to February 1961, receiving a Bachelor of Science in Chemical Engineering in June 1959 and a Master of Science in Geology and Geophysics in February 1961. During the final phases of his MS work and for 18 months thereafter he was employed as a member of the DSR research staff by the Radioactivity Center at MIT. During this period he worked in geophysical radiochemistry. He reentered the MIT graduate school in September 1962.

## PUBLICATIONS

- Schroeder, G. L. and J. W. Winchester, "Determination of Sodium in Silicate Minerals and Rocks by Neutron Activation Analysis", *Anal. Chem.* 34, 96 (1962).
- Evans, R. D., H. W. Kraner, and G. L. Schroeder; Edgerton, Germeshausen and Grier, Inc., Report B-2516, 6 December 1962.
- Kraner, H. W., G. L. Schroeder, and R. D. Evans, "Measurements of the Effects of Atmospheric Variables on Rn<sup>222</sup> Flux and Soil Gas Concentrations", *The Natural Radiation Environment*, eds. J. A. S. Adams and W. M. Lowder, pp. 191-215, University of Chicago Press, 1964.
- Kraner, H. W., G. L. Schroeder, R. D. Evans, and A. R. Lewis, "Large Volume Scintillation Chamber for Radon Counting", *Rev. Sci. Instr.* 35, 1259-1265 (1964).
- Schroeder, G. L., "Radon-222 in Mine Atmospheres", *Science* 145, 727 (1964).
- Schroeder, G. L., H. W. Kraner, and R. D. Evans, "Diffusion of Radon in Several Naturally Occurring Soil Types", to be published *J. Geophys. Res.* 1965.